TIMING, PROVENANCE, AND PALEOCLIMATE IMPLICATIONS OF THE CENOZOIC EOLIAN DEPOSITION IN THE CENTRAL ROCKY MOUNTAINS, USA

by

JILLIAN ROWLEY

Presented to the Faculty of the Graduate School of

The University of Texas at Arlington in Partial Fulfillment

of the Requirements

for the Degree of

MASTER OF SCIENCE IN GEOLOGY

THE UNIVERSITY OF TEXAS AT ARLINGTON

December 2013

Acknowledgements

I would like to express my gratitude to Dr. Majie Fan, who presented me with this project and guided me through the process of collecting data and analyzing results. I am grateful for her advice to attend GSA and present my work. I appreciate the insight and guidance of my two committee members, Dr. Asish Basu and Dr. John Wickham.

I would like to acknowledge Shariva Darmaoen for her assistance in formatting my document. I am particularly grateful for the assistance given by Joseph Girani in the statistical analysis as well as the support he has provided me throughout the process. Finally, I would like to extend my deepest appreciation to my family for their lifelong support.

November 25, 2013

Abstract

TIMING, PROVENANCE, AND PALEOCLIMATE IMPLICATIONS OF THE CENOZOIC EOLIAN DEPOSITION IN THE CENTRAL ROCKY MOUNTAINS, USA

Jillian Rowley, MS

The University of Texas at Arlington, 2013

Supervising Professor: Majie Fan

This study applies detrital zircon U-Pb geochronology and sandstone petrography to constrain the timing and provenance of Cenozoic eolian sandstone in the central Rocky Mountains. Four samples, collected at the transition to eolian deposition along a west-east transect, have maximum depositional ages of 35.9±0.7 Ma, 35.4±2.0 Ma, 33±0.9 Ma, and 30±1.0 Ma, suggesting the transition initiated during the latest Eocene-earliest Oligocene and became younger eastward. A total of 766 zircon grains consist of a 17-44 Ma population, derived from the distal ignimbrite flare-up in western and southwestern North America, and a population older than 45 Ma, recycled from local Laramide uplifts. Sandstone petrography results indicate detritus from the distal ignimbrite flare-up and local Laramide uplifts. The transition to eolian deposition could represent regional drying caused by both global cooling due to initiation of Antarctic glaciation and the development of rain shadow in the central Rocky Mountains due to regional uplift.

Table of Contents

List of Illustrations

List of Tables

Chapter 1

Introduction

The central Rocky Mountains (central Rockies) in Wyoming and northern Colorado are an intracontinental plateau with high mountain ranges with elevations up to 4 km high and intervening sedimentary basins with the basin floor at ~1.5 km. The topography gradually decreases eastward to the western Great Plains with an elevation of ~1.0 km in western Nebraska. This portion of the western U.S.A. has been studied extensively in order to understand how the central Rockies attained its current topography and landscape (e.g., Dickinson and Snyder, 1978; DeCelles, 2004; Pelletier, 2009; Duller et al., 2012; Roberts et al., 2012). The Laramide orogeny, caused by the low-angle subduction of the Farallon oceanic plate during the late Cretaceous to early Eocene, has been viewed as the last major mountain building process in the region (Dickinson and Snyder, 1978; DeCelles, 2004), producing high basement-cored mountain ranges and deep intermontane sedimentary basins (e.g., Fan and Dettman, 2009; Fan et al., 2011; Cather et al., 2012). After the end of the Laramide orogeny, the central Rockies may have experienced several episodes of uplift, including dynamic uplift caused by mantle upwelling associated with the extensional tectonics forming the Rio Grande Rift (Heller et al., 2003; McMillian et al., 2006), removal of the Farallon flat slab beneath the western U.S.A. (Cather et al., 2012), and/or removal of thick lithospheric mantle beneath a broader region centered on Yellowstone (Duller et al., 2012; Roberts et al., 2012). In addition to tectonics, middle-late Cenozoic climate has experienced dramatic changes including the most prominent early Oligocene cooling caused by Antarctic glaciation and the late Cenozoic cooling caused by Northern Hemisphere glaciation (Zachos et al., 2001a, b). Climate change also impacts the evolution of regional landscape. For example, snowmelt runoff associated with late Miocene global cooling may have caused up to 1.5 km of erosion from the middle Miocene to present (Pelletier, 2009), possibly resulting in isostatic uplift. Despite many studies, it remains unclear how post-Laramide tectonics and climate change influence regional landscape and sedimentation.

Cenozoic deposition in the central Rockies underwent a transition from river-dominated deposition to eolian deposition (Figure 1.1) (McKenna and Love, 1972; Flanagan and Montagne, 1993; Buffler, 2003). Based on available age constraints, including mammalian biostratigraphy, K-Ar, ^{40}Ar-^{39}Ar, and U-Pb dating of biotites, feldspars, and zircons in ash beds, the earliest transition to eolian deposition occurred during the latest Eocene (Evanoff et al., 1992; Larson and Evanoff, 1998). The sporadic preservation of Cenozoic eolian deposits indicates eolian deposition sustained into the Miocene (e.g., Love, 1970; Honey and Izett, 1988; Scott, 2002). Locally preserved eolian deposits are also documented in the northern New Mexico and Arizona part of the Colorado Plateau. The timing of eolian deposition is narrowed to 33.5-27 Ma for the Chuska and western Mongollon-Datil eolianite and 33.5-22 Ma for the eolianite in the Albuquerque Basin (May and Russell, 1994; Tedford and Barghoorn, 1999; Cather et al., 2008). Cather et al. (2008) suggested the eolian deposition in the central Rockies may have occurred during the same time as the eolian deposition in the Colorado Plateau. Cather et al. (2008) further suggested this transition from fluvial to eolian deposition represented a regionally synchronous event, onset during the earliest Oligocene associated with global cooling due to Antarctic glaciation. Alternatively, Evanoff et al. (1992) proposed a west-east diachronous transition from fluvial to eolian deposition that occurred during the late Eocene-middle Oligocene in the central Rockies. Additional study is needed in order to test whether the transition to eolian deposition has temporal and spatial patterns and whether the patterns were governed by tectonic uplift or global climate change.

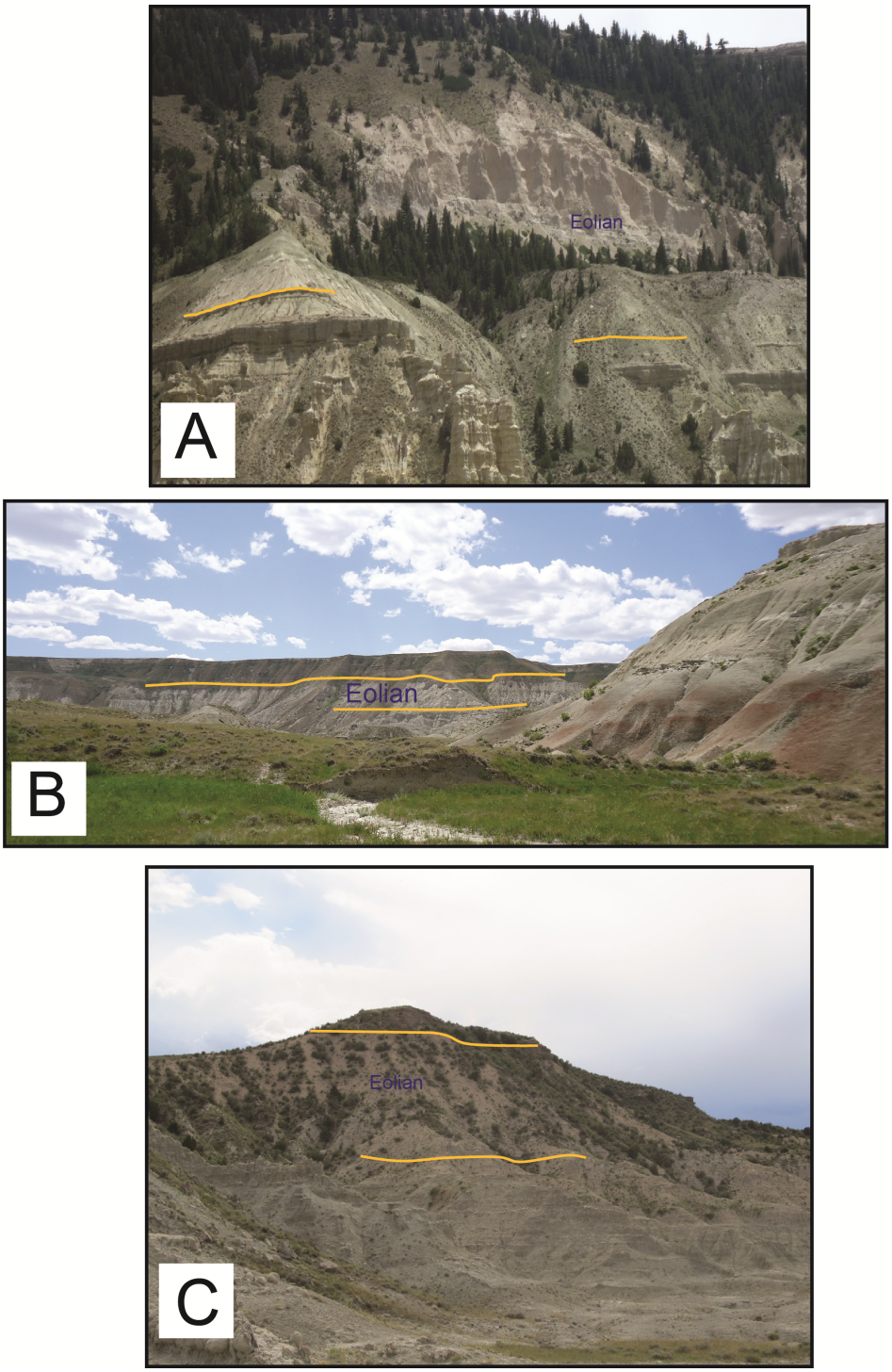

Figure 1.1 Regional transition from fluvial to eolian deposition in Wyoming.

A. Western part of Beaver Divide, Fremont County, Wyoming. B. Flagstaff Rim section, North Fork of Lone Tree Gulch, Natrona County, Wyoming C. Dilts Ranch, Converse County, Wyoming.

The Paleocene-early Eocene deposits in the central Rockies have been studied extensively in order to understand the Laramide basin evolution, exhumation, and surface uplift of the Laramide mountain ranges (e.g., Dickinson et al., 1988; Fan et al., 2011). Few studies have provided details to the latest Eocene-Miocene deposits. This study addresses questions of when, how, and why the eolian deposition occurred within the central Rockies and adjacent Great Plains during the Cenozoic. The provenance and maximum depositional ages of the Cenozoic eolian sandstone will be determined by using detrital zircon U-Pb geochronology and sandstone petrography. Samples were collected from various locations in the central Rockies and adjacent Great Plains including Wyoming, northern Colorado, and western Nebraska (Figure 1.2), in order to spatially and temporally characterize the Cenozoic eolian deposition, reconstruct paleogeography, and explore the implications to paleoclimate and tectonics.

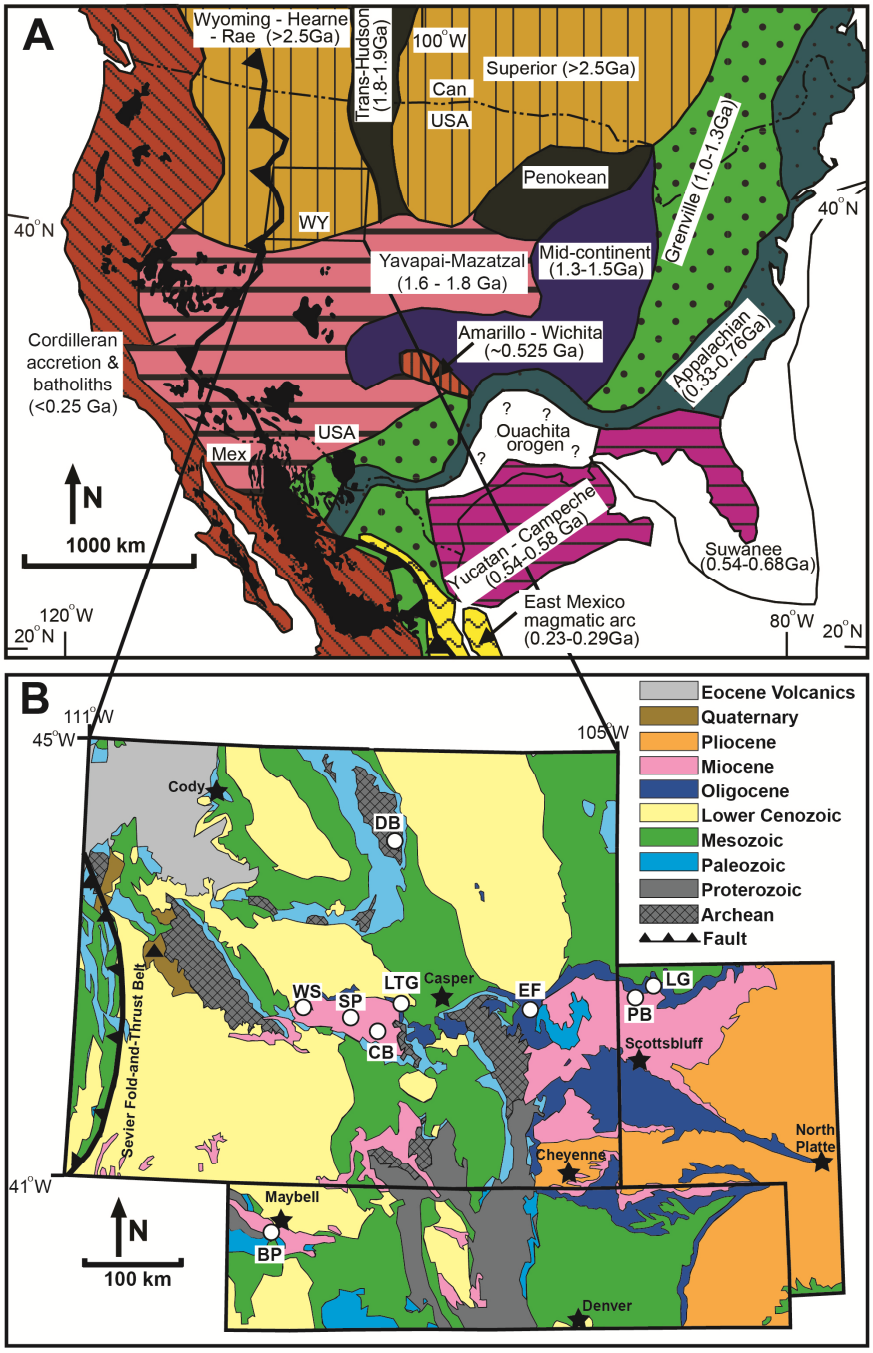

Figure 1.2 Geologic maps of North America (A) and the study area (B).

A. Map showing locations of provinces of various age (after Dickinson and Gehrels, 2009; Mackey et al., 2012), Cenozoic ignimbrite flare-up in black polygons (after Best et al., 2013), Sevier fold-and-thrust belt (after DeCelles, 2004).
B. Geological map of study area including central Rockies and adjacent western Great Plains, circles represent sample locations.

1.1 Geologic Background

1.1.1 Regional geological settings

The study area is located in the central Rockies and adjacent western Great Plains (Figure 1.2). Modern landscape of the study area is characterized by high basement-cored uplifts and intermontane sedimentary basins in the central Rockies that gradually change eastward to low, flat plains in Nebraska. Starting in the late Jurassic, the high-angle subduction of the Farallon oceanic plate underneath the North American plate caused significant crustal shortening and thickening and produced the Sevier fold-and-thrust belt in the area of modern eastern Idaho, central Utah, and western Wyoming as well as the Cordilleran magmatic arc in the area of Nevada (DeCelles, 2004). During the Cretaceous, the studied area was in the foreland basin of the Sevier fold-and-thrust belt, with the basin developing underneath the Western Interior Seaway (DeCelles, 2004). The Laramide orogeny disrupted the Sevier foreland and formed a series of basement-cored uplifts and intervening sedimentary basins during ~80-45 Ma, caused by the change from high-angle normal subduction to low-angle subduction of the Farallon plate (Dickinson and Snyder, 1978; Dickinson et al., 1988; DeCelles, 2004). Post-Laramide tectonics is highly debated due to the lack of continuous sedimentary record. McMillan et al. (2006) argues that these intermontane basins experienced continuous and slow subsidence during the late Eocene-middle Miocene. However, Cather et al. (2012) suggests intense exhumation in Wyoming during 42-37 Ma, based on the widespread paleovalley incision and scarcity of Duchesnean deposition. During the latest Miocene-Pliocene, central Wyoming may have collapsed (Love, 1970; Steidtmann and Middleton, 1991), possibly due to the west-to-east migration of thermal cooling of the Yellowstone hotspot during the last 10 Ma (Anders et al., 2009). Other studies suggest that the central Rockies and Great Plains experienced differential dynamic uplift during the latest Miocene-Pliocene (McMillan et al., 2006; Duller et al., 2012; Roberts et al., 2012), likely due to hot mantle upwelling associated with Yellowstone hotspot or extension of the Rio Grande Rift (e.g., Heller et al., 2003; Moucha et al., 2008; Roberts et al., 2012).

Tertiary volcanism and ignimbrite activity became prolific during the latest Eocene in much of western and southwestern North America (e.g., Best and Chrisitansen, 1991; McIntosh and Cather, 1994; McIntosh and Chamberlin, 1994; Chapin et al., 2004a, b). Magmatism, particularly in the Indian Peak-Caliente caldera complex and the central Nevada caldera complex in the Great Basin area in Nevada, persisted from 36 to 18 Ma, with an estimated volume of erupted volcanic ash of 50,000 km^3 over an area of >71,000 km^2 (Best and Christiansen, 1991, Best et al., 2013). During the early Miocene, extensional tectonics in the Basin and Range province impacted the central Rockies. The extensional tectonics have been attributed to a thermally weakened lithosphere as well as overthickened and gravitationally unstable crust in the Sevier hinterland (e.g., Eaton, 1982; Liu, 1996).

1.1.2 Climate Setting

Modern climate of the study area is arid to semi-arid. The hydroclimate is dominated by the competing influences of the dry polar air mass, the Westerlies, and the moist tropical-subtropical air masses from the Gulf of Mexico, the Atlantic Ocean, and the Pacific Ocean (namely the North American Monsoon) (Bryson and Hare, 1974). During summer time, the North American Monsoon brings moisture from the Gulf of Mexico and subtropical Atlantic into the Great Plains and from the equatorial Pacific into the central Rockies (Bryson and Hare, 1974). During winter time, moisture is mainly transported from the high-latitude Pacific with minor contributions from the Arctic region (Bryson and Hare, 1974).

Global climate, represented by the oxygen isotope ratios of benthic foraminifera, show several cooling events during the late Cenozoic, which include the Oi-1 Glaciation at 34 Ma and Mi-1 Glaciation at 27-26 Ma (Zachos et al., 2001a, b). Reconstructed mean annual precipitation from paleosols Bk depth in Nebraska show a warm-wet and humid-subhumid climate during the late Eocene, changing to a cooler and dryer climate during the early Oligocene (Retallack, 2007). Retallack (2007) suggested the change of local climate was related to the development of rain shadow in the central Rockies. A sub-humid and warm-temperate climate persisted with a marked dry season during the Oligocene, while climate became cooler and drier during the

Miocene (Van Houten, 1964, Evanoff et al., 1992). Late Cenozoic climate change is also supported by changes of phytolith assemblages, which indicate a closed, dry woodland ecosystem during the early Oligocene, changing to an open savanna/woodland type habitat during the Miocene (Stromberg, 2004).

1.1.3 Potential sediment provenance

The potential provenance of the late Cenozoic sediment in the study area may include recycled grains from the nearby Laramide basement-cored uplifts as well as direct input of grains formed during the late Cenozoic magmatism in western and southwestern North America. The Archean Wyoming craton (~3.2-2.5 Ga) is exposed in the cores of Laramide uplifts in the vast majority of Wyoming (Figure 1.2). Proterozoic basement rocks, formed by the Yavapai-Mazatzal orogeny (1.8-1.6 Ga), outcrop in the southeast corner of Wyoming and western Colorado (Whitmeyer and Karlstrom, 2007). Paleozoic and Mesozoic sedimentary rocks, bounding the Laramide uplifts, and lower Tertiary sedimentary rocks, deposited in the Laramide intermontane basins, include grains recycled from the Archean and Proterozoic basement, the Grenville orogeny (1.3-0.9 Ga), the Appalachian orogeny (700-300 Ma), Permian-Triassic magmatic arcs (290-230 Ma) in eastern Mexico, and the Cretaceous Cordillera magmatic arc (220-80 Ma) in the western U.S.A. (Dickinson and Gehrels, 2003; Whitmeyer and Karlstrom, 2007; Dickinson and Gehrels, 2009; Fan et al., 2011). Lower Cenozoic sedimentary rocks, distributed in the Laramide intermontane basins, should include grains derived from the Challis and Absaroka volcanic supergroups (60-42 Ma) (Armstrong and Ward, 1993), which are currently distributed in Idaho, northwest Wyoming, and southeast Montana. The ignimbrite flare-up in western and southwestern North America resulted in large eruptions of rhyolitic ash from ~44 to 17 Ma (Best and Christiansen, 1991; McIntosh and Chamberlin, 1994; Chapin et al., 2004a, b) and may input grains directly into the late Cenozoic sediments.

1.2 Studied strata and age constraints

Latest Eocene-Oligocene and Miocene sediments are sporadically distributed in Wyoming, northern Colorado and western Nebraska with an area of 3000 km^2 (MacFadden and

Hunt, 1998, Figure 1.2). In general, upper Cenozoic strata are characterized by lenticular, trough cross-stratified sandstone and conglomerate beds interlayered with massive, well-sorted, fine-grained sandstone beds, and volcanic ash beds of 10 cm to 2 m thick (Love, 1970; McKenna and Love, 1972; Honey and Izett, 1988; Evanoff et al., 1992; Larson and Evanoff, 1998). These strata have thicknesses varying between 0 m and 1500 m and color changing from white to light gray to green (Love, 1970; McKenna and Love, 1972; Honey and Izett, 1988; Evanoff et al., 1992; Larson and Evanoff, 1998). Latest Eocene-Oligocene strata are commonly cemented by carbonate, but the Miocene strata often lack cementation.

Samples were collected from the massive, well-sorted, fine-grained sandstones in the White River Formation (WS 121.5, LTG 171, EF 15-60), Split Rock Formation (SP 15, DB 37), and Moonstone Formation (CB 26) in Wyoming, Browns Park Formation (BP 110) in northern Colorado, and Brule Formation of the White River Group (LG 6-29) and Monroe Creek Formation of the Arikaree Group (PB 1397) in western Nebraska (Figure 1.3, Table 1.1). In four studied localities (WS 121.5, LTG 171, EF 15-60, and LG 6-29), the massive, fine-grained sandstone conformably overlies a succession of interlayered lenticular, pebbly conglomerate, coarse-grained sandstone with erosional bases, and thinly bedded medium to fine-grained sandstone, siltstone, and mudstone (Emry, 1973, 1975; Evanoff, 1990a; LaGarry and LaGarry, 1997). The interlayered successions are interpreted as fluvial depositional environments (Evanoff, 1990a; LaGarry and LaGarry, 1997). The massive, fine-grained sandstone contains abundant volcanic glass shards, thus is interpreted as volcaniclastic deposits (Evanoff et al., 1992; MacFadden and Hunt, 1998). In northwestern Colorado, large-scale trough cross-stratifications, formed by eolian processes, are described in the volcaniclastic sandstone of early Miocene age (Honey and Izett, 1988). The volcaniclastic sandstone appears to be similar to the eolian loess in the Chinese Loess Plateau and Quaternary loess in North America based on grain-size distribution (Liu, 1988; Muhs et al., 2008); therefore, the sandstone in the central Rockies represents eolian deposition (Swinehart and Diffendal, 1987; Pye and Tsoar, 1990). In the other five localities, samples were collected from the eolian sandstone with unconformable contact relationship to the overlying and

underlying strata. Although the stratigraphic nomenclature of the upper Cenozoic strata is complex (e.g., Denson, 1965; Love, 1970; Lillegraven, 1993; Scott, 2002), radiometric dating of interlayered ash beds, studies of mammal fossils, magnetostratigraphy, and stratigraphic correlation provide precise chronostratigraphic framework of estimated ages for the studied eolian sandstone samples of Latest Eocene-Miocene age (Figure 1.4 and Figure 1.5). Detailed description of each formation and their age controls are summarized in Table 1.1.

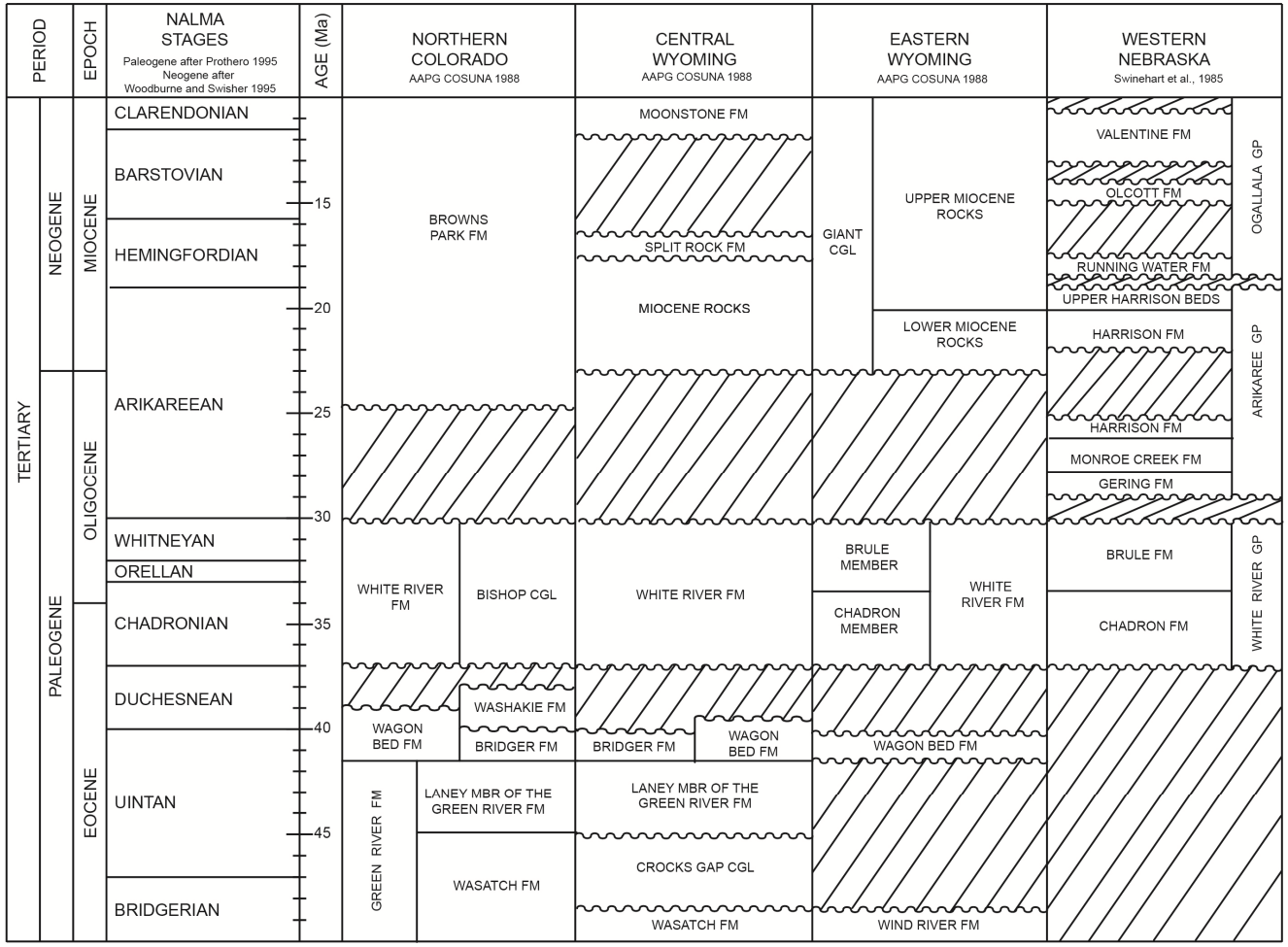

Figure 1.3 Chronostratigraphy of the studied strata.

Western Nebraska: Modified from Swinehart et al., 1985, Eastern and Central Wyoming and Northern Colorado: Modified from Childs et al., 1988.

Table 1.1 Sample location and age constraints.

Sample Name	Formation Name	GPS Location		Age Constraints				
		Lat. (°N)	Long. (°W)	NALMA Stage	Radiometric age (Ma)	Magnetostratigraphy (Ma)	Max. Depositional Age (Ma)	n
WS 121.5	White River	42.614	108.271	Middle Chadronian (Van Houten, 1964; Emry, 1975, Emry et al., 1987)	N/A	Chrons C13r-C15r [34.0-35.3] (Prothero and Sanchez, 2004)	35.9±0.7	5
LTG 171		42.647	106.735	Middle Chadronian (Swisher and Prothero, 1990)	K/Ar dating: Ash F: 34.6 (biotite), 26.6 (anorthosite), Ash G: 33.5 (Evernden et al, 1964); 40Ar/39Ar dating: Ash F: 35.72±0.38 (biotite), 35.81±0.09 (anorthosite), Ash G: 35.57±0.17 (biotite), 35.72±0.07 (anorthosite) (Swisher and Prothero,1990)	N/A	35.3±2.0	5
EF 15-60		42.610	105.249	Late Chadronian to Late Whitneyan (Evanoff et al., 1992)	High-precision zircon U-Pb geochronology: tuff 5: 34.0±0.2; tuff 7: 32.9±0.2; tuff 6a: 31.2±0.1 (Scott and Bowring, 2000); Biotite 40Ar/39Ar dating: tuff 5: 33.6±1.2, 33.9±0.1; tuff 7: 30.7±0.6, tuff 6a: 31.24±0.06 (Scott and Bowring, 2000; Swisher and Prothero, 1990)	N/A	33.0±0.9	6
LG 6-29	Brule	42.823	103.585	Whitneyan (Swisher and Prothero, 1990)	Lower tuff bed (LWA) anorthoclase, biotite, and plagioclase 40Ar/39Ar dates of 31.85±0.01, 31.81±0.03 and 31.67±0.16; Upper tuff bed (UWA) biotite 40Ar/39Ar date of 30.58±0.18 (Swisher and Prothero, 1990)	N/A	30.0±0.9	6

Table 1.1-*Continued*

Sample Name	Formation Name	GPS Location		Age Constraints			Max. Depositional Age (Ma)	n
		Lat. (°N)	Long. (°W)	NALMA Stage	Radiometric age (Ma)	Magnetostratigraphy (Ma)		
PB 1397	Monroe Creek	42.748	103.808	Late early Arikareean (Hayes, 2005)	N/A	Chrons C9r-C7r [28.95-27.05] (Hayes, 2005; MacFadden and Hunt, 1998)	28.3±1.4	6
BP 110	Browns Park	40.616	108.329	Hemingfordian to early Clarendonian (Honey and Izett, 1988)	Biotite K-Ar dating: near base of formation: 24.8±0.8 (Izett, 1975); Zircon fission track date: near top of formation: 9.9±0.4 (Naeser et al., 1980)	N/A	25.7±1.0	7
DB 37	Split Rock	44.118	107.119	Late Hemingfordian (McKenna and Love, 1972)	Sanidine 40Ar/39Ar dating: 17.4 +- 0.08 (Izett and Obradovich, 2001)	Chron C5r [16.7-17.4] (Liter et al., 2008)	25.2 ±1.6	9
SP 15		42.443	107.560		N/A	N/A	19.5±1.3	4
CB 26	Moonstone	42.369	107.051	Late Barstovian to early Hemphillian (Cassiliano, 2008)	Electron microbe analysis of glass shards: upper tuff (UT-01): 10.2 +- 0.1, 9.8 +- 0.2; Zircon U/Pb geochronology: lower tuff (LT-02): 11.3 +- 0.5 (Scott, 2002)	N/A	26.8 ±1.4	7

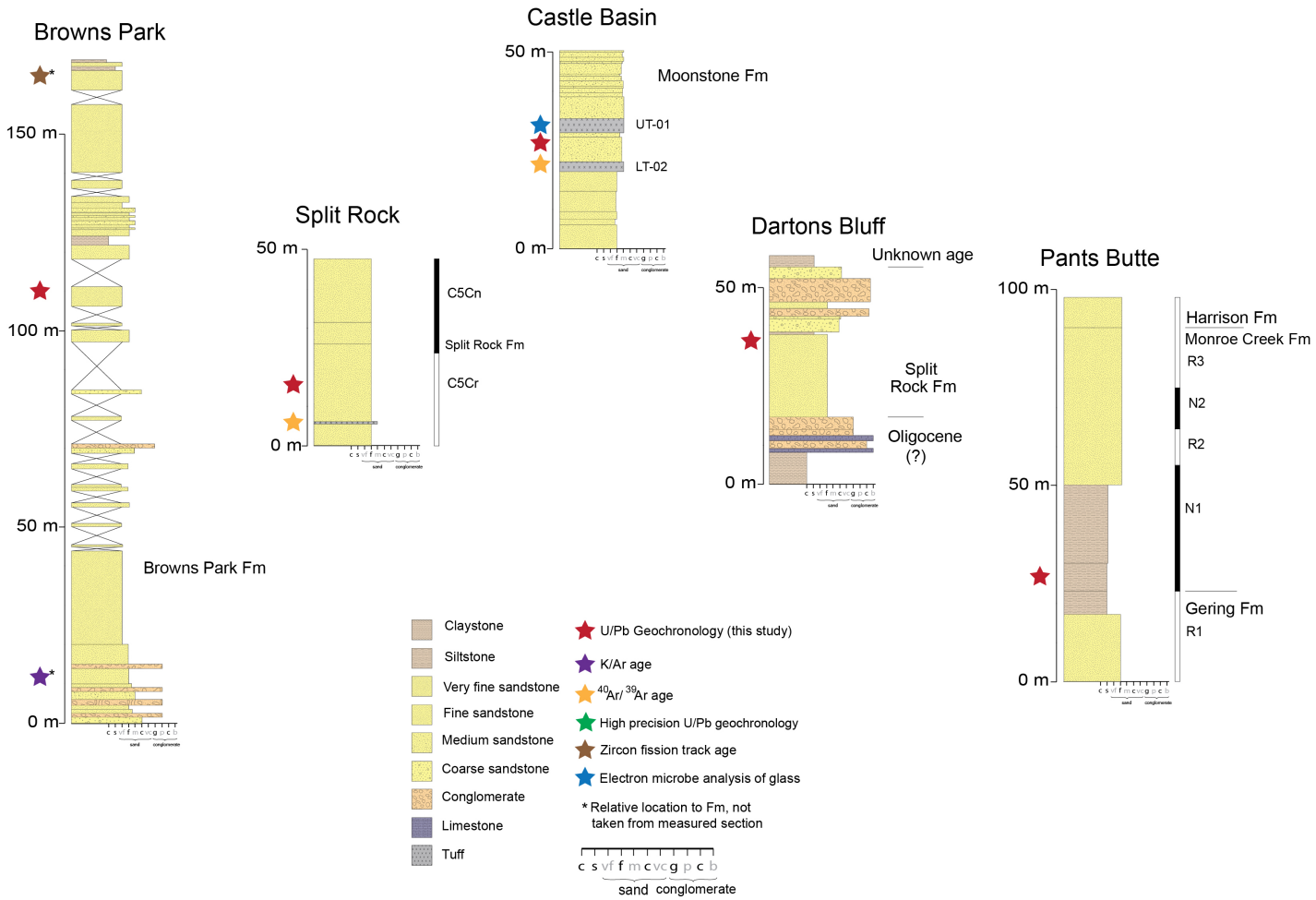

Figure 1.4 Stratigraphic framework of the Miocene sample measured sections.

Reference age constraints in Table 1.1.

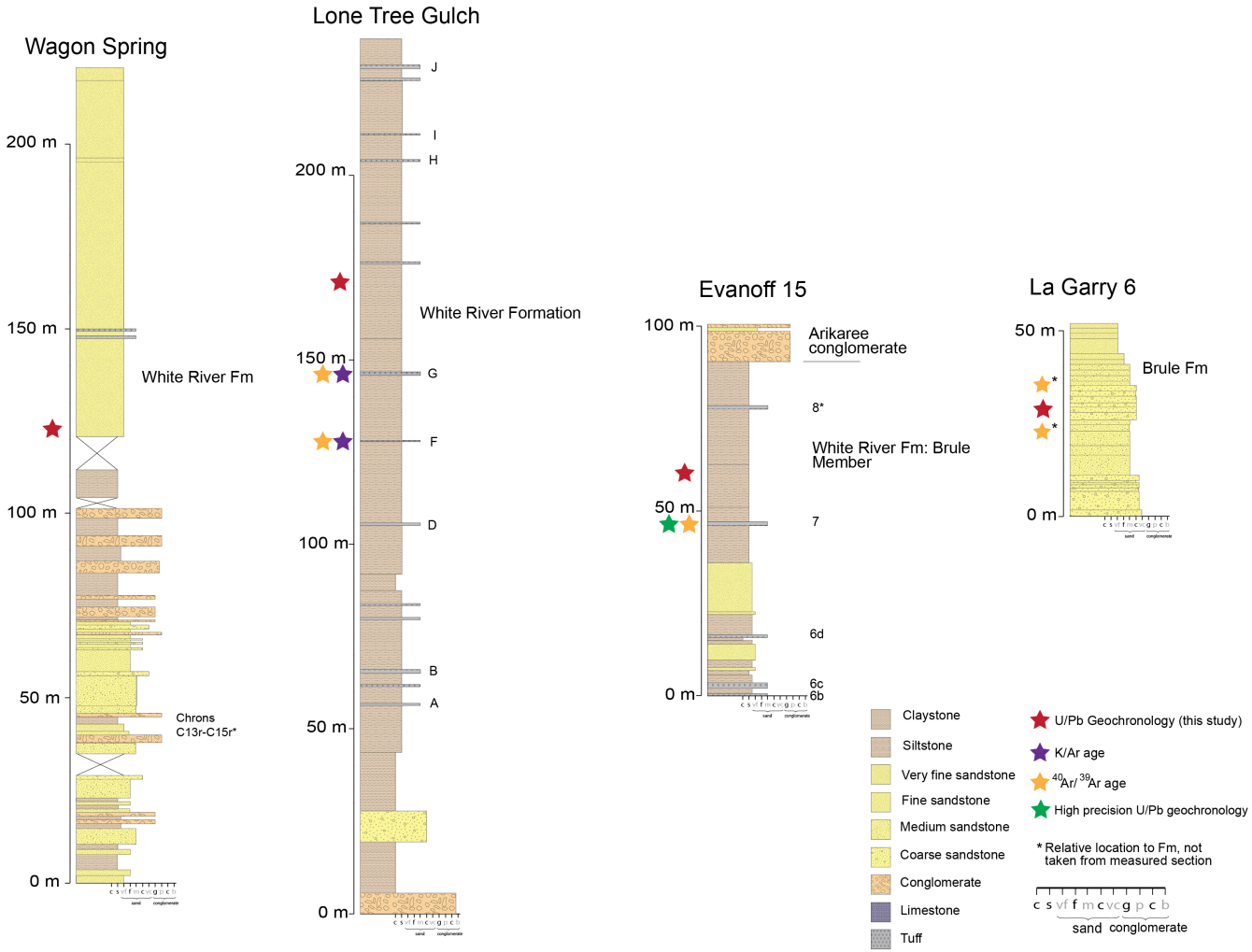

Figure 1.5 Stratigraphic framework of the Latest Eocene-Oligocene sample measured sections.

Reference age constraints in Table 1.1.

1.2.1 White River Formation

The White River Formation in eastern Wyoming is divided into the fluvial Chadron Member and fluvial/eolian Brule Member, which are lithologically similar to the Chadron and Brule formations of the White River Group in western Nebraska (Swisher and Prothero, 1990; Larson and Evanoff, 1998). In central and eastern Wyoming, the formation unconformably overlies the late Eocene Wagon Bed Formation and unconformably underlies the Miocene Split Rock Formation, with a maximum thickness of 300 m (Evanoff, 1990a). The formation consists of tuffaceous fine-grained sandstone, bentonitic mudstone, and lenses of arkosic sandstone and conglomerate (Van Houten, 1964; Evanoff, 1990a; Evanoff et al., 1992). The mammalian fauna of the White River Formation place the depositional age to the Chadronian, Orellan, and Whitneyan stages (Evanoff et al., 1992). Near the city of Douglas in eastern Wyoming, a tuff bed (tuff 5) in the lower half of the section was dated as 33.91±0.06 Ma by biotite $^{40}Ar/^{39}Ar$ geochronology (Swisher and Prothero, 1990), 33.59±0.02 Ma by sanidine $^{40}Ar/^{39}Ar$ geochronology (Izett and Obradovich, 2001), and 34.0±0.2 Ma by high-precision zircon U-Pb geochronology (Scott and Bowring, 2000). A second tuff bed (tuff 7) stratigraphically higher than tuff 5 was dated to 30.7±0.6 Ma by biotite $^{40}Ar/^{39}Ar$ geochronology and 32.9±0.2 Ma by zircon U-Pb geochronology (Scott and Bowring, 2000). A third tuff bed (tuff 6a) stratigraphically in between tuff 5 and tuff 7 was dated to 31.2±0.1 Ma by zircon U-Pb geochronology (Scott and Bowring, 2000). Sample EF 15-60 was collected stratigraphically above tuff 7. Near Fremont County, in central Wyoming, the White River Formation was correlated to Chrons C13r-C15r with an age of 35.3-34.0 Ma (Prothero and Sanchez, 2004). Several interlayered tuff beds were dated to 36.6-34.6 Ma by biotite and anorthosite $^{40}Ar/^{39}Ar$ and biotite and anorthosite K-Ar geochronology (tuff F), and 35.72-33.5 Ma by biotite and anorthosite $^{40}Ar/^{39}Ar$ and biotite K-Ar geochronology (tuff G) (Evernden et al., 1964; Swisher and Prothero, 1990). Sample LTG 171 was taken from between these two tuffs. Sample WS 121.5 was collected from the undivided White River Formation in central Wyoming. There is no available radiogenic age constraint, and the estimated age based on lithostratigraphic correlation to the other two sites is of 36-33 Ma.

1.2.2 Brule Formation

In western Nebraska, the White River Group rests unconformably on the Cretaceous Pierre Shale and is unconformably overlain by the Miocene Arikaree Group (Swinehart and Diffendal, 1987; LaGarry, 1998; Terry, 1998). The group comprises the Chadron and Brule formations. The Brule Formation includes the Orellan, Whitney, and Brown Siltstone members (Swinehart and Diffendal, 1987; LaGarry, 1998). The Brule Formation is ~350 m thick and consists of massive volcaniclastic fine-grained sandstone and interbedded lenticular sandstone, siltstone, and mudstone (Swinehart et al., 1985; Swinehart and Diffendal, 1987). The Whitney Member is of Whitneyan stage (Swisher and Prothero, 1990). Anorthoclase, biotite, and plagioclase $^{40}Ar/^{39}Ar$ dating give ages of 31.85±0.01 Ma, 31.81±0.03 Ma, and 31.67±0.16 Ma, respectively, to the lower tuff bed (LWA), and biotite $^{40}Ar/^{39}Ar$ dating yields an age of 30.58±0.18 Ma to the upper tuff bed (UWA) (Swisher and Prothero, 1990). Sample LG 6-29 is collected from this formation, and the estimated age is of ~31 Ma.

1.2.3 Browns Park Formation

The Browns Park Formation is distributed in southern Wyoming, northwestern and central Colorado and northeastern Utah (Honey and Izett, 1988). The formation has a maximum thickness of 555 m and lies unconformably on older formations including the Bishop Conglomerate (Honey and Izett, 1988). An erosional unconformity bounds the top of the formation (Honey and Izett, 1988). The formation consists of a basal conglomerate unit, a middle large-scale, trough cross-stratified to planar-laminated sandstone unit, and an upper interlayered massive sandstone and tuff unit (Honey and Izett, 1988). The eolian nature of the sandstone is evident from the large-scale trough cross-stratification (Honey and Izett, 1988). Mammal fossils, although scarce, place the depositional age of the formation to span the Hemingfordian, Barstovian, and early Clarendonian stages (Honey and Izett, 1988). Biotite K-Ar dating to a tuff bed near the base of the formation gives 24.8±0.8 Ma (Izett, 1975). Zircon fission track dating of a tuff bed near the top of the formation gives 9.9±0.4 Ma (Naeser et al.,1980). Glass K-Ar dating to a vitric tuff within the formation yields 11.8±0.4 Ma (Damon, 1970). Volcanic rocks of 11.4-7.8 Ma

old intrude or overlie the formation, suggesting the formation is older than 7.8 Ma (Buffler, 2003). Sample BP 110 is collected from the middle sandstone unit, and the estimated age is between 24.8 and 10 Ma.

1.2.4 Monroe Creek Formation

The Monroe Creek Formation is distributed in northeastern Colorado, southeastern Wyoming, southwestern South Dakota and western Nebraska and belongs to the Arikaree Group (Swinehart et al., 1985; MacFadden and Hunt, 1998; Hayes, 2005). The Arikaree Group is <240 m thick and is unconformably underlain and overlain by the White River Group and Ogallala Group, respectively (Swinehart et al., 1985; MacFadden and Hunt, 1998). The Monroe Creek Formation is described as interlayered, buff, siltstone and fine-grained sandstone (Swinehart et al., 1985; MacFadden and Hunt, 1998). Fossil assemblages place the formation to the late early Arikareean stage (Hayes, 2005). Magnetostratigraphy correlates the Monroe Creek Formation at the Pants Butte locality to Chrons C9r-C7r, which is of 28.95-27.05 Ma (MacFadden and Hunt, 1998; Hayes, 2005). Sample PB 1397 is collected from Chron C9n and is of 27.05-27.95 Ma (MacFadden and Hunt, 1998).

1.2.5 Split Rock Formation

The Split Rock Formation was deposited in central Wyoming, with a thickness ranging between 100 m and 1000 m (Love, 1961; McKenna and Love, 1972). The formation overlies the White River Formation with an erosional unconformity except on the Bighorn Mountains where the formation overlies Archean basement directly (McKenna and Love, 1972). The formation is overlain by the Moonstone Formation with an angular unconformity on the Granite Mountains (Love, 1961; Love, 1970). The formation consists of predominately buff, poorly consolidated, fine-grained volcaniclastic sandstone (Love, 1961; McKenna and Love, 1972). Samples DB 37 and SP 15 were collected from this formation, following the described sections in McKenna and Love (1972) and Love (1961), respectively. Fossil assemblages found in the DB 37 locality place this formation to the late Hemingfordian stage (McKenna and Love, 1972). A tuff bed ~20 m below the DB 37 sample was dated to 17.4±0.08 Ma by sanidine $^{40}Ar/^{39}Ar$ chronology (Izett and

Obradovich, 2001). Magnetostratigraphy correlates the sampled section to Chron C5r, which is of 16.7-17.4 Ma old (Liter et al., 2008).

1.2.6 Moonstone Formation

The Moonstone Formation overlies the Split Rock Formation unconformably and is overlain by the Kortes Formation unconformably in central Wyoming (Love, 1970; Flanagan, 1990; Scott, 2002). The formation has an average thickness of 300 m and consists of interlayered massive, fine-grained sandstone, tuff, and thinly-bedded siltstone and limestone (Love, 1970; Flanagan, 1990; Scott, 2002). Mammal fossil assemblages place the formation to late Barstovian to early Hemphillian stages (Cassiliano, 2008). A zircon fission track date of an ash in the formation provides a depositional age of 11 Ma (Flanagan, 1990). Sample CB 26 was collected from an interval between two tuff beds, following the described section in Scott (2002). High-precision zircon U-Pb geochronology yields 11.3±0.5 Ma for the lower tuff, and electron microbe analysis of glass shards yields between 10.2±0.1 Ma and 9.8±0.2 Ma for the upper tuff (Scott, 2002).

Chapter 2

Methods

2.1 Sandstone Petrography

Ten fine-grained sandstone samples were studied for sandstone petrography by using a modified Gazzi-Dickinson method (Ingersoll et al., 1984). This method considers grains larger than 0.0062 mm in lithic fragments as individual crystals (i.e. monocrystalline quartz). Modal framework grain compositions were determined by point counting 400 grains of each standard petrographic thin section. Four thin sections were stained for potassium and calcium feldspars, one thin section was impregnated with blue-dyed epoxy, and the remaining five sections were not stained. For the slides not stained, feldspars were determined by brownish coloring in plane-polarized light, maintenance of crystal structure, and degree of reworking. For the purpose of this study, the grain size of the samples is very fine-grained sand and silt, so grains larger than 0.005 mm within lithic fragments are considered as individual crystals. Framework grains are categorized based on the parameters in Table 2.1. Point count data is provided in Appendix A. Sandstone petrography data are displayed on a QtFL ternary diagram for sandstone classification following Folk (1974) and on QmFLt and QmPK ternary diagrams to assist in interpretation of sediment provenance following Dickinson and Suczek (1979) (Figure 3 2).

Table 2.1 Modal petrographic parameters.

Symbol	Description
Qm	Monocrystalline quartz
Qp	Polycrystalline quartz
C	Chert
Qt	Total quartzose grains (Qm + Qp + C)
K	Potassium feldspar (perthite and microcline)
P	Plagioclase feldspar (Na and Ca varieties)
Lvi	Volcanic grains (mafic, felsic, mirolitic, lathwork)
Lvv	Vitric volcanic grains
Lv	Total volcanic lithic grains (Lvi + Lvv)
Lsh	Mudstone
Lc	Carbonate lithic grains
Lm	Metamorphic lithic grains
Ls	Total Sedimentary lithic grains (Lsh + Lc + C)
Lt	Total lithic grains (Ls + Lv + Lm + Qp)
L	Total nonquartzose lithic grains (Lv + Ls + Lc)
Note: Accessory minerals: chlorite, biotite, zircon, magnetite	

2.2 Detrital zircon U-Pb Geochronology

Nine fine-grained sandstone samples were selected for detrital zircon U-Pb geochronology. Four of the nine samples were collected at the transition from fluvial to eolian deposition, thus represent the oldest eolian deposition. Following crushing and grinding of the bulk samples, zircons were separated using a Wilfley table, heavy liquids, and a Frantz magnetic separator. Zircon grains were analyzed on a GVI Isoprobe multicollector magnetic sector laser ablation-inductively coupled plasma-mass spectrometry (LA-ICP-MS) at the University of Arizona LaserChron Center following Gehrels et al. (2006). Zircon grains were randomly selected for analysis to avoid bias to size or shape. For each sample, approximately 105 individual zircon grains were analyzed in an attempt to identify the predominate age groups. It has been determined that 117 grains should be analyzed to have a 95% confidence of seeing all age populations (Vermeesch, 2004). The laser beam size used has a diameter of 35 μm with a pit 12

μm deep. For samples with smaller grain sizes, the laser beam size was reduced to 25 μm in diameter.

The ages and concentrations of two mineral standards (R33 and SL2) were used for the correction and check of isotope ratios (Gehrels, et al., 2008). The $^{206}Pb/^{207}Pb$ ages are used for grains greater than 900 Ma, and $^{206}Pb/^{238}U$ ages are used for grains less than 900 Ma. Discordance of zircon U-Pb ages occurs due to lead loss, inheritance, and overgrowths. Individual grain ages were filtered by 30% discordance. Broader discordance tolerances were used for younger grains due to the inherent inaccuracy in the measurement of $^{207}Pb^*$ in young grains, which often exceeds the analytical uncertainty of the measurement. Age groups were determined by identifying three or more grains with overlapping $^{206}Pb^*/^{238}U$ and $^{207}Pb^*/^{206}Pb^*$ ages in the aggregate data set. After filtering the data for discordance, concordia diagrams were constructed using Ludwig's excel program Isoplot (Ludwig, 2008) (Figure 3.3). Each zircon crystal is plotted as an ellipse to include all errors. Cumulative age probability plots and normalized relative age probability diagrams were constructed from concordant data (Figure 3.4, Figure 3.5).

To calculate relative abundance, each sample was divided into identified zircon populations with at least three overlapping ages, and the numbers of grains were counted for each age group (Figure 3.6). Archean grains, which experienced Pb loss, were excluded from the concordia and normalized distribution diagrams; however, the grains were added to calculate relative abundance of grain groups. A total of five Archean grains were added to sample LTG 171, and one Archean grain was added to each sample WS 121.5 and PB 1397.

Chapter 3

Results

3.1 Sandstone Petrography

The studied sandstone samples are typically moderately-sorted, fine-grained, subangular to subround, arkose, lithic arkose, and feldspathic litharenite (Figure 3.1; Figure 3.2; Folk, 1974). Quartz grains frosted by clay minerals and quartz growth rims are common. Most samples are cemented by calcite, which formed during early diagenesis. The carbonate cements are mostly micritic but locally sparry. Framework grains include monocrystalline quartz, polycrystalline quartz, chert, K-feldspar (microcline and some perthite), plagioclase, volcanic lithic fragments (vitric glass shards and felsic volcanic grains), sedimentary lithic fragments (siltstone, mudstone, and carbonate grains), and minor contributions of metamorphic lithics. Accessory minerals include: chlorite, hematite, magnetite, biotite, zircon, hornblende, and glauconite. The ratio of K-feldspar and plagioclase (K/P) ranges from 0.1 to 0.7 with an average of 0.3. Volcanic lithic fragments dominate the lithic population. The ratio of volcanic lithics to sedimentary lithics (Lv/Ls) ranges from 0.2 to 6.3 with an average of 3.46. Chert abundance ranges from 3.3% to 10.5% with an average of 4.9%. Samples of latest Eocene-Oligocene ages and Miocene ages have average modal compositions of $Qm_{44}F_{26}Lt_{30}$ $Qt_{46}F_{26}L_{28}$, $Qm_{64}P_{29}K_{7}$, and $Qm_{44}F_{27}Lt_{26}$, $Qt_{48}F_{27}L_{25}$, $Qm_{64}P_{27}K_{9}$, respectively. The modal compositions of the samples of latest Eocene-Oligocene ages and Miocene ages are identical (Figure 3.2).

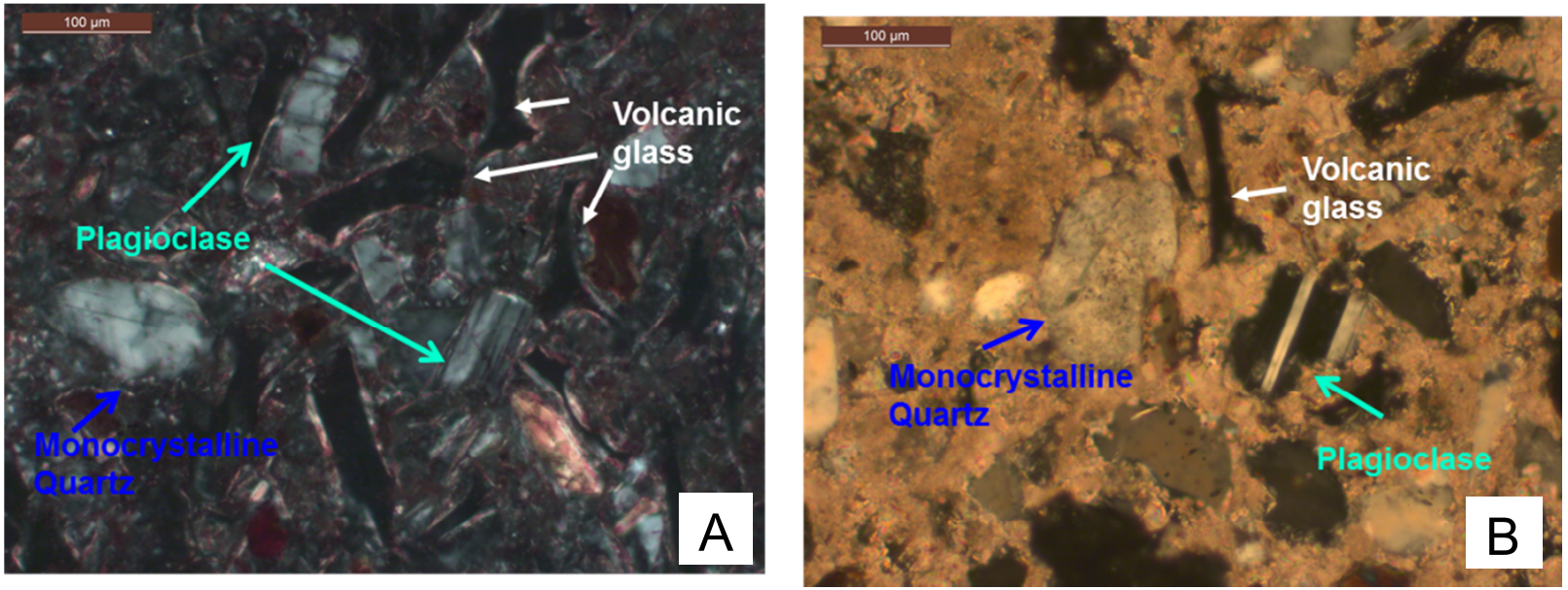

Figure 3.1 Petrographic thin sections of studied strata.

A. Thin section of DB16. B. Thin section of LTG 740.

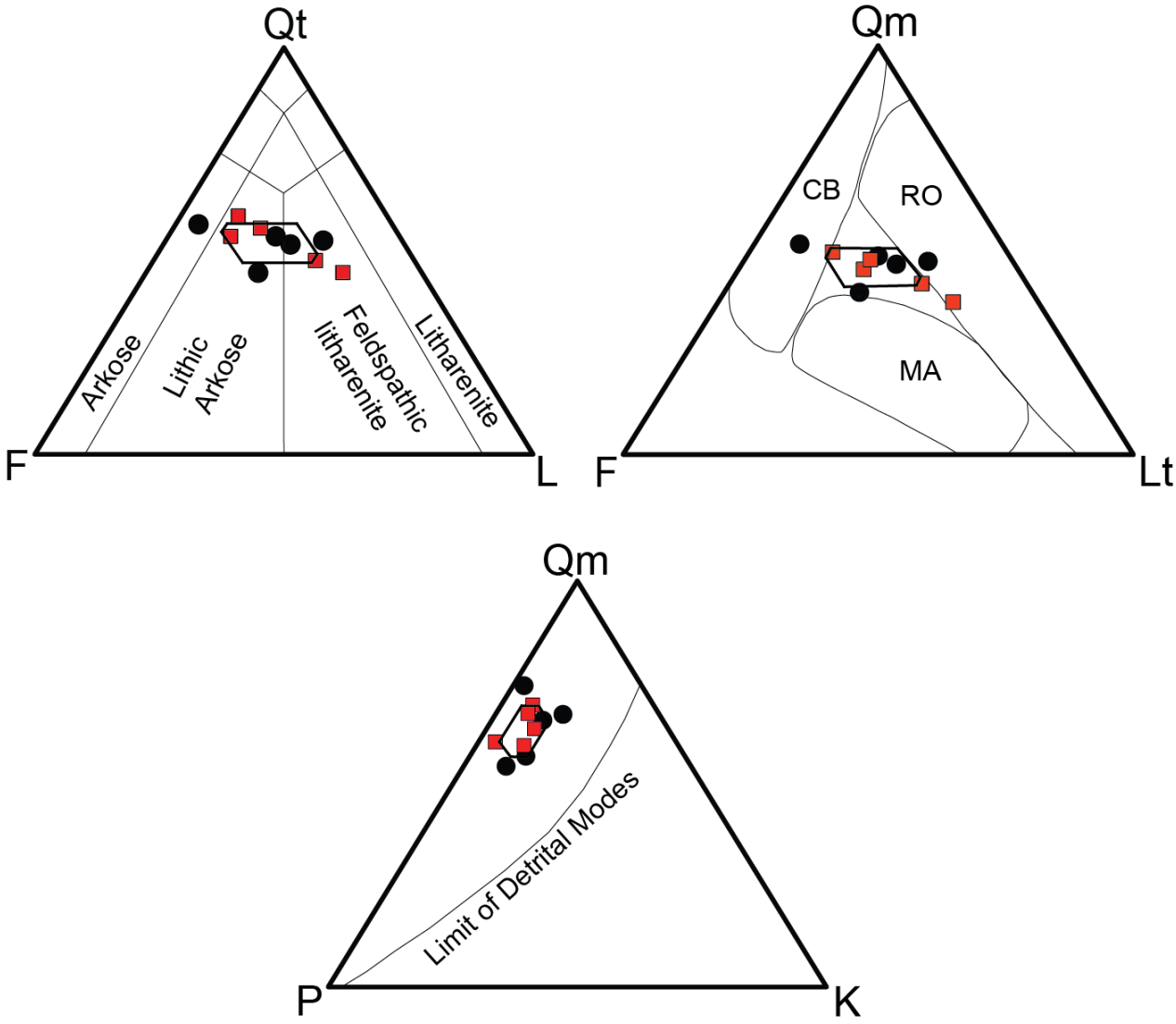

Figure 3.2 Ternary diagrams showing modal-framework grain compositions of Cenozoic eolian sandstone.

Provenance fields after Dickinson and Suczek (1979). Lithology identification after Folk (1974). RO—recycled orogen; CB—continental block; MA—magmatic arc. Modal petrographic data listed in Appendix A. Black circles are latest Eocene-Oligocene samples. Red squares are Miocene samples. Hexagons indicate one standard deviation uncertainties for average compositions of all samples.

3.2 Detrital zircon U-Pb geochronology

3.2.1 Zircon populations

Detrital zircon geochronology data reveal that zircon grains in the studied sandstone samples have ages ranging between 17 Ma and 3314 Ma. A total of 156 analyses from the nine samples were filtered from further analysis, including 47 grains for high $^{206}Pb/^{238}U$ error, two grains for high $^{206}Pb/^{237}U$ error, 58 grains for high ^{204}Pb, 24 grains for reverse discordance, 17 grains for discordance, and eight grains for low $^{206}Pb/^{204}Pb$ error. Of the ages not included, 116 grains (74%) have a best age of >900 Ma. A total of 766 grains are included in the analysis after filters were applied. Concordant grains are plotted on concordia and cumulative probability diagrams (Figure 3.3; Figure 3.4). Six zircon populations are defined based on grouping relative age peaks observed in the normalized age probability diagram (Figure 3.5), including late Eocene-middle Miocene (44-17 Ma) zircons of population F, late Triassic-middle Eocene (218-45 Ma) zircons of population E, Neoproterozoic-middle Triassic (708-222 Ma) zircons of population D, Mesoproterozoic-Neoproterozoic (1326-948 Ma) zircons of population C, Paleoproterozoic-Mesoproterozoic (1816-1332 Ma) zircons of population B, and Archean-Paleoproterozoic (3314-1825 Ma) zircons of population A. Populations A, B and F are subdivided into subpopulations of A1, A2, A3, B1, B2, B3, F1, and F2, respectively. The majority of the studied zircon grains are of populations B, C and F. Relative abundances of defined zircon populations are displayed in Figure 3.6 and Table 3.1. Abundance of population F is shown in Figure 3.7.

Six Kolmogorov-Smirnov (K-S) tests were conducted to compare the defined populations of the Latest Eocene-Oligocene and Miocene samples in this study. Populations A-C have p-values of 0.08, 0.19, and 0.97, respectively. Populations D-F have p-values of 0.01, 0.03, and 0.00, respectively. A comparison of normalized U-Pb probability plots of the Latest Eocene-Oligocene and Miocene samples illustrates the variations in age ranges as well as the proportions of age ranges (Figure 3.8).

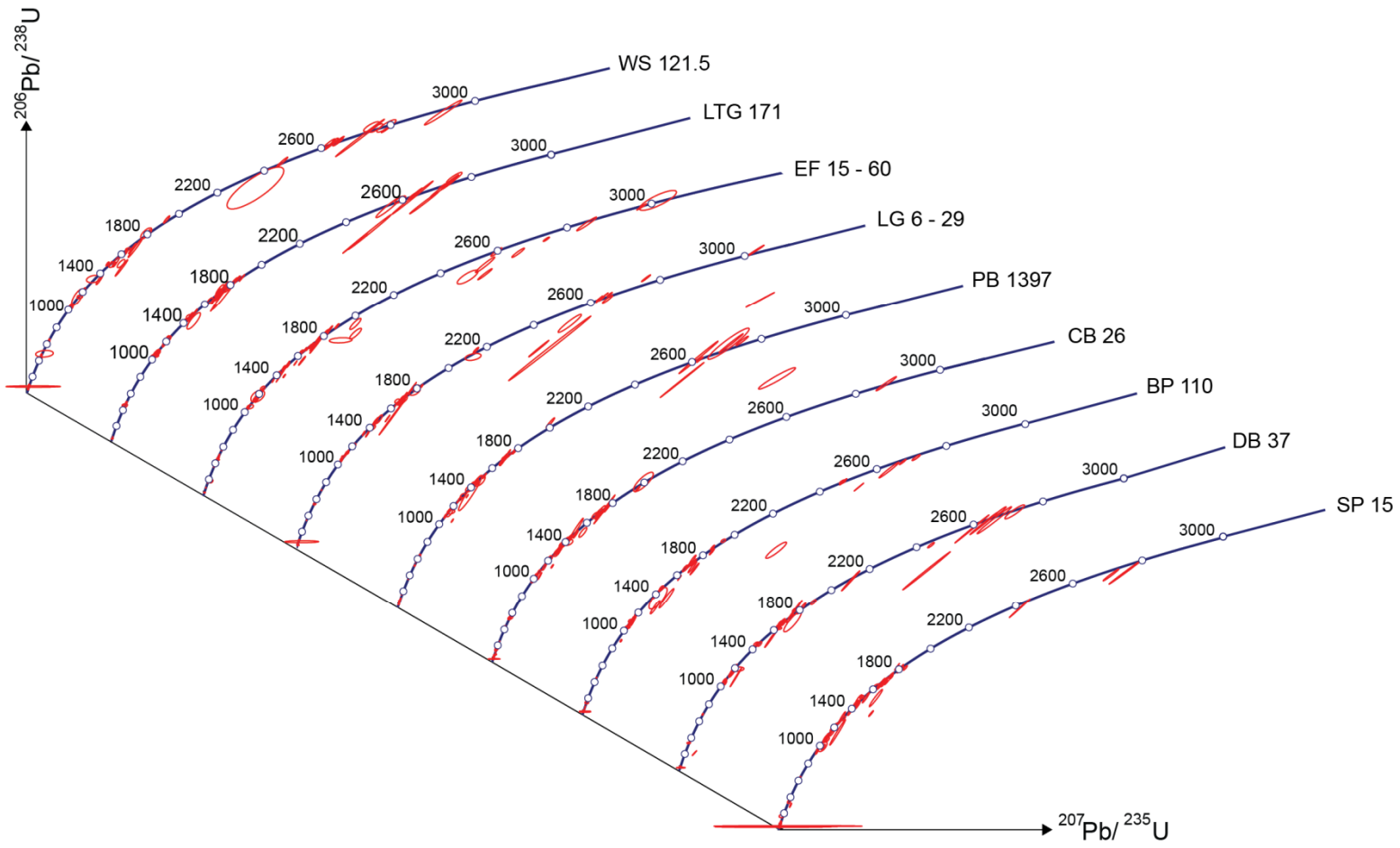

Figure 3.3 U/Pb concordia diagrams for detrital zircon samples of the nine Cenozoic eolian sandstone samples.

Error ellipses are shown for 2-sigma level of uncertainty, and only analyses that are <30% discordant are plotted. See text for discussion.

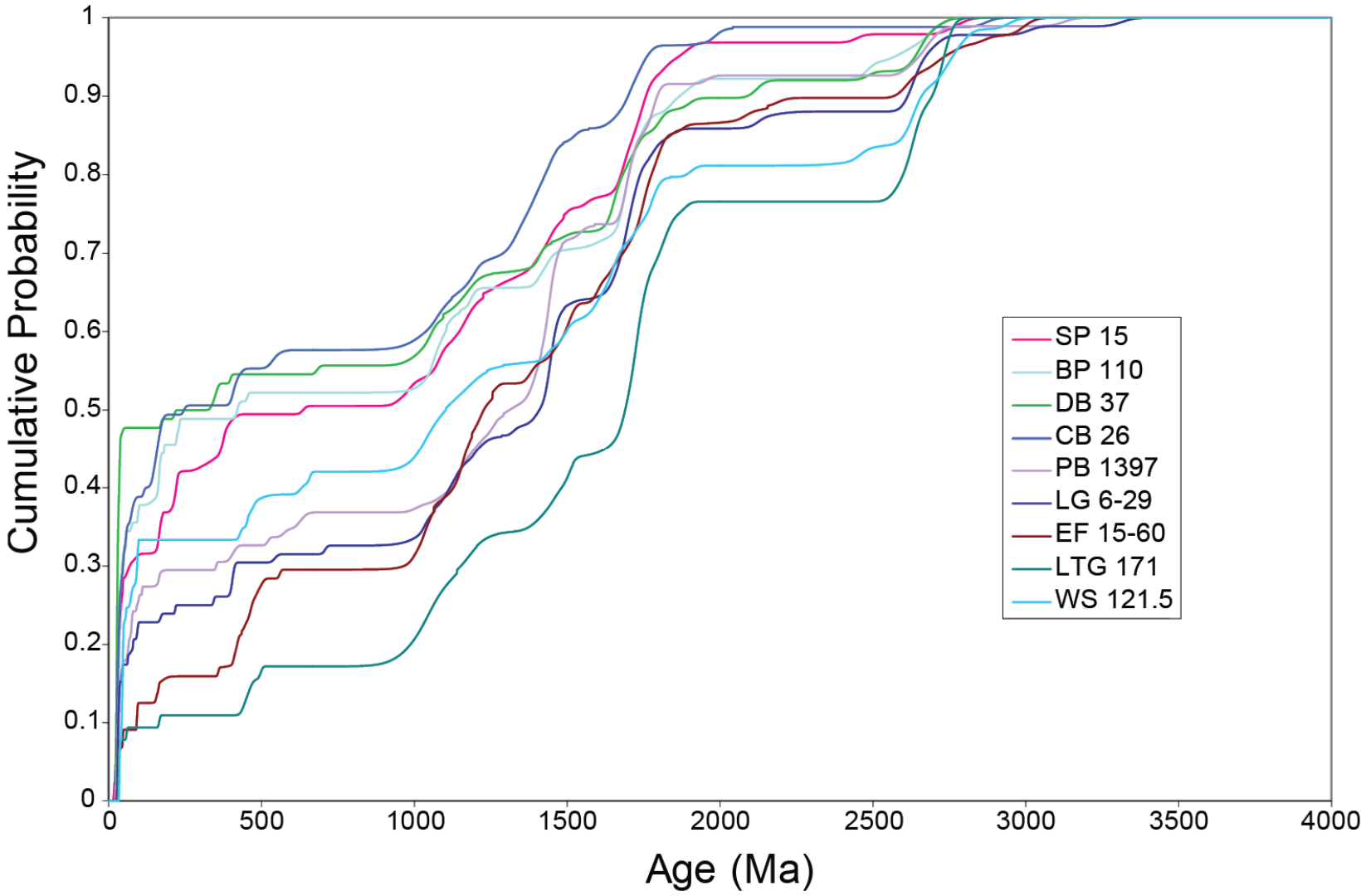

Figure 3.4 Cumulative probability plot of the nine Cenozoic eolian sandstone samples.

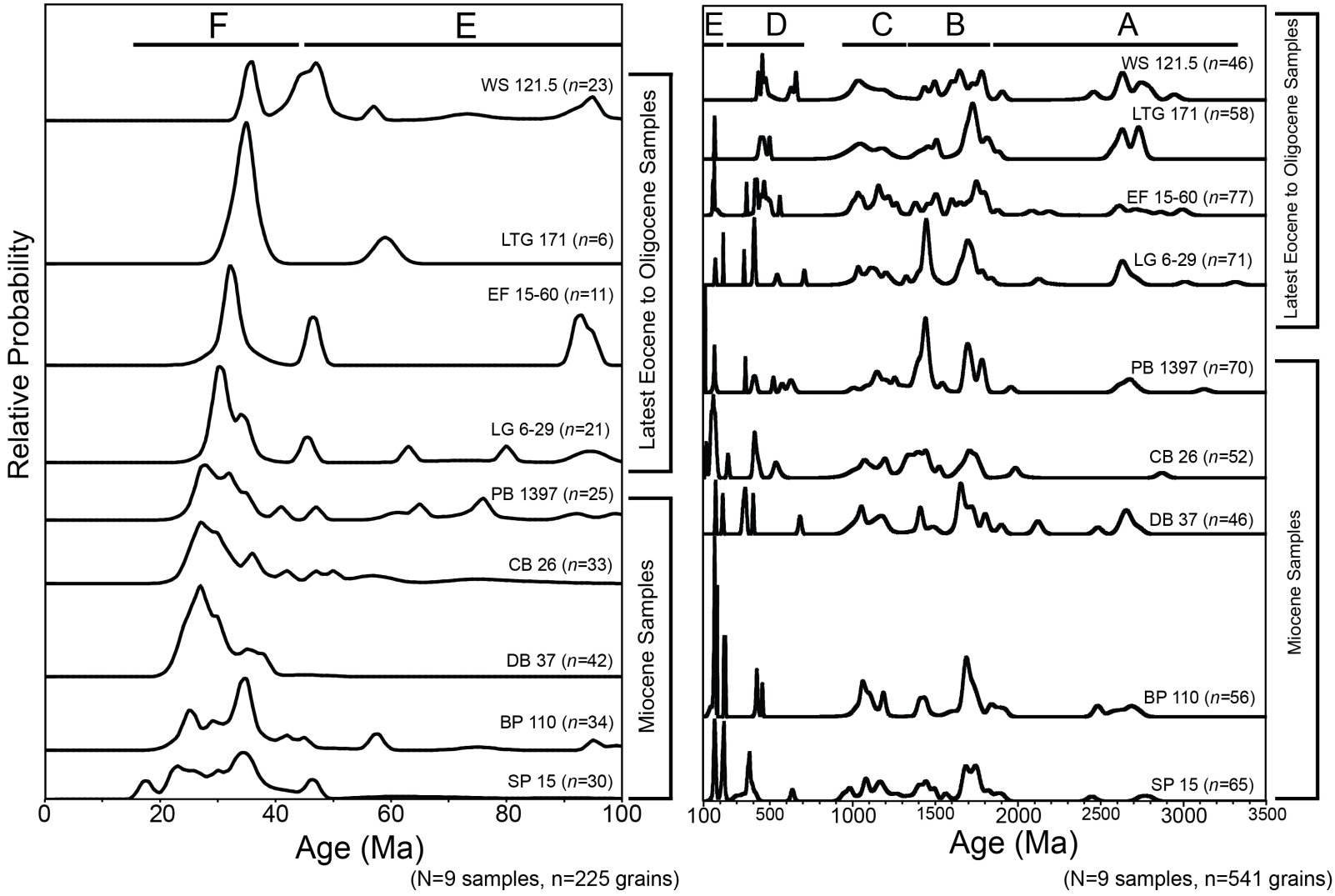

Figure 3.5 Normalized detrital zircon U-Pb age probability plots for the nine Cenozoic eolian sandstone samples.

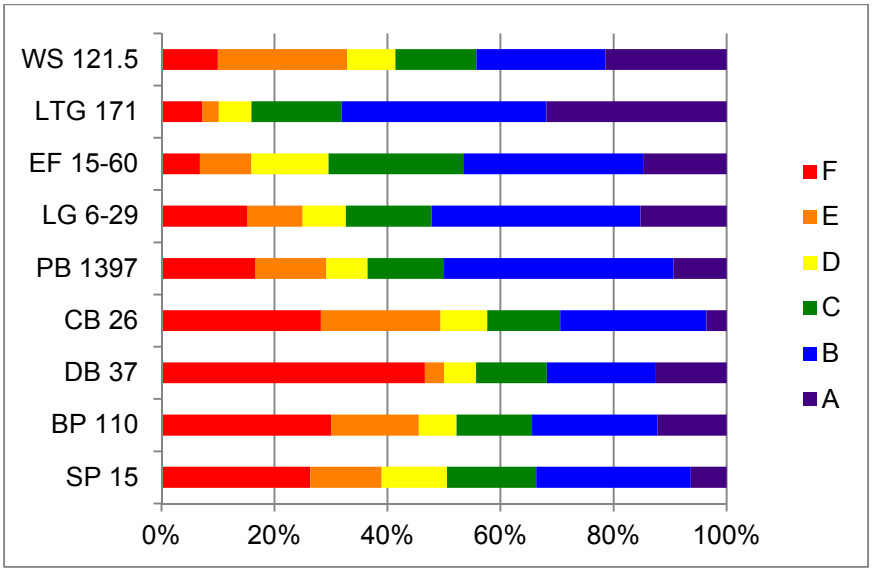

Figure 3.6 Relative abundance of defined zircon populations for the nine Cenozoic eolian sandstone samples.

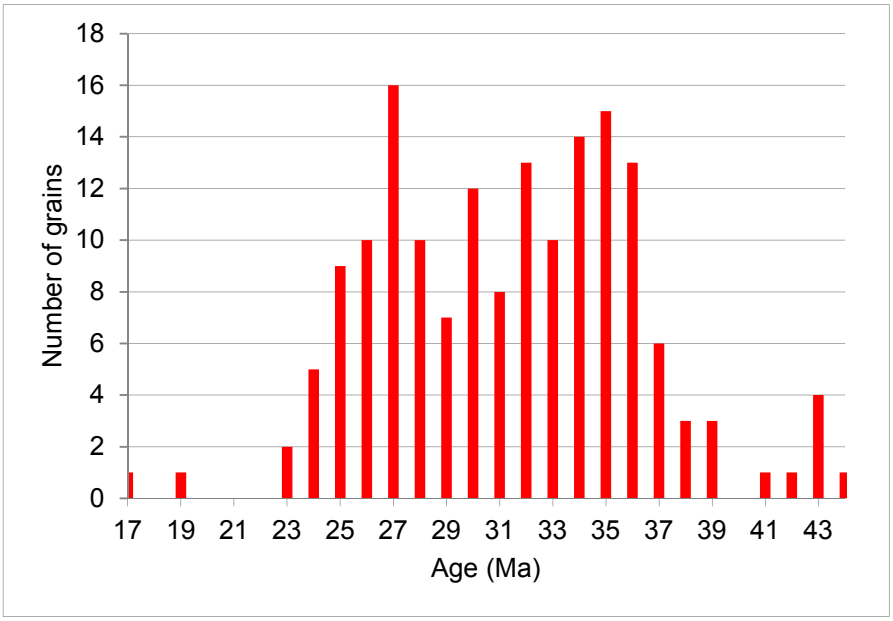

Figure 3.7 Total zircon grains of population F of all nine Cenozoic eolian sandstone samples.

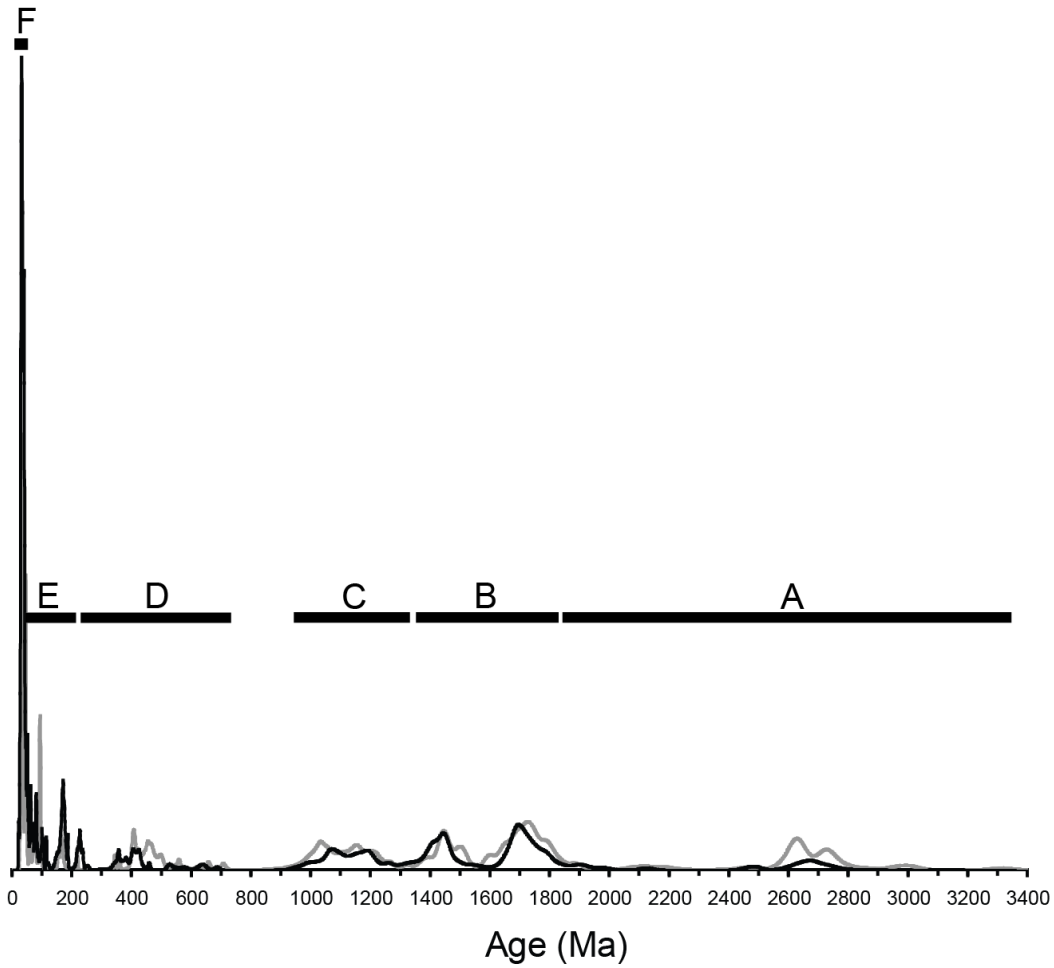

Figure 3.8 Comparison of normalized U-Pb age probability plots of total grain ages of Latest Eocene-Oligocene and Miocene sandstone.

Latest Eocene-Oligocene in gray and Miocene in black.

Table 3.1 Zircon population ages with relative abundance.

Age group	Age range (Ma)	Proportion of total samples (%)	Proportion of Oligocene (%)	Proportion of Miocene (%)
F2	17-32	11.9	3.1	18.1
F1	33-44	9.4	6.9	11.2
E	218-45	12.2	11.0	13.0
D	708-222	8.4	9.1	7.9
C	1326-948	15.3	17.6	13.7
B3	1498-1332	10.0	8.8	10.8
B2	1564-1500	1.4	1.9	1.1
B1	1816-1587	18.0	21.6	15.4
A3	1907-1825	1.7	1.6	1.8
A2	2485-1922	2.2	2.2	2.2
A1	3314-2569	9.6	16.3	4.8
F	44-17	21.3	10.0	29.3
E	218-45	12.2	11.0	13.0
D	708-222	8.4	9.1	7.9
C	1326-948	15.3	17.6	13.7
B	1816-1332	29.4	32.3	27.3
A	3314-1825	13.5	20.1	8.8

3.2.2 Maximum depositional age

The maximum age of deposition for the nine samples are reported with both a final age, calculated from the weighted mean of more than three youngest grains, and a MSWD (Figure 3.9; Figure 3.10). From west to east, the maximum depositional ages of the samples WS 121.5, LTG 171, EF 15-60, and LG 6-29 are of 35.9±0.7 Ma (n=5, MWSD=0.1), 35.3±2.0 (n=5, MWSD=0.2), 33.0±0.9 Ma (n=6, MWSD=0.3), and 30.0±0.9 Ma (n=6, MWSD=0.6), respectively (Figure 3.9). These four ages display an eastward younging trend. These ages are consistent with the estimated ages based on the North American Land Mammal stages, magnetostratigraphy, and radiometric dating (Table 1.1). The maximum depositional age of samples LTG 171 and WS 121.5 are of latest Eocene age, and samples EF 15-60 and LG 6-29 are of earliest Oligocene age. The maximum depositional ages of samples PB 1397, DB 37, SP 15, BP 110 and CB 26 are of 28.3±1.4 Ma (n=6, MWSD=0.5), 25.2 ±1.6 Ma (n=9, MWSD=0.1), 19.5±1.3 Ma (n=4,

MWSD=1.6), 25.7±1.0 Ma (n=7, MWSD=0.2), and 26.8 ±1.4 Ma (n=7, MWSD=0.3), respectively (Figure 3.10). The maximum depositional age of sample PB 1397, DB 37, BP 110, and SP 15 are 1-2 Ma older than the depositional ages constrained by radiometric dating and magnetostratigraphy (Table 1.1). The maximum depositional age of sample CB 26 is ~17 Ma older than the depositional age.

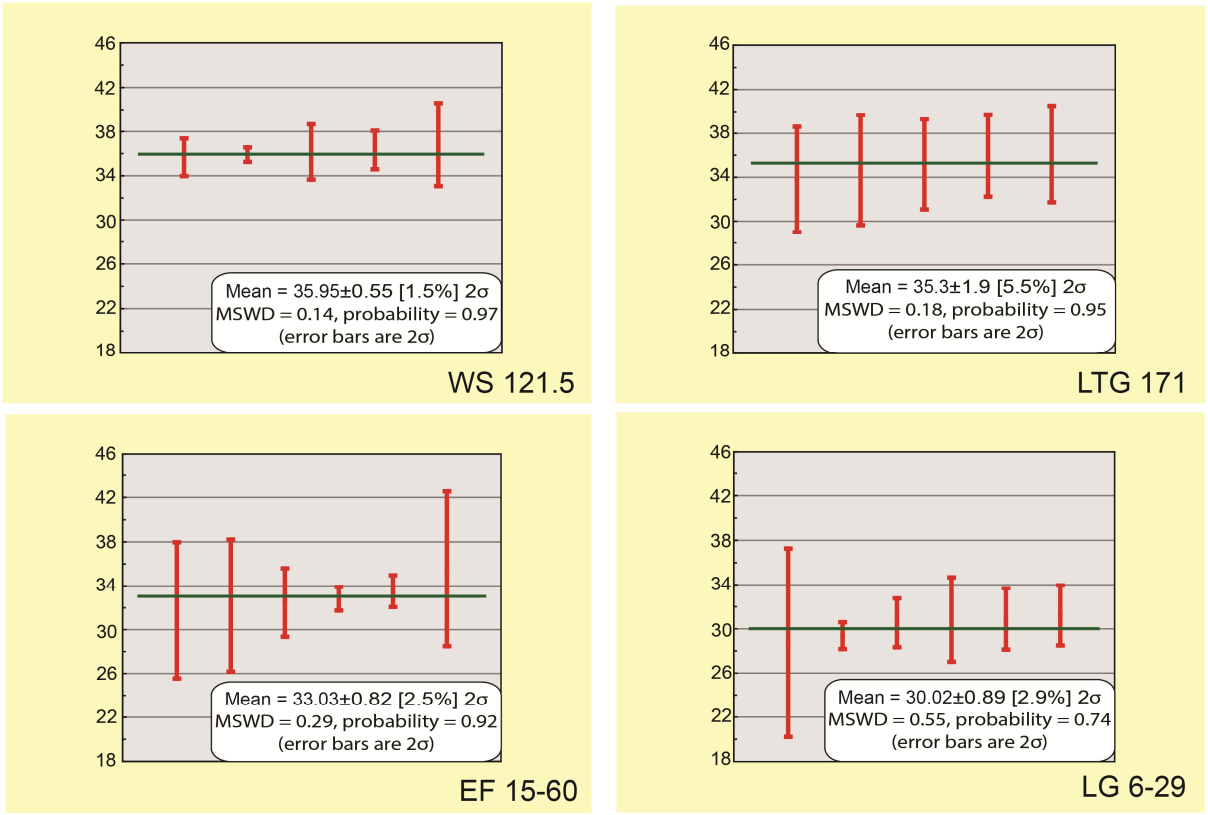

Figure 3.9 Maximum depositional ages of Latest Eocene-Oligocene sandstone samples. Data-point error symbols are 2σ.

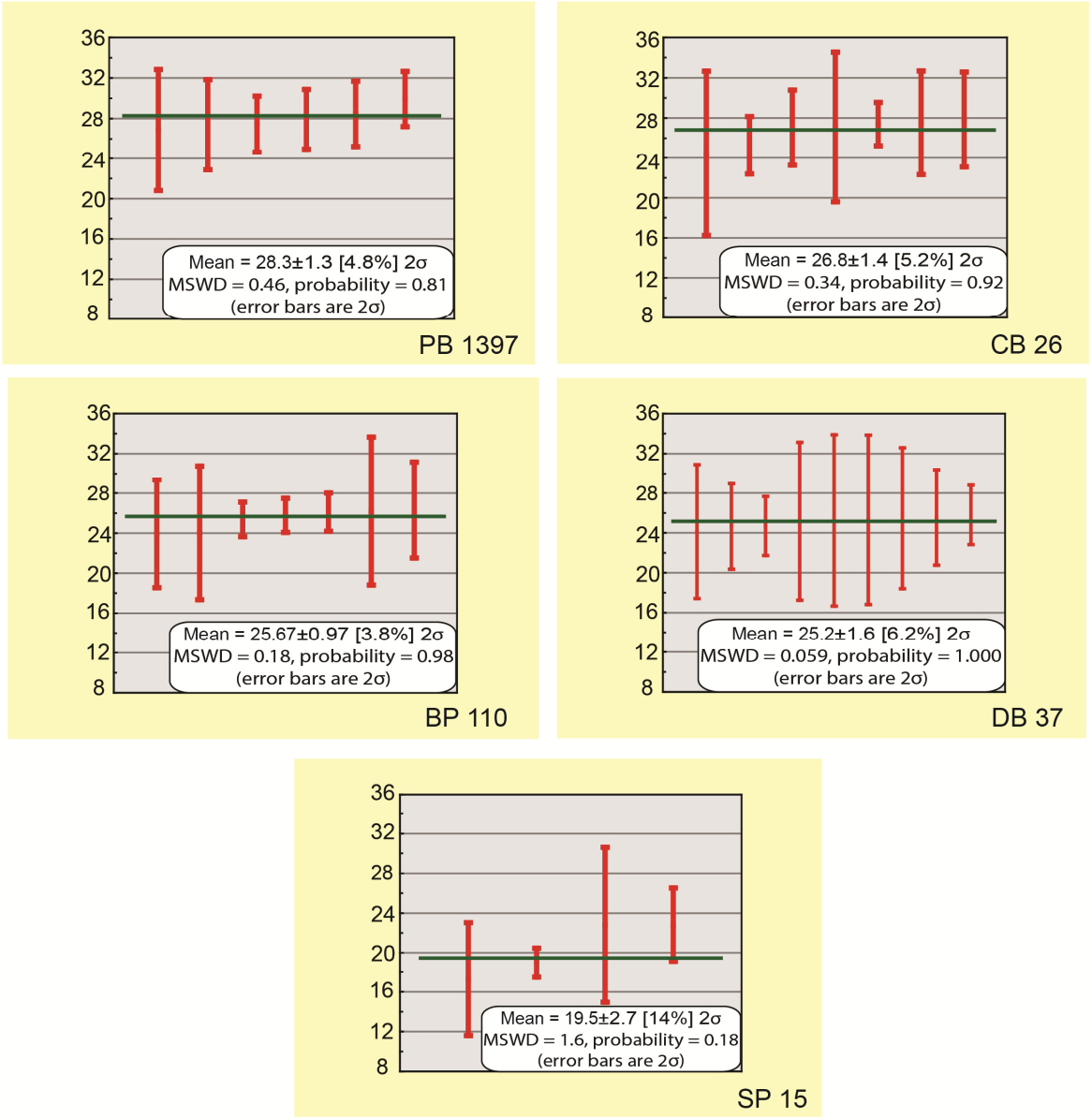

Figure 3.10 Maximum depositional ages of Miocene sandstone samples.

Data-point error symbols are 2σ.

Chapter 4

Discussion and Conclusions

4.1 Sandstone Petrography

The maturity of sandstone is determined by the modal composition (Dickinson and Suczek, 1979). Rounded monocystalline quartz grains with occasional overgrowths are indicative of reworked detrital grains (Folk, 1980; Ingersoll et al. 1987). Quartz grains rimmed by hematite are possibly recycled from the Jurassic and Triassic red beds, which are distributed along the flanks of the Laramide uplifts. These hematite rimmed quartz grains experienced oxidation when the early Mesozoic climate alternated between wet and dry conditions (Robinson, 1973). Polycrystalline quartz grains are derived from metamorphic basement and formed due to grain deformation under tectonic strain and low-grade metamorphism (Folk, 1980). These grains are most likely recycled from the Precambrian cores of the Laramide uplifts. Reworked detrital chert is indicative of older sedimentary sources due to its chemical and mechanical durability (Folk, 1980). Chert grains are likely recycled from Paleozoic carbonate rocks (Love and Christiansen, 1985) and formed by either carbonate replacement or deposition of siliceous pelagic sediment. Plagioclase and potassium feldspars can be recycled from the Precambrian basement, which outcrops in the core of the Laramide uplifts (Love and Christiansen, 1985), or directly sourced and/or recycled from the Eocene-middle Miocene magmatic arc sources in western and southwestern North America (Best and Christiansen, 1991; McIntosh et al., 1992; Cunningham et al., 2007; Ferrari et al., 2007; Lipman, 2007; Best et al., 2013). Fresh volcanic rocks have more plagioclase than plutonic basement (Dickinson, 1985); therefore, the results of low K/P and high Lv/Ls ratios suggest that the distal volcanism is likely a major contributor to sand grains. The Cenozoic ignimbrite flare-up in western and southwestern North America is characterized by rhyolitic eruptions (Best and Christiansen, 1991; Best et al., 2013), which could provide abundant plagioclase and volcanic lithic grains. These Cenozoic volcanic sources include, but are not limited to, the Absaroka and Challis volcanic fields, the Great Basin ignimbrite province, volcanic activities in Colorado, Idaho, Arizona, New Mexico, Utah, and the Sierra Madre Occidental in

western Mexico (Ewing, 1979; Moye et al., 1988; Best and Christiansen, 1991; McIntosh et al., 1992; Cunningham et al., 2007; Ferrari et al., 2007; Lipman, 2007; Best et al., 2013). The clastic sedimentary lithics are of low abundance, which is typically the result of the breakdown of grains by weathering. The presence of clastic sedimentary lithics suggests recycling of the local Mesozoic and lower Cenozoic clastic sedimentary rocks. The occurrence of carbonate lithics suggests recycling of local Paleozoic carbonate. Overall, the Latest Eocene-Miocene eolian sandstone samples in the central Rocky Mountains and western Great Plains have low maturity, suggesting the sources of the framework grains are proximal with significant volcanic arc contribution.

Sandstone modal composition also reflects provenance types, which are governed by tectonics (Dickinson and Suczek, 1979). The Latest Eocene-Miocene sandstone samples show different contributions of recycled orogen, magmatic arc, and continental block sources (Figure 3.2). Recycled orogen and continental block sources in the study area include the Precambrian basement rocks and the Phanerozoic strata distributed on the cores and flanks of the Laramide uplifts (Love and Christiansen, 1985). The magmatic arc source is the ignimbrite activity in western and southwestern North America (Best et al., 2013). Overall, the Cenozoic eolian sandstone samples in the central Rocky Mountains and western Great Plains show a mixed source of recycled Precambrain-early Cenozoic rocks and young volcanic rocks.

The eolian samples were divided into the Miocene group and the Latest Eocene-Oligocene group based on estimated ages. The two groups are of indistinguishable modal composition, suggesting the provenances and their relative contributions did not change for ~30 Ma. However, it is important to note sandstone composition is also subject to the influence of climate, transport mechanisms, and diagenesis (Dickinson et al., 1983). The provenance interpretation can be strengthened by detrital zircon U-Pb geochronology.

4.2 Detrital zircon U-Pb Geochronology

4.2.1 Major populations

Major sources of the eolian sandstone samples include populations B and C, derived predominantly from the Yavapai-Mazatzal and Grenville orogenic belts, and population F, derived from the late Eocene-Miocene ignimbrite activities in western and southwestern North America (Table 3.1; Figure 1.2).

Population B includes three subpopulations (B1-3). Zircons of B1 subpopulation are 1.82-1.59 Ga old and were formed in the Yavapai-Mazatzal orogenic belts, distributed currently in Arizona, New Mexico, Colorado, and northern Mexico (Figure 1.2) (Anderson and Silver, 1981; Condie, 1982; Grambling et al., 1988; Hoffman, 1989; Pedrick et al., 1998; Karlstrom et al., 2004; Nourse et al., 2005; Amato et al., 2008; Daniel et al., 2013; Jones et al., 2013). These basement rocks form the core of the Laramide uplifts south of the Archean-Proterozoic Wyoming shear suture zone (Condie, 1982), particularly in western Colorado and New Mexico (Jones and Thrane, 2012; Daniel et al., 2013; Jones et al., 2013). The Mojave basement rocks exposed in southern California and Arizona are of the same age and could also contribute zircons to B1 (Miller et al., 1992; Barth et al., 2009). Zircons of this subpopulation could be transported into the samples either by direct weathering of the Laramide uplifts south of the Archean-Proterozoic Wyoming shear suture zone or by recycling Paleozoic-lower Cenozoic older sedimentary rocks. Subpopulation B2 (1.56-1.50 Ga) is a minor component and has an ultimate source of the Gawler craton of Australia. Zircons of this subpopulation have been found in a wide range of strata from Alaska to Mexico (Stewart et al., 2001; Nourse et al., 2005; Gleason et al., 2007; Gehrels et al., 2011). Zircons of this age were most likely recycled into the Cenozoic rocks by eroding the Paleozoic-Mesozoic strata. Subpopulation B3 (1.50-1.33 Ga) is likely derived from anorogenic magmatism in south-central Laurentia (Anderson, 1983; Amato et al., 2008). Approximately 70% of Proterozoic magmatism occurred during 1.49-1.41 Ga, with the volume of magmatism decreasing during 1.41-1.34 Ga (Anderson, 1983; Snoke, 1993). Granitic intrusions of this age are generally underlying the Great Plains (Anderson, 1983; Bickford et al., 1986; Hoffman, 1988,

1989; Karlstrom et al., 1997, 2004; Amato et al., 2008) and Sonora (Anderson and Silver, 1981; Nourse et al., 2005), with limited exposure in northern New Mexico (Daniel et al., 2013). Subpopulations B1 and B3 are common in the Mesoproterozoic-lower Tertiary strata in the western United States and northern Mexico (Gehrels and Dickinson, 1995; Gehrels et al., 1995; Gehrels and Stewart, 1998; Stewart et al., 2001; Dickinson and Gehrels, 2003; Dickinson et al., 2009). Sporadic local exposures of magmatism of 1.50-1.33 Ga old are limited to the Laramie Anorthosite Complex (1.44 Ga) and Sherman batholith (1.43 Ga) in southeastern Wyoming (Snoke, 1993). Zircons of subpopulation B3 may be transported into the samples either by direct weathering of the Laramie Anorthosite Complex and Sherman batholith or by recycling from the Mesoproterozoic-lower Tertiary strata. Because many samples were collected from north of the Laramie Anorthosite Complex and Sherman batholith, zircons of subpopulation B3 are mainly recycled from older sedimentary rocks.

Mesoproterozoic Grenvillian grains of 1.33 Ga-948 Ma comprise population C. This population was originally derived from the Grenvillian basement rocks, formed by the Grenville orogeny, and were distributed in a belt along the eastern flank of Laurentia (Dickinson and Gehrels, 2003). Although volumetrically less significant, the Pikes Peak Batholith (1.1 to 1.0 Ga) of Colorado may contribute zircons to this population (Anderson, 1983). Grenville-aged zircons occur in a high abundance in Phanerozoic sedimentary rocks due to high zircon fertility (Moecher and Samson, 2006; Dickinson, 2008). Grenville-aged zircons were mixed into Cenozoic sedimentary rocks by eroding the Paleozoic-lower Cenozoic sedimentary rocks.

Population F of 44-17 Ma includes two subpopulations (F1 and F2). Zircons of population F were formed by the widespread Cenozoic ignimbrite flare-up events in southwestern and western North America. Volcanism began in the northern portion of the Great Basin around 44 Ma and migrated in a southward and eastward direction across Nevada by Miocene time (Best and Christiansen, 1991). Prolific volcanism in multiple caldera sources in western and southwestern North America are potential contributors to the population, including the Great Basin peak volcanism at 31-20 Ma (Best and Christiansen, 1991); the four ignimbrite pulses of

the Mongollon-Datil field in New Mexico at 36.2-34.3 Ma, 32-31.4 Ma, 29.1-27.3 Ma, and 24.3 Ma (McIntosh et al., 1992); the two ignimbrite pulses of the Sierra Madre Occidental in Mexico at 32-28 Ma and 24-20 Ma (Ferrari et al., 2007); the peak volcanism of the southern Rocky Mountain field in Colorado at 29-27 Ma (Lipman, 2007); volcanism of the Marysvale volcanic field in Utah at 32-17 Ma (Cunningham et al., 2007); and volcanism of the Snake River Plain and Yellowstone hotspot during the last ~17 Ma (Tolan et al., 1989). Subpopulation F1 (44-33 Ma) contains zircons primarily derived from high-K andesite, dacite, and rhyolite lavas with minor pyroclastic material and are dominantly derived from the Indian Peak-Caliente and central Nevada caldera complexes of the Great Basin (Best and Christiansen, 1991). Subpopulation F2 (32-17 Ma) was derived from magma with similar composition to F1, but volumes of pyroclastic material were far greater (Best and Christiansen, 1991). Volcanism waned after ~20 Ma (Best and Christiansen, 1991), and only two grains less than 20 Ma occurred in the nine studied samples (Figure 3.7). The zircons of population F were derived from direct ash fall out as well as erosion of latest Eocene-Miocene sedimentary rocks.

4.2.2 Minor populations

Population A (3.31-1.83 Ga) includes three subpopulations (A1-3). Subpopulation A1 includes only Archean-age zircons (3.31-2.57-Ga). The study area overlies the Archean Wyoming craton (Whitmeyer and Karlstrom, 2007), with direct sources exposed as the cores of the major Laramide ranges in Wyoming. Late Archean magmatism (2.95-2.55 Ga) produced a major part of the Wyoming craton (Chamberlain et al., 2003). Archean terranes, including Wyoming, Hearne, Rae and Superior provinces, are exposed in western and central North America (Whitmeyer and Karlstrom, 2007). Subpopulation A2 (2.49-1.92 Ga) was formed by igneous activity in Canada (Hoffman, 1989), since 2.49-1.92 Ga is a period of tectonic quiescence in the United States. Subpopulation A3 (1.91-1.83 Ga) was formed by the Trans-Hudson orogeny, which represents the collision of the Wyoming Archean craton, the Superior province, and the Hearne-Rae province (Whitmeyer and Karlstrom, 2007). Population A is dominated by subpopulation A1 with minor contribution of subpopulations A2 and A3. Population A1 could be mixed into the Cenozoic

eolian sandstone by direct erosion of the Laramide basement-cored uplifts in Wyoming or recycling from the Paleozoic-lower Cenozoic sedimentary rocks. However, A2 and A3 can only be recycled from older sedimentary rocks.

Population D is comprised of zircon grains of 708-222 Ma old, which record the creation of the central and southern Appalachian orogen and Permian-Triassic arc (284-232 Ma). The tectonomagmatic events of the Appalachian orogeny include the Avalonian-Carolinian at 640-580 Ma, Potomac at ~500 Ma, Taconian at 500-430 Ma, Acadian at 400-350 Ma, and Alleghanian at 325-265 Ma (Eriksson et al., 2003). An additional source is the magmatism associated with the Antler-Sonoma orogeny (450-330 Ma) in Nevada and Idaho (Dickinson, 2004). The nine studied samples have four zircon grains older than 245 Ma, which were likely sourced from northern and eastern Mexico arcs (Torres et al., 1999). These zircons are mixed into the studied samples by recycling from the Paleozoic-lower Cenozoic strata.

Population E is comprised of zircons of 218-45 Ma old and are derived from the Cordilleran magmatic arc in broad western North America (Chen and Moore, 1982; Barth and Wooden, 2006). Major episodes of Sierra Nevada magmatism occurred during the Jurassic (200-150 Ma) and Late Cretaceous (120-85 Ma) (Armstrong and Ward, 1993). Two major episodes of Baja Peninsula magmatism occurred during the Early Cretaceous (135-115 Ma) and Late Cretaceous (100-80 Ma) (Kauffman, 1985; Armstrong and Ward, 1993). Southern Californian peak magmatism occurred during the Late Cretaceous (85-70 Ma) (Jacobson et al., 2011). Magmatism in the western United States was very sporadic during ~70-45 Ma, due to the low-angle subduction of the Farallon oceanic plate (Dickinson and Snyder, 1978). The sparse volcanism near the study area includes the Black Hills (69-47 Ma), Sanpoil (53-45 Ma), Challis (51-44 Ma), Absaroka (49-44 Ma), and Rattlesnake Hills (44 Ma). These zircons are mixed into the studied samples by recycling from the Triassic-lower Cenozoic strata.

In summary, zircon populations present in the latest Eocene-Miocene eolian sandstone in the central Rocky Mountains and western Great Plains suggest sediment sources of recycled Precambrian-lower Cenozoic rocks as well as middle-late Cenozoic magmatism in western and

southwestern North America. The distal and local provenances represented by the zircon populations are consistent with the interpretation of the sandstone petrography results. The recycled Precambrian-lower Cenozoic source is most likely the local Laramide uplifts. However, wind deflation of older rocks in other localities in North America cannot be ruled out.

4.2.3 Comparison between Latest Eocene-Oligocene and Miocene sandstone

K-S test results of the different populations of the Latest Eocene-Oligocene samples and Miocene samples show that populations D-F have p values <0.05, but populations C-A have p values >0.05, with a p value of population C as high as 0.97. The results suggest that the zircon populations >948 Ma are likely of similar proportional contribution to the Latest Eocene-Oligocene and Miocene samples, but zircon populations <708 Ma are of different proportional contribution. The major difference of populations D and E is the Miocene samples have proportionally more early Mesozoic grains, which may suggest early Mesozoic clastic rocks became a larger contributor to the provenance of zircons during the Miocene. The major difference of population F is the Miocene samples have more grains in the range of 32-26 Ma, which is most likely caused by the increased intensity of magmatism. This is a period when peak volcanism in the Great Basin, Sierra Madre Occidental, and southern Rocky Mountain, Mongollon-Datil and Marysvale fields was concurrent (Best and Christiansen, 1991; McIntosh et al., 1992; Cunningham et al., 2007; Ferrari et al., 2007; Lipman, 2007). Population F is predominately of Oligocene age (Figure 3.7), which is older than the depositional ages of the Miocene samples. The higher abundance of population F during Miocene time may suggest large volumes of loose sediment available for wind erosion and transport.

The abundance of Archean zircons in the Latest Eocene-Oligocene samples is higher than the Miocene samples (Figure 3.6), which can be explained by the reduced Archean basement exposure during the Miocene. The other possibility is that the high abundance of population F in the Miocene samples may dilute the Archean population. However, the abundance of A1 relative to populations A-D, not including population F, is 18% in Latest Eocene-Oligocene samples and 7% in the Miocene samples. This suggests that the high abundance of

population F is not the reason for lower abundance of Archean zircons. The smaller exposure of the Archean basement during the Miocene is the result of widespread eolian deposition, which largely covered the Laramide uplifts. A similar scenario is proposed by Evanoff et al., (1992). This is additionally supported by the preservation of Miocene eolian deposition on the top of the Bighorn Mountains (McKenna and Love, 1972) and Granite Mountains (Love, 1961).

4.2.4 Maximum depositional age and timing of fluvial-eolian transition

The maximum depositional ages of most samples are at most 1-2 Ma older than the available radiometric age dates. This is expected because volcanic eruptions produce broad coverage on the landscape, and loose ash can be easily eroded, transported, and deposited by wind processes. Late Miocene sample CB 26 has a maximum depositional age of ~27 Ma, which is ~17 Ma older than the ash layers stratigraphically below and above the sample (Scott, 2002). This is particularly intriguing because the slightly older sample, SP 15, contains syndepositional zircons of ~17 Ma and 19 Ma old. This may be caused by the cessation of the ignimbrite flare-up at 17 Ma (Best and Christiansen, 1991).

The four samples (WS121.5, LTG 171, EF 15-60, LG 6-29) that represent the regional transition from fluvial sedimentation to eolian sedimentation have maximum depositional ages of latest Eocene-early Oligocene, which is consistent with the compiled NALMA ages, radiometric ages and ages constrained by magnetostratigraphy. The transition also shows an eastward younging trend, consistent to the proposed eastward transition to dryland in the western United States by Evanoff et al. (1992).

4.3 Significance for Tectonics, Paleoclimate, and Paleogeography

For eolian sediment to be deposited and accumulated, three factors must be met including a source for sediment generation, wind regime and energy for sediment transport, and location for sediment accumulation (Tsoar and Pye, 1987). Accumulation of eolian deposition requires large amounts of easily erodible source material. Eolian deposition, which was extensive in Asia, North America, South America, Europe, and New Zealand during the last 2 Ma, is often tied to glacial periods when the climate is cold and dry with loose glacial till or desert available

upwind (e.g. An et al., 1990; Muhs et al., 1999a, b; Muhs and Bettis, 2003; Roberts et al., 2003; Aleinikoff et al., 2008). There is no documented desert or glaciation in the Northern Hemisphere during the latest Eocene-Oligocene; therefore, other loose sediment sources have to be considered. Direct wind deflation of Precambrian basement and lithified Paleozoic-Mesozoic strata is a potential way to produce loose sediment. However, this mechanism requires strong wind energy and often forms eolian erosion remnant landscapes. A typical example is the dry and strong Asian Winter Monsoon from Siberia, which caused significant erosion in northwestern China and resulted in Yardang landscapes (e.g. Kapp et al., 2011). Because similar landscapes are not documented in the western U.S.A., it is suggested here that the loose sediment source of the recycled grains >45 Ma is dominantly the late Eocene fluvial sedimentary fills in the Laramide intermontane basins. These rocks were not lithified during the early stage of eolian deposition and could be easily deflated and transported by wind. Wind deflation of loose riverbank sediment provides a major source for wind transport and eolian sedimentation (Muhs et al., 2003). This interpretation is additionally supported by the large, deep valleys that cut several Laramide uplifts, including the Wind River Range and the Laramie Range, during the late Eocene (Steidtmann et al., 1989; Evanoff, 1990b; Steidtmann and Middleton, 1991; Evanoff and Chapin, 1994).

Eolian deposition is inherently tied to climate change and can initiate as a result of global cooling or regional drying or a combination of these effects (e.g., Liu et al., 2009; Sun et al., 2010). Cather et al. (2008) documented eolian deposition in northern New Mexico as old as 33.5 Ma and suggested the initiation of eolian deposition on the Colorado Plateau and the central Rockies was caused by the global cooling event of Oi-1 due to glaciation in Antarctica (Zachos et al., 2001b). The maximum depositional ages of the four samples that represent the regional depositional environment transition, as well as the compiled NALMA and radiometric ages, show the transition is diachronous rather than regionally synchronous. Global cooling as the sole cause for eolian deposition initiation would result in a regionally synchronous transition thus is not well supported by the data. A possible mechanism of regional drying is the rainshadow effect caused by the renewed uplift of the central Rockies as well as the broad uplift in the Cordillera hinterland.

Mix et al., (2011) suggested that the Cordillera hinterland experienced southward uplift up to 3.4 km during the middle Eocene-Oligocene, possibly induced by deep mantle processes. The highland in western North America could have blocked the moisture from the Pacific Ocean and caused leeward drying. This may explain the transition in western Wyoming starting as early as Latest Eocene. However, in eastern Wyoming and Nebraska, moisture should be mainly contributed from the Gulf of Mexico, and the blocking of moisture from the Pacific Ocean should have a very small impact. It is suggested here that the uplift of the central Rockies expelled the reach of the Gulf moisture southeastward and gradually caused drying and an eastward younging trend of the transition to eolian deposition. Renewed uplift of the central Rockies may have occurred in Wyoming during the late middle Eocene associated with both the lack of Duchesnean age strata in Wyoming and the exhumation episode of 42-37 Ma in the southern Rockies (Cather et al., 2012). Uplift in the western Great Plains may have lasted into the Latest Eocene, supported by the White River Group resting unconformably on the Cretaceous Pierre Shale in western Nebraska (Swinehart and Diffendal, 1987; LaGarry, 1998; Terry, 1998). Cather et al (2012) attributed this uplift to the foundering of the subducted Farallon oceanic slab, a mechanism that caused additional uplift of the Colorado Plateau during the Eocene (Liu and Gurnis, 2010). The regional aridification caused by the uplift of the Rockies is also documented by low reconstructed mean precipitation amount in Montana and western Nebraska (Sheldon and Retallack, 2004; Retallack, 2007; Sheldon, 2009).

Transport of the loose Eocene-Oligocene fluvial deposits flanking the Laramide uplifts as well as pyroclastic sediment mantling the broad western U.S.A. may not require a strong wind regime. In Asia, the Siberia pressure high is strengthened during the winter time and glacial period, causing a strong Asian Winter Monsoon (Gong et al., 2001; Wu and Wang, 2002). The southeastward transport direction of the eolian dust is indicative of the wind regime (Zhisheng et al., 2001). In the central Rockies, the only documented large-scale trough cross stratification, caused by eolian transport, is in northwest Colorado, which shows northeastward wind flow direction (Honey and Izett, 1988; Buffler, 2003). Because the study period is earlier than the

establishment of Northern Hemisphere glaciation (Zachos et al., 2001a), dry polar airflow might not be established during this time. The short distance of wind transportation likely does not require a strong wind regime. The dry upper troposphere westerlies and near-ground southwestern Summer Monsoon are the wind flow that transported pyroclastic and local fluvial deposits to form the eolian sandstone. It is also possible that the latest Eocene-Oligocene loose sediments were eroded and redeposited by wind during Miocene time.

The interpretation of the sediment provenance and inferred tectonics, paleoclimate, and wind regime help to reconstruct the paleogeography (Figure 4.1). During the Latest Eocene-early Oligocene, uplift of the Cordillera hinterland and central Rockies expelled the reach of moisture from the Pacific Ocean and Gulf of Mexico, causing local aridification in the Rockies. Widespread volcanism in western and southwestern North America and large valleys draining the local Laramide highlands produced abundant loose material for wind transport. Dry westerlies and near-ground monsoonal wind reworked these loose materials and formed massive eolian sandstone in the Rocky Mountains and the western Great Plains. Although large fluvial valleys of Miocene age are not documented, the basal Arikaree Conglomerate was deposited in a fluvial depositional environment (Hoganson et al., 1998) and is widely distributed in Wyoming and western Nebraska, possibly providing loose sediment to Miocene deposition. The Oligocene eolian sedimentation may also be eroded and reworked by wind processes during the Miocene time. This is supported by the poor preservation of Oligocene eolian sedimentation in the Rockies, the high abundance of zircon grains <45 Ma preserved in the Miocene sandstone, and less prevalent volcanism after ~24 Ma.

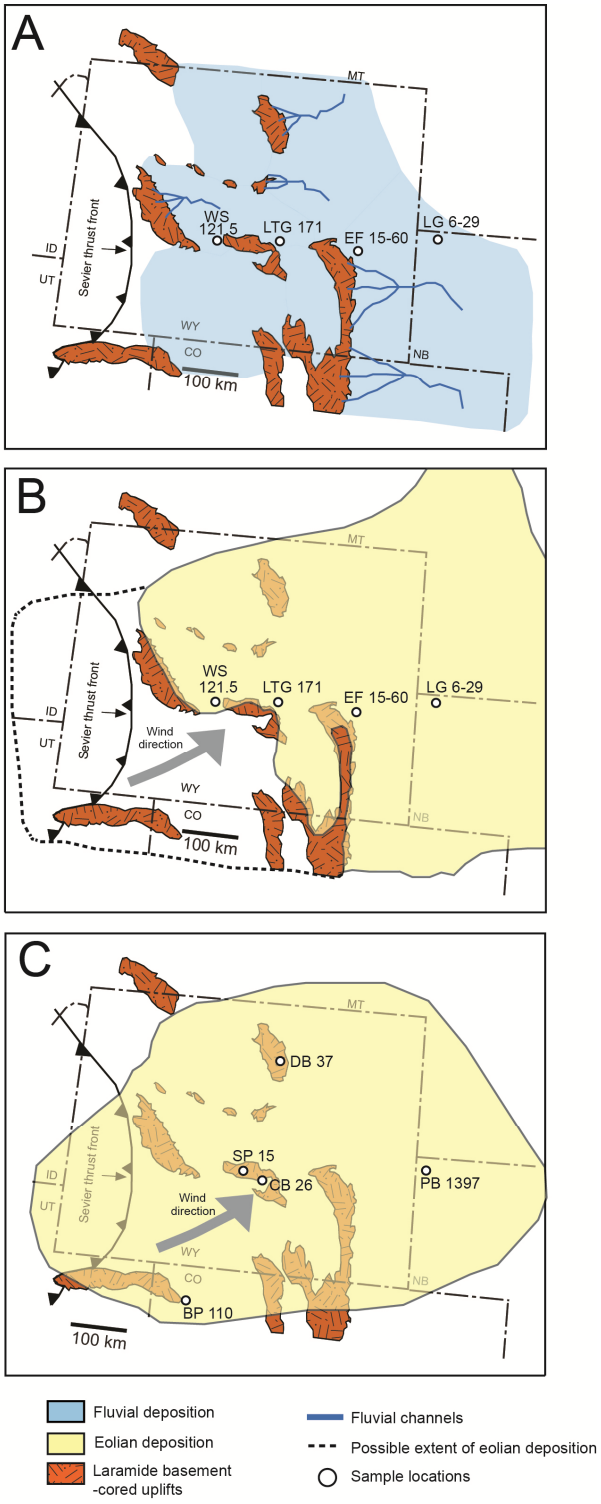

Figure 4.1 Paleogeographic interpretation of late Eocene through early Miocene.

A. Late Eocene B. Oligocene C. Early Miocene, figures are modified from Galloway et al., 2011.

4.4 Conclusion

Sandstone petrography and detrital zircon U-Pb geochronology of nine Latest Eocene-Miocene eolian sandstones of the central Rocky Mountains and adjacent Great Plains are studied to constrain the timing of a regional transition to eolian deposition and the provenance of the eolian sandstone. A total of 766 detrital zircon ages show populations of 17-44 Ma, 45-218 Ma, 220-708 Ma, 948-1326 Ma, 1332-1816 Ma, and 1825-3314 Ma. The youngest population (17-44 Ma) was derived from volcanism of the distal ignimbrite flare-up in western and southwestern North America. The populations older than 45 Ma were derived from the local Precambrian basement-cored Laramide uplifts and Paleozoic-lower Cenozoic strata distributed along the flanks of the uplifts. These older zircon populations were eroded and transported by fluvial processes during the Late Eocene. The loose fluvial deposits were then transported and deposited by wind processes. Sandstone petrography samples have average modal compositions of $Qm_{44}F_{26}Lt_{30}$ $Qt_{46}F_{26}L_{28}$, $Qm_{64}P_{29}K_{7}$, (Latest Eocene-Oligocene) and $Qm_{44}F_{27}Lt_{26}$, $Qt_{48}F_{27}L_{25}$, $Qm_{64}P_{27}K_{9}$ (Miocene), which suggests sand grains were derived from distal volcanism as well as local recycled Laramide uplifts. Distal ash from the ignimbrite flare-up and local reworked sediment may be transported northeastward by both the dry westerlies and summer monsoon winds.

Maximum depositional ages of the four samples collected at the eolian transition suggest the onset of the eolian deposition has an eastward younging trend, beginning in central Wyoming at ~37 Ma. This time-transgressive transition suggests the uplift of the Cordillera hinterland and renewed uplift of the central Rockies developed a rainshadow in the study area. This transition occurred during the early Oligocene global cooling caused by Antarctic glaciation. Uplift and global cooling resulted in regional drying and initiation of eolian deposition.

During the latest Eocene-early Oligocene, sediment was sourced from large paleovalleys that drained the local Laramide highlands as well as the widespread volcanism in western and southwestern North America. Winds reworked the abundant loose sediment to form the massive eolian sandstone of Wyoming, northern Colorado and western Nebraska. Eolian deposition lasted

into the Miocene, with Miocene samples having less abundant Archean zircons than the Latest Eocene-Oligocene samples. This difference in abundance suggests wind activity may have nearly covered the basement cores in the Laramide uplifts and reduced the contribution of Archean zircons during the Miocene. Miocene eolian sediment was potentially derived from fluvial depositional environments, supported by the widely distributed Arikaree Conglomerate, as well as reworked Oligocene eolian sedimentation, supported by the poor preservation of the Oligocene deposits and the abundance of Oligocene age zircon grains in the Miocene samples. This study of the Latest Eocene-Miocene eolian sandstones of the central Rocky Mountains and adjacent Great Plains improved our understanding of provenance of sediment and Late Cenozoic landscape evolution. Improved age constraints and relative proportions of zircon populations have implications for uplift and paleoclimatic changes, which influence the depositional environment.

Appendix A

Sandstone petrography modal petrographic data

Sample	Qm(%)	Qp(%)	C(%)	Lsh(%)	Lc(%)	K(%)	P(%)	Lvv(%)	Lvi(%)	Lm(%)	O(%)*
WS 208	38.5	0.0	5.0	0.8	0.5	6.0	26.3	11.8	7.8	0.0	3.5
LTG 740	45.0	1.0	4.0	0.8	0.0	9.0	13.0	10.5	13.0	0.0	3.8
EF 15-90	47.0	1.3	3.3	0.0	0.0	7.3	17.3	13.3	7.3	0.0	3.5
LG 6-20	50.8	1.3	3.5	2.3	0.8	10.0	28.5	0.0	1.3	0.0	1.8
LG 6-34	46.3	0.5	5.0	1.5	0.3	1.0	15.0	20.3	7.8	0.0	2.5
PB 4636	39.8	1.5	3.8	0.8	0.8	3.8	15.5	7.5	21.5	0.0	5.3
CB R4	48.5	0.5	4.0	1.5	0.3	7.8	25.3	7.0	2.8	0.3	2.3
BP 65	44.5	3.0	10.5	0.0	1.0	2.5	26.8	0.0	9.5	0.3	2.0
DB 16	35.8	2.5	4.3	1.8	0.5	3.3	12.5	22.8	12.3	0.0	4.5
SP 20	46.8	1.8	6.0	0.3	0.3	7.0	19.8	5.5	10.5	0.0	2.3

Appendix B

Detrital zircon U-Pb geochronology raw data

U (ppm)		206 Pb/ 204 Pb					Isotopic Ratios				Apparent ages (Ma)		
		207 Pb*/ 235 U	I+/- (%)	206 Pb*/238 U	I +/- (%)	Error Corr.	206 Pb*/238 U	I +/- (Ma)	207 Pb*/ 235 U	I +/- (Ma)	206 Pb*/207 Pb*	I +/- (Ma)	Discordance
WS 121.5													
143	188008	10.3597	1.8	0.4687	1.7	0.97	2477.7	35.6	2467.5	16.5	2459.0	7.0	1.01
282	31562	0.5677	4.7	0.0730	1.1	0.22	454.5	4.6	456.6	17.2	467.1	101.0	0.97
564	5404	0.0401	34.8	0.0071	7.3	0.21	45.3	3.3	39.9	13.6	-276.9	887.0	-0.16
266	94932	5.6659	1.8	0.3523	1.7	0.94	1945.6	28.9	1926.2	15.8	1905.4	11.5	1.02
1710	13176	0.0360	13.8	0.0056	3.5	0.25	36.2	1.3	35.9	4.9	19.5	322.2	1.86
434	44871	4.2702	2.9	0.2933	2.9	0.98	1658.1	41.7	1687.6	23.8	1724.5	9.2	0.96
203	122047	1.8289	2.3	0.1780	1.3	0.56	1055.9	12.5	1055.9	14.9	1056.0	37.8	1.00
476	10138	3.8159	3.3	0.2628	2.6	0.77	1504.4	34.4	1596.1	26.9	1719.4	39.4	0.87
780	254450	3.6102	3.3	0.2671	3.0	0.91	1526.3	41.1	1551.8	26.4	1586.6	25.7	0.96
143	32875	2.3020	2.5	0.2090	1.8	0.74	1223.4	20.4	1212.9	17.6	1194.2	33.0	1.02
533	13909	14.5402	0.9	0.5340	0.9	0.95	2758.5	19.3	2785.6	8.5	2805.4	4.4	0.98
463	9470	0.0394	36.7	0.0077	6.4	0.17	49.1	3.1	39.2	14.1	-532.5	995.4	-0.09
606	32202	9.2697	10.2	0.4160	8.3	0.82	2242.4	158.0	2365.0	93.4	2472.4	98.1	0.91
1040	10153	0.0445	21.1	0.0074	2.6	0.12	47.2	1.2	44.3	9.2	-113.6	521.5	-0.42
113	33931	1.7544	3.4	0.1737	1.7	0.48	1032.5	15.8	1028.8	22.2	1020.8	60.8	1.01
157	38196	1.8072	2.7	0.1785	1.0	0.37	1058.7	9.6	1048.1	17.4	1025.9	50.1	1.03
111	72586	4.1019	2.0	0.2922	0.7	0.35	1652.7	10.2	1654.7	16.3	1657.1	34.6	1.00
48	15432	2.0471	9.6	0.1942	7.2	0.74	1144.1	75.0	1131.3	65.6	1106.9	128.3	1.03
120	8859	0.7044	41.6	0.0783	7.0	0.17	485.7	33.0	541.4	176.3	783.5	898.5	0.62
157	166543	12.2702	1.5	0.5066	1.5	0.95	2642.1	31.8	2625.3	14.5	2612.3	7.9	1.01
370	8588	0.0725	24.5	0.0149	9.2	0.37	95.0	8.6	71.1	16.8	-674.9	634.5	-0.14
645	7256	0.0548	27.6	0.0090	3.0	0.11	57.5	1.7	54.2	14.6	-89.4	683.3	-0.64
465	36546	12.3060	1.6	0.5028	1.6	0.99	2625.7	34.5	2628.0	15.3	2629.8	4.6	1.00
421	11407	0.0893	20.7	0.0146	3.0	0.15	93.2	2.8	86.9	17.2	-83.0	505.1	-1.12
72	21458	4.8362	3.8	0.3244	2.7	0.72	1811.4	42.9	1791.2	31.8	1767.8	48.0	1.02
131	23277	0.4978	17.7	0.0691	1.5	0.09	430.5	6.4	410.2	59.9	297.7	405.8	1.45

352	25424	0.5746	4.5	0.0760	2.1	0.48	472.1	9.7	461.0	16.5	406.1	87.6	1.16
433	195590	4.3884	5.4	0.2944	5.3	0.99	1663.5	77.9	1710.2	44.6	1767.8	16.3	0.94
2349	14540	0.0338	10.1	0.0057	2.4	0.24	36.3	0.9	33.7	3.3	-149.0	242.6	-0.24
533	7488	0.0424	32.5	0.0074	4.9	0.15	47.7	2.3	42.2	13.4	-260.9	833.2	-0.18
513	245917	3.4059	0.9	0.2642	0.8	0.88	1511.1	11.1	1505.7	7.4	1498.2	8.6	1.01
362	5934	0.0367	46.0	0.0068	6.8	0.15	43.5	3.0	36.6	16.6	-389.9	1240.8	-0.11
944	11969	0.0406	22.8	0.0071	8.1	0.35	45.3	3.6	40.4	9.0	-246.2	542.9	-0.18
249	39786	1.8073	1.6	0.1783	1.0	0.61	1057.7	9.5	1048.1	10.5	1028.1	25.8	1.03
306	45313	0.9032	2.0	0.1076	0.5	0.27	658.9	3.4	653.4	9.8	634.4	42.1	1.04
482	14530	4.0025	1.1	0.2871	1.1	0.93	1626.9	15.3	1634.7	9.3	1644.7	7.8	0.99
350	89781	3.2643	1.5	0.2620	1.3	0.85	1500.0	17.4	1472.6	11.9	1433.3	15.6	1.05
169	96551	12.5169	0.8	0.5129	0.7	0.86	2669.1	15.1	2644.0	7.5	2624.9	6.7	1.02
277	4326	2.9445	3.9	0.2307	3.7	0.94	1337.9	44.9	1393.4	29.9	1479.5	25.0	0.90
424	133188	3.5526	1.7	0.2608	1.5	0.89	1493.9	19.8	1539.0	13.2	1601.5	14.1	0.93
885	166420	4.0097	1.6	0.2840	1.6	0.99	1611.3	23.0	1636.2	13.3	1668.3	4.9	0.97
981	15450	0.0442	11.9	0.0074	4.2	0.35	47.2	2.0	43.9	5.1	-132.2	276.3	-0.36
842	4660	3.8309	5.4	0.2540	5.4	0.99	1459.1	70.2	1599.3	43.8	1789.2	14.9	0.82
167	5185	0.2491	362.6	0.0117	9.9	0.03	75.2	7.4	225.8	928.0	2389.7	425.5	0.03
4164	33562	0.0358	5.5	0.0056	0.9	0.16	35.9	0.3	35.8	1.9	26.7	130.9	1.35
331	117056	4.8597	2.4	0.3228	2.3	0.98	1803.6	36.4	1795.3	19.9	1785.6	8.9	1.01
3786	43892	0.0453	4.1	0.0070	1.4	0.34	44.8	0.6	45.0	1.8	56.2	91.3	0.80
1029	63810	13.5170	6.0	0.5177	6.0	1.00	2689.5	131.6	2716.5	56.7	2736.6	6.0	0.98
107	79305	14.1706	1.6	0.5376	1.3	0.84	2773.2	29.4	2761.2	14.8	2752.4	14.1	1.01
1114	11215	0.0371	18.0	0.0055	2.4	0.13	35.7	0.8	37.0	6.5	123.6	423.5	0.29
1249	30815	0.0990	5.0	0.0150	2.0	0.40	96.0	1.9	95.8	4.6	91.6	108.2	1.05
546	6415	0.0422	39.6	0.0057	5.1	0.13	36.8	1.9	41.9	16.3	344.6	921.0	0.11
86	12668	2.1334	4.4	0.1949	1.4	0.33	1148.0	15.0	1159.7	30.1	1181.7	81.4	0.97
62	19514	3.4470	3.2	0.2608	1.8	0.55	1493.7	23.8	1515.2	25.5	1545.3	50.7	0.97
86	57086	14.5905	2.2	0.5421	1.9	0.88	2792.1	43.6	2788.9	20.7	2786.6	16.8	1.00
345	3463	0.0259	58.7	0.0066	8.0	0.14	42.2	3.3	25.9	15.0	NA	NA	#VALUE!
339	20554	12.7004	1.1	0.5142	1.1	0.97	2674.5	23.6	2657.7	10.5	2644.9	4.6	1.01
330	198966	16.8955	3.7	0.5692	3.6	0.99	2904.5	84.8	2928.9	35.3	2945.8	10.2	0.99
82	67639	13.9844	1.9	0.5404	1.5	0.81	2785.2	34.4	2748.7	17.7	2721.9	18.0	1.02

448	9520	0.0724	19.7	0.0146	3.8	0.19	93.4	3.5	71.0	13.5	-634.1	532.9	-0.15
690	8158	0.0406	33.6	0.0075	3.4	0.10	48.4	1.7	40.4	13.3	-411.9	894.9	-0.12
283	63760	12.6196	1.3	0.5094	1.3	0.94	2653.9	27.6	2651.7	12.6	2650.0	7.3	1.00
1174	11951	0.0461	14.8	0.0071	3.8	0.26	45.7	1.8	45.8	6.6	48.8	341.9	0.94
195	28691	0.8640	5.4	0.1026	2.3	0.43	629.6	14.0	632.3	25.4	641.9	104.5	0.98
195	46627	1.7740	4.5	0.1725	2.7	0.59	1026.0	25.5	1036.0	29.5	1057.2	73.7	0.97
390	130529	4.0270	0.9	0.2893	0.8	0.86	1638.0	11.4	1639.7	7.4	1641.8	8.6	1.00
829	35155	0.0759	12.8	0.0115	4.9	0.38	73.7	3.6	74.3	9.2	92.9	280.5	0.79
32	20978	2.7021	8.8	0.2316	2.6	0.30	1342.8	32.0	1329.0	65.5	1306.9	163.9	1.03
277	107957	2.0939	2.0	0.1970	0.6	0.29	1159.1	6.1	1146.8	13.9	1123.7	38.6	1.03
LG 6-29													
109	1114	0.0452	97.5	0.0045	14.9	0.15	28.7	4.3	44.9	42.9	1025.8	#####	#VALUE!
378	6581	0.0242	40.8	0.0046	2.1	0.05	29.4	0.6	24.3	9.8	-458.2	1114.0	#VALUE!
452	10887	0.0315	16.9	0.0047	3.6	0.22	30.5	1.1	31.5	5.2	108.1	392.3	#VALUE!
501	10147	0.0334	13.8	0.0048	6.2	0.45	30.8	1.9	33.4	4.5	219.1	285.8	#VALUE!
325	5195	0.0345	17.7	0.0048	4.5	0.26	30.9	1.4	34.4	6	288.2	394.5	#VALUE!
445	7818	0.0314	10.6	0.0049	4.4	0.41	31.2	1.4	31.4	3.3	46.6	232.1	#VALUE!
1535	27481	0.0308	8.6	0.0049	1.1	0.13	31.7	0.3	30.8	2.6	-34.3	207.3	#VALUE!
294	3858	0.0312	24.8	0.0049	3.8	0.15	31.8	1.2	31.2	7.6	-18.3	599.3	#VALUE!
204	2867	0.0228	43.7	0.0051	6.4	0.15	33.1	2.1	22.9	9.9	-956.6	1318.1	#VALUE!
256	3169	0.0446	26.1	0.0052	7.2	0.27	33.3	2.4	44.3	11.3	693.3	543.8	#VALUE!
322	3770	0.0323	22.6	0.0053	9.6	0.43	34.4	3.3	32.3	7.2	-120.8	508.2	#VALUE!
131	1476	0.0337	46.6	0.0054	14.8	0.32	34.4	5.1	33.7	15.4	-16.8	1117.2	#VALUE!
461	8240	0.0364	30.7	0.0054	3.7	0.12	34.5	1.3	36.3	11	157.9	728.4	#VALUE!
356	5174	0.031	23.2	0.0055	4.5	0.19	35.2	1.6	31	7.1	-278	584.4	#VALUE!
314	6620	0.0374	17.7	0.0071	3.3	0.19	45.8	1.5	37.3	6.5	-479.3	463.3	#VALUE!
2607	69549	0.0478	4.1	0.0072	0.9	0.23	46.6	0.4	47.4	1.9	90.7	95.5	#VALUE!
867	22148	0.0638	6.1	0.0099	1.6	0.27	63.5	1	62.8	3.7	37.7	140.7	#VALUE!
50	1502	0.2048	273.3	0.0115	14.6	0.05	73.7	10.7	189.1	510.8	2086.0	369.4	#VALUE!
465	13214	0.0817	12.7	0.0126	1.5	0.12	80.9	1.2	79.7	9.8	43.8	302.8	#VALUE!
868	67121	0.0938	4.0	0.0145	2.4	0.60	93.0	2.2	91.1	3.5	40.4	76.4	#VALUE!

400	17222	0.0948	12.4	0.0151	2.7	0.22	96.9	2.6	92.0	10.9	-33.6	294.8	#VALUE!
180	16785	0.1857	7.5	0.0267	2.5	0.34	170.0	4.3	173.0	12.0	213.2	164.7	#VALUE!
1348	64117	0.2397	1.4	0.0344	1.1	0.78	218.1	2.4	218.2	2.8	219.1	20.9	#VALUE!
718	132818	0.3999	1.2	0.0549	0.9	0.75	344.3	3.0	341.5	3.5	323.2	17.9	#VALUE!
235	35633	0.4857	2.3	0.0644	1.0	0.45	402.5	4.0	402.0	7.6	399.1	45.7	1.01
227	44301	0.4826	3.4	0.0647	2.1	0.63	403.8	8.2	399.8	11.1	376.6	58.8	1.07
727	36737	0.4980	1.9	0.0654	1.7	0.90	408.3	6.8	410.4	6.4	422.0	18.1	0.97
179	3064	0.5295	4.2	0.0655	1.1	0.27	408.8	4.5	431.5	14.9	554.3	89.1	0.74
122	3433	0.7273	6.2	0.0881	2.0	0.32	544.3	10.3	554.9	26.3	598.7	126.4	0.91
509	371850	1.0074	0.9	0.1161	0.7	0.72	708.1	4.4	707.5	4.7	705.8	13.5	1.00
72	93540	1.7131	3.2	0.1713	1.0	0.33	1019.4	9.7	1013.4	20.3	1000.6	60.9	1.02
111	46747	1.8154	2.3	0.1788	1.4	0.61	1060.3	13.7	1051.0	14.9	1031.9	36.4	1.03
412	234168	1.7968	1.1	0.1768	0.9	0.85	1049.4	8.8	1044.3	7.0	1033.7	11.5	1.02
59	23771	1.8875	2.7	0.1841	0.9	0.32	1089.5	8.6	1076.7	18.0	1051.0	51.9	1.04
151	18596	1.8240	2.3	0.1771	1.9	0.82	1050.9	18.2	1054.1	15.1	1060.9	26.8	0.99
72	48524	1.9742	1.3	0.1872	1.1	0.79	1106.4	10.7	1106.8	9.0	1107.5	16.4	1.00
70	74009	2.0048	2.3	0.1899	1.8	0.79	1120.8	18.6	1117.1	15.4	1110.0	27.7	1.01
82	31822	2.0560	2.2	0.1924	1.2	0.53	1134.6	12.2	1134.3	15.2	1133.7	37.6	1.00
127	94729	2.0850	1.4	0.1942	1.1	0.77	1144.4	11.3	1143.9	9.6	1143.0	17.9	1.00
62	51701	2.0663	2.1	0.1918	1.2	0.60	1131.3	12.8	1137.7	14.2	1150.0	33.0	0.98
298	22595	2.2387	1.2	0.2027	1.0	0.79	1190.0	10.5	1193.3	8.6	1199.2	14.6	0.99
44	27591	2.3016	3.7	0.2067	1.7	0.46	1211.3	18.8	1212.8	26.0	1215.5	63.9	1.00
83	64832	2.3012	1.7	0.2056	1.3	0.79	1205.5	14.8	1212.7	12.1	1225.3	20.6	0.98
217	252616	2.7210	1.7	0.2311	1.5	0.93	1340.1	18.7	1334.2	12.3	1324.8	11.5	1.01
99	73218	2.9329	2.0	0.2424	1.6	0.77	1399.2	19.7	1390.4	15.5	1377.0	25.3	1.02
251	210230	3.0019	0.8	0.2454	0.8	0.92	1414.8	9.6	1408.1	6.2	1398.1	6.0	1.01
174	84090	2.9751	2.2	0.2387	2.1	0.96	1379.7	26.0	1401.3	16.5	1434.2	11.6	0.96
194	109277	3.1122	2.2	0.2493	2.2	0.97	1434.8	28.1	1435.7	17.3	1437.1	10.2	1.00
231	89184	2.8794	2.4	0.2303	2.3	0.97	1335.8	27.8	1376.5	17.9	1440.2	11.0	0.93
103	88755	3.1877	1.6	0.2546	1.2	0.73	1462.3	15.2	1454.2	12.3	1442.3	20.8	1.01
234	259364	3.1483	1.2	0.2511	1.1	0.96	1444.4	14.3	1444.6	8.9	1444.9	6.1	1.00
73	48904	3.1125	1.8	0.2479	0.7	0.41	1427.4	9.2	1435.8	13.5	1448.2	30.6	0.99
260	224194	3.1685	1.8	0.2523	1.7	0.94	1450.3	21.5	1449.5	13.7	1448.3	11.9	1.00

250	13945	3.1647	4.0	0.2517	3.8	0.94	1447.1	49.0	1448.6	31.0	1450.7	25.8	1.00
121	136843	3.1721	1.2	0.2521	0.9	0.75	1449.3	11.4	1450.4	9.0	1452.0	14.7	1.00
54	22671	3.1606	1.6	0.2512	1.4	0.85	1444.4	17.8	1447.6	12.6	1452.2	16.5	0.99
236	136387	3.1822	1.3	0.2523	1.0	0.74	1450.2	12.7	1452.9	10.3	1456.7	17.1	1.00
62	47466	3.1051	2.5	0.2430	1.6	0.64	1402.1	20.0	1434.0	19.1	1481.5	36.2	0.95
78	98360	3.3477	3.2	0.2600	2.7	0.84	1489.6	36.3	1492.3	25.3	1496.0	32.8	1.00
41	38059	4.0751	1.8	0.2969	1.1	0.59	1675.8	16.0	1649.3	15.0	1615.7	27.8	1.04
865	601861	3.9881	2.9	0.2860	2.9	1.00	1621.6	40.9	1631.8	23.2	1644.9	2.8	0.99
77	68588	4.0924	1.1	0.2923	0.7	0.64	1653.3	10.3	1652.8	8.9	1652.2	15.5	1.00
848	659431	3.6888	2.1	0.2614	2.1	0.99	1496.8	28.1	1568.9	17.0	1667.4	5.9	0.90
72	130559	4.3177	1.8	0.3031	1.3	0.69	1706.4	18.9	1696.7	15.1	1684.8	24.4	1.01
476	370015	4.1855	1.5	0.2935	1.5	0.99	1659.0	22.3	1671.2	12.6	1686.5	3.5	0.98
252	77101	4.3707	2.2	0.3062	2.1	0.99	1721.9	32.3	1706.8	17.8	1688.3	5.4	1.02
157	98788	4.2602	1.2	0.2979	1.1	0.92	1680.7	15.7	1685.7	9.5	1691.9	8.6	0.99
221	272641	4.2802	1.5	0.2993	1.5	0.98	1687.6	21.6	1689.6	12.2	1691.9	5.6	1.00
104	53770	4.2967	1.3	0.2984	1.1	0.86	1683.2	16.1	1692.7	10.5	1704.5	12.0	0.99
52	16411	4.3259	3.1	0.2995	2.0	0.64	1688.9	29.6	1698.3	25.8	1709.9	44.4	0.99
275	366971	4.4969	0.6	0.3101	0.6	0.96	1741.0	8.8	1730.4	5.0	1717.5	3.2	1.01
145	300243	4.2900	2.5	0.2956	2.4	0.97	1669.7	35.6	1691.4	20.6	1718.5	11.4	0.97
401	87380	4.5861	4.9	0.3156	4.9	1.00	1768.2	75.8	1746.7	41.0	1721.1	5.3	1.03
128	133819	4.2867	1.1	0.2931	0.9	0.79	1656.9	13.2	1690.8	9.4	1733.1	12.7	0.96
356	47075	3.8746	11.1	0.2640	11.1	1.00	1510.4	149.6	1608.4	90.0	1739.2	9.6	0.87
291	335499	4.9029	0.8	0.3262	0.7	0.93	1820.1	11.8	1802.8	6.7	1782.8	5.2	1.02
331	138538	4.8147	1.2	0.3198	1.1	0.96	1788.7	17.2	1787.5	9.7	1786.0	6.2	1.00
156	70552	4.7966	3.7	0.3162	2.0	0.55	1771.1	31.7	1784.3	31.1	1799.8	56.2	0.98
207	19648	5.0597	1.1	0.3262	1.0	0.91	1819.8	16.2	1829.4	9.6	1840.3	8.6	0.99
87	181001	7.2784	1.2	0.3999	1.1	0.93	2168.5	21.0	2146.2	11.0	2124.8	8.1	1.02
12	22183	7.1635	3.7	0.3862	1.5	0.41	2105.0	27.0	2132.0	32.9	2158.1	58.9	0.98
1333	848001	12.2952	0.8	0.5063	0.8	1.00	2640.6	18.0	2627.2	7.8	2616.9	1.0	1.01
541	24613	9.8307	3.4	0.4028	3.4	1.00	2182.0	62.9	2419.0	31.5	2624.9	4.9	0.83
931	22920	11.0892	3.5	0.4542	3.3	0.95	2414.0	66.5	2530.7	32.3	2625.5	17.7	0.92
644	1078748	12.4005	1.6	0.5077	1.6	1.00	2646.9	35.1	2635.2	15.2	2626.2	1.4	1.01
744	237715	12.3880	0.7	0.5053	0.7	0.99	2636.6	14.8	2634.3	6.5	2632.5	1.5	1.00

186	308755	12.7097	0.7	0.5145	0.7	0.95	2675.7	14.5	2658.4	6.5	2645.2	3.4	1.01
43	85312	12.6257	1.3	0.5046	1.3	0.95	2633.4	27.6	2652.1	12.6	2666.4	6.8	0.99
385	7002	10.2770	13.3	0.4036	13.3	1.00	2185.5	246.0	2460.0	123.5	2695.4	10.1	0.81
160	432169	14.1882	1.1	0.5474	1.0	0.98	2814.5	23.8	2762.4	10.1	2724.5	3.6	1.03
160	532572	18.6381	1.5	0.6034	1.5	0.99	3043.7	36.4	3023.3	14.6	3009.7	2.7	1.01
300	14270	18.8241	2.5	0.5030	2.5	1.00	2626.8	54.1	3032.8	24.2	3314.2	1.1	0.79
LTG 171													
491	6700	0.0368	38.2	0.0056	5.2	0.14	36.0	1.9	36.7	13.8	86.6	927.2	0.42
129	40400	3.1884	2.7	0.2563	1.2	0.45	1471.0	16.0	1454.3	20.7	1430.0	45.6	1.03
235	46381	1.8949	2.9	0.1829	1.9	0.65	1082.9	18.8	1079.3	19.4	1072.1	44.7	1.01
366	210929	3.4763	1.3	0.2677	1.2	0.94	1529.1	16.7	1521.8	10.4	1511.8	8.7	1.01
329	253720	4.4230	4.2	0.3046	4.2	0.99	1713.9	63.3	1716.7	35.1	1720.0	9.3	1.00
408	6084	0.0354	44.0	0.0053	7.1	0.16	33.8	2.4	35.4	15.3	142.9	1064.5	0.24
96	28080	1.8959	5.2	0.1820	2.9	0.56	1077.8	29.2	1079.6	34.9	1083.3	87.2	0.99
229	8655	3.3809	6.6	0.2472	5.6	0.84	1424.0	71.6	1500.0	52.0	1609.0	66.3	0.89
504	70762	4.3471	2.0	0.3051	1.9	0.96	1716.6	29.3	1702.4	16.7	1684.9	10.1	1.02
149	68468	4.5012	3.7	0.3054	3.5	0.94	1717.9	53.0	1731.2	30.9	1747.3	22.5	0.98
158	96135	4.8662	2.1	0.3183	1.6	0.76	1781.6	25.1	1796.4	17.9	1813.7	25.2	0.98
121	158109	1.8580	5.0	0.1804	2.1	0.41	1069.0	20.4	1066.3	33.0	1060.8	91.5	1.01
280	122997	12.8149	3.7	0.4907	3.7	1.00	2573.7	79.1	2666.1	35.3	2737.0	5.7	0.94
58	9125	1.7934	7.1	0.1753	1.5	0.21	1041.5	14.0	1043.1	46.0	1046.4	139.4	1.00
477	718	0.0359	38.5	0.0054	7.3	0.19	34.7	2.5	35.8	13.5	112.0	921.1	0.31
223	102905	3.2507	2.6	0.2569	2.4	0.92	1473.9	31.3	1469.3	20.1	1462.7	19.7	1.01
1298	11732	0.0624	9.7	0.0093	4.5	0.46	59.7	2.7	61.5	5.8	132.9	203.1	0.45
635	116304	13.9971	1.4	0.5391	1.4	0.99	2779.7	31.9	2749.5	13.5	2727.4	3.8	1.02
90	54579	4.4564	2.0	0.3077	1.1	0.52	1729.2	16.1	1722.9	16.8	1715.2	31.8	1.01
306	36953	13.8402	1.8	0.5298	1.8	0.99	2740.6	39.9	2738.8	17.1	2737.5	4.7	1.00
1179	6560	0.0301	23.0	0.0055	5.8	0.25	35.2	2.0	30.2	6.8	-354.8	581.2	-0.10
329	22894	0.6271	4.1	0.0804	1.5	0.36	498.3	7.0	494.3	15.9	476.0	83.6	1.05
294	146776	12.3481	5.6	0.5015	5.6	1.00	2620.4	119.5	2631.2	52.3	2639.5	6.1	0.99
94	44785	4.0491	2.5	0.2894	1.9	0.75	1638.7	27.8	1644.1	20.8	1651.1	31.1	0.99

845	17017	4.1770	2.1	0.2743	2.1	0.99	1562.6	28.9	1669.5	17.2	1806.7	4.8	0.86
535	37613	2.2340	5.2	0.2052	4.6	0.89	1203.0	50.4	1191.8	36.2	1171.4	46.5	1.03
128	28418	1.7773	3.7	0.1766	1.2	0.31	1048.5	11.2	1037.2	24.3	1013.4	72.0	1.03
434	182656	4.6683	0.9	0.3182	0.8	0.84	1780.7	12.2	1761.6	7.7	1739.0	9.1	1.02
144	126275	4.7196	1.2	0.3184	0.6	0.51	1782.0	9.6	1770.7	10.0	1757.4	18.7	1.01
552	6257	10.5914	6.8	0.4310	6.8	1.00	2310.0	131.3	2488.0	63.0	2636.6	8.1	0.88
73	34988	11.8402	1.6	0.4974	1.2	0.78	2602.8	26.6	2591.8	14.8	2583.3	16.4	1.01
324	108985	2.2100	2.2	0.2019	1.5	0.71	1185.4	16.6	1184.2	15.2	1182.0	30.3	1.00
210	137287	13.6436	3.3	0.5246	3.3	0.99	2718.5	73.5	2725.3	31.6	2730.3	5.8	1.00
739	759163	12.4233	1.0	0.5074	1.0	0.99	2645.7	21.8	2636.9	9.5	2630.2	2.0	1.01
532	213781	14.0555	1.9	0.5423	1.7	0.90	2792.9	38.1	2753.5	17.6	2724.6	13.0	1.03
316	87833	1.8220	2.8	0.1781	2.3	0.82	1056.7	22.4	1053.4	18.3	1046.5	31.8	1.01
351	194863	12.5878	1.1	0.5147	1.0	0.98	2676.9	22.6	2649.3	9.9	2628.3	3.7	1.02
153	11179	0.5073	7.1	0.0708	2.2	0.31	441.1	9.4	416.7	24.2	283.6	153.8	1.56
128	15573	0.5617	15.2	0.0736	4.3	0.28	458.0	18.9	452.6	55.7	425.4	327.9	1.08
167	112810	14.0241	1.0	0.5392	0.9	0.94	2780.0	20.3	2751.3	9.1	2730.3	5.6	1.02
109	38354	2.3522	3.5	0.2106	2.2	0.64	1232.2	25.1	1228.2	25.1	1221.2	53.4	1.01
745	217443	9.9975	4.1	0.4084	4.1	1.00	2207.4	77.4	2434.6	38.3	2630.2	2.9	0.84
503	291166	5.3569	1.7	0.3369	1.7	0.99	1871.6	27.5	1878.0	14.6	1885.1	3.9	0.99
200	74408	4.3841	1.9	0.3026	1.7	0.85	1704.4	24.7	1709.3	16.1	1715.4	18.8	0.99
257	64054	5.1829	1.7	0.3347	1.6	0.94	1861.1	25.1	1849.8	14.1	1837.2	10.2	1.01
680	28588	0.1782	6.4	0.0262	2.2	0.34	166.6	3.6	166.5	9.9	165.5	141.9	1.01
503	269067	13.5620	0.9	0.5249	0.8	0.98	2719.7	18.7	2719.6	8.1	2719.5	2.5	1.00
160	24478	4.6588	8.9	0.3045	8.8	0.99	1713.4	132.7	1759.9	74.9	1815.5	26.8	0.94
109	22689	1.7532	3.9	0.1739	1.7	0.43	1033.7	16.1	1028.4	25.2	1017.0	71.3	1.02
626	73340	3.3573	2.6	0.2593	2.6	0.98	1486.2	34.1	1494.5	20.5	1506.2	10.3	0.99
105	31781	4.6917	2.5	0.3130	1.6	0.63	1755.7	24.1	1765.8	20.7	1777.7	34.9	0.99
138	60291	1.7065	2.7	0.1706	1.0	0.39	1015.3	9.8	1011.0	17.3	1001.6	50.5	1.01
958	455699	4.4072	2.5	0.2988	2.5	1.00	1685.4	37.4	1713.7	20.9	1748.4	4.1	0.96
78	10365	3.1080	3.0	0.2485	1.1	0.36	1430.9	14.1	1434.7	23.1	1440.2	53.5	0.99
119	11582	0.5163	10.5	0.0743	2.3	0.22	461.9	10.4	422.7	36.5	214.2	238.8	2.16
182	96363	3.0178	3.2	0.2452	2.7	0.82	1413.5	33.9	1412.1	24.7	1410.0	35.1	1.00
1542	657115	4.3347	0.9	0.2981	0.9	0.99	1682.0	13.7	1700.0	7.7	1722.2	2.7	0.98

301	201343	4.4539	1.4	0.3058	1.3	0.93	1719.9	20.3	1722.4	12.0	1725.5	9.8	1.00
163	61517	4.4564	3.0	0.3131	2.7	0.90	1755.8	42.1	1722.9	25.2	1683.1	24.6	1.04
248	1721	0.0429	87.4	0.0056	6.1	0.07	36.1	2.2	42.7	36.6	428.3	2615.6	0.08
153	66915	4.4029	1.9	0.3085	1.6	0.89	1733.4	25.0	1712.9	15.3	1687.8	15.8	1.03
234	43033	4.4487	6.2	0.3062	6.2	1.00	1722.2	93.3	1721.5	51.4	1720.6	10.5	1.00
239	84807	11.3807	3.8	0.4823	3.7	0.97	2537.4	77.2	2554.8	35.6	2568.7	16.6	0.99
438	356486	12.3880	1.4	0.5057	1.3	0.93	2638.1	28.4	2634.3	13.3	2631.3	8.7	1.00
EF 15-60													
236	3501	0.0555	27.6	0.0049	9.8	0.35	31.8	3.1	54.8	14.8	1234.1	515.7	0.03
300	4361	0.0320	60.3	0.0050	9.4	0.16	32.2	3.0	32.0	19.0	17.1	1567.5	1.88
340	4149	0.0399	22.0	0.0050	4.8	0.22	32.5	1.6	39.7	8.6	502.3	477.1	0.06
1750	7585	0.0336	7.1	0.0051	1.7	0.23	32.8	0.5	33.5	2.4	83.6	164.6	0.39
927	8123	0.0329	10.3	0.0052	2.2	0.21	33.5	0.7	32.9	3.3	-14.2	244.8	-2.36
173	2645	0.0283	100.3	0.0055	9.9	0.10	35.5	3.5	28.3	28.0	-548.1	#VALUE!	-0.06
1167	46770	0.0466	7.9	0.0072	1.6	0.21	46.3	0.7	46.3	3.6	44.5	184.7	1.04
700	5523	0.0505	12.4	0.0074	1.9	0.15	47.8	0.9	50.1	6.1	161.2	287.8	0.30
580	30777	0.0930	8.5	0.0145	1.6	0.19	92.8	1.5	90.3	7.4	25.6	201.5	3.62
779	29428	0.0933	5.3	0.0146	2.1	0.39	93.4	1.9	90.6	4.6	17.6	116.2	5.29
519	55727	0.0963	8.1	0.0150	2.0	0.25	95.8	1.9	93.4	7.2	32.6	188.5	2.94
606	48071	0.1641	3.2	0.0246	2.0	0.61	156.5	3.0	154.3	4.6	121.5	59.7	1.29
390	22530	0.1702	4.0	0.0259	1.6	0.40	164.9	2.6	159.6	5.9	80.9	86.9	2.04
317	10411	0.3134	18.3	0.0277	9.5	0.52	175.8	16.5	276.8	44.3	1250.2	307.0	0.14
254	40438	0.4228	3.9	0.0574	1.1	0.28	359.5	3.7	358.0	11.8	348.2	84.7	1.03
574	13327	0.5103	4.3	0.0656	0.9	0.20	409.7	3.5	418.7	14.8	468.2	93.5	0.88
1295	40674	0.5257	3.4	0.0668	1.3	0.37	416.6	5.2	428.9	12.0	495.9	70.3	0.84
223	31214	0.5022	8.0	0.0676	6.9	0.87	421.5	28.3	413.2	27.0	367.0	88.2	1.15
328	19238	0.5203	3.5	0.0678	1.0	0.30	423.2	4.2	425.4	12.0	437.2	73.6	0.97
93	26642	0.5711	10.1	0.0714	1.6	0.16	444.7	6.8	458.7	37.2	529.8	218.2	0.84
190	88875	0.5611	3.2	0.0743	1.9	0.61	461.8	8.7	452.3	11.7	403.8	57.2	1.14
716	88529	0.5808	1.8	0.0750	1.4	0.78	466.5	6.2	465.0	6.6	457.4	24.7	1.02
189	12523	0.6129	4.3	0.0759	3.1	0.71	471.7	14.1	485.4	16.7	550.4	66.2	0.86

379	74774	0.6137	2.6	0.0784	1.7	0.68	486.4	8.1	485.9	9.9	483.7	41.6	1.01
383	90610	0.6370	2.1	0.0812	1.8	0.85	503.5	8.7	500.5	8.4	486.6	24.8	1.03
256	57977	0.7428	3.4	0.0908	0.8	0.23	560.4	4.1	564.0	14.7	578.5	71.8	0.97
185	87338	1.7525	1.6	0.1751	1.3	0.83	1040.3	12.9	1028.1	10.4	1002.2	17.9	1.04
58	25604	1.7416	2.8	0.1730	2.0	0.70	1028.4	18.8	1024.1	18.3	1014.8	41.1	1.01
135	67597	1.7467	1.9	0.1727	1.5	0.77	1026.9	13.8	1025.9	12.1	1023.9	24.1	1.00
67	51603	1.7163	3.1	0.1693	1.2	0.39	1008.1	11.1	1014.6	19.8	1028.7	57.6	0.98
413	110955	1.7579	1.1	0.1730	1.0	0.93	1028.4	9.7	1030.1	7.1	1033.7	8.2	0.99
115	24259	1.7846	2.4	0.1747	1.9	0.79	1037.8	18.3	1039.9	15.8	1044.2	30.3	0.99
434	234935	1.8302	1.1	0.1778	0.9	0.84	1055.1	8.7	1056.3	7.1	1059.0	11.9	1.00
242	16145	1.8948	5.6	0.1790	1.9	0.34	1061.5	18.8	1079.3	37.3	1115.4	105.3	0.95
145	145756	2.0636	2.0	0.1942	1.3	0.65	1144.1	14.0	1136.8	14.0	1122.9	30.8	1.02
181	123697	2.0813	1.9	0.1936	0.9	0.47	1140.6	9.1	1142.7	12.7	1146.5	32.5	0.99
239	86164	2.1485	1.6	0.1989	1.3	0.80	1169.6	14.1	1164.6	11.4	1155.3	19.5	1.01
338	171764	2.1307	1.0	0.1973	0.8	0.84	1160.6	9.0	1158.8	6.9	1155.6	10.8	1.00
164	77764	2.1565	1.5	0.1992	1.2	0.76	1170.9	12.5	1167.1	10.7	1160.1	20.1	1.01
23	5172	2.1988	10.4	0.2004	4.9	0.48	1177.2	53.1	1180.7	72.4	1187.0	180.1	0.99
53	42593	2.1863	3.7	0.1991	0.8	0.21	1170.6	8.2	1176.7	25.6	1187.8	71.1	0.99
101	48189	2.1187	1.4	0.1925	0.9	0.62	1134.9	9.0	1154.9	9.6	1192.6	21.6	0.95
88	46462	2.1709	2.9	0.1971	2.0	0.68	1159.8	21.3	1171.8	20.4	1193.9	42.1	0.97
46	51091	2.4019	3.1	0.2164	1.5	0.48	1262.8	16.9	1243.2	22.1	1209.3	53.3	1.04
647	18006	2.2758	2.8	0.2039	2.8	0.98	1196.1	30.3	1204.8	20.1	1220.5	12.0	0.98
96	42965	2.2590	6.1	0.2022	5.8	0.96	1187.0	62.9	1199.6	42.8	1222.4	35.3	0.97
814	189313	2.4024	1.1	0.2102	1.1	0.99	1230.0	12.0	1243.3	7.8	1266.5	3.0	0.97
271	85221	2.8925	0.8	0.2400	0.8	0.97	1386.8	9.6	1380.0	6.0	1369.3	3.9	1.01
508	57735	2.8158	1.1	0.2314	1.1	0.94	1341.6	13.0	1359.7	8.5	1388.4	7.3	0.97
106	94862	3.0570	2.0	0.2469	1.2	0.63	1422.2	15.7	1422.0	15.0	1421.6	29.0	1.00
290	150978	3.2394	1.5	0.2574	1.4	0.96	1476.5	19.1	1466.6	11.7	1452.3	8.2	1.02
156	167749	3.2834	1.7	0.2581	1.4	0.83	1479.9	19.2	1477.1	13.6	1473.1	18.4	1.00
390	21035	3.2205	6.9	0.2502	6.9	1.00	1439.7	89.1	1462.1	53.6	1494.8	7.8	0.96
510	122906	3.3394	0.8	0.2587	0.7	0.86	1483.4	8.9	1490.3	6.1	1500.1	7.5	0.99
318	210294	3.4603	0.9	0.2658	0.7	0.82	1519.6	9.9	1518.2	7.0	1516.2	9.7	1.00
263	48135	3.4170	1.4	0.2622	1.2	0.82	1501.2	15.4	1508.3	11.1	1518.3	15.2	0.99

233	524702	3.2763	1.3	0.2413	1.2	0.91	1393.7	14.8	1475.4	10.1	1595.0	9.9	0.87
517	79811	3.8715	2.2	0.2847	2.1	0.98	1614.8	30.3	1607.8	17.5	1598.6	8.3	1.01
156	137114	3.9536	1.9	0.2883	1.6	0.83	1632.8	23.1	1624.7	15.6	1614.2	19.9	1.01
529	33400	3.7333	1.4	0.2674	1.4	0.98	1527.8	18.9	1578.5	11.3	1647.0	4.7	0.93
545	67634	4.1276	1.2	0.2948	1.2	0.97	1665.6	17.1	1659.8	9.8	1652.4	5.2	1.01
829	1755052	4.2271	1.1	0.2967	1.1	0.98	1675.0	16.2	1679.3	9.2	1684.6	4.1	0.99
165	99775	4.3449	1.0	0.3024	0.8	0.80	1703.4	11.4	1701.9	7.9	1700.2	10.7	1.00
218	282106	4.3893	1.7	0.3030	1.7	0.98	1706.2	25.5	1710.3	14.3	1715.3	6.1	0.99
207	191926	3.9798	2.4	0.2710	2.4	0.98	1546.1	32.8	1630.1	19.9	1740.2	9.7	0.89
750	12337	4.0592	1.7	0.2758	1.6	0.96	1569.9	22.4	1646.1	13.7	1744.8	8.7	0.90
143	127006	4.6093	1.0	0.3130	0.8	0.82	1755.3	12.0	1750.9	8.0	1745.7	10.1	1.01
771	141931	4.5236	3.8	0.3067	3.8	1.00	1724.7	57.7	1735.3	31.7	1748.1	2.8	0.99
131	156571	4.6852	2.4	0.3167	2.2	0.93	1773.7	34.0	1764.6	19.7	1753.8	15.9	1.01
501	105618	4.5989	1.3	0.3103	1.3	0.99	1742.4	20.0	1749.1	11.1	1757.0	3.7	0.99
672	8133	4.5899	4.9	0.3058	4.9	0.99	1719.8	74.0	1747.4	41.1	1780.7	9.3	0.97
194	155716	4.8629	1.3	0.3216	1.2	0.94	1797.4	19.1	1795.9	10.9	1794.0	8.0	1.00
91	51333	4.9869	1.9	0.3292	1.6	0.82	1834.6	25.4	1817.1	16.4	1797.1	20.0	1.02
100	102399	4.9690	2.0	0.3266	1.8	0.88	1821.9	27.8	1814.1	16.8	1805.1	17.0	1.01
206	307177	5.1150	2.0	0.3351	1.9	0.97	1862.9	31.5	1838.6	17.1	1811.2	9.0	1.03
118	107546	5.4152	1.3	0.3423	1.2	0.95	1897.5	20.1	1887.3	11.0	1876.0	7.5	1.01
177	95946	5.5676	6.8	0.3137	1.4	0.20	1758.7	21.1	1911.1	58.3	2080.8	116.8	0.85
66	15562	6.1658	3.0	0.3469	2.7	0.89	1919.8	44.2	1999.6	26.3	2083.1	24.5	0.92
401	88581	6.1706	3.2	0.3271	2.8	0.87	1824.4	43.7	2000.3	27.7	2187.2	27.3	0.83
56	70099	11.8903	1.5	0.4943	1.5	0.95	2589.2	30.9	2595.8	14.4	2600.9	8.4	1.00
1230	2507	10.7227	3.2	0.4436	2.6	0.81	2366.5	51.6	2499.4	29.8	2609.2	31.3	0.91
515	6520	11.4338	2.8	0.4685	2.7	0.97	2476.9	56.2	2559.2	26.2	2625.0	10.5	0.94
185	3998	11.4290	2.1	0.4494	2.0	0.98	2392.6	40.9	2558.8	19.5	2693.2	6.7	0.89
138	281804	12.7754	1.6	0.4929	1.6	0.96	2583.3	33.3	2663.2	15.4	2724.5	7.8	0.95
324	20499	13.9190	0.7	0.5203	0.7	0.92	2700.5	15.1	2744.2	7.0	2776.5	4.7	0.97
171	405274	15.5590	2.1	0.5515	2.1	0.97	2831.2	47.3	2850.1	20.2	2863.5	7.8	0.99
361	726167	17.7918	0.9	0.5860	0.9	0.98	2973.2	21.4	2978.5	8.8	2982.1	2.6	1.00
48	123234	18.4541	3.3	0.5992	2.7	0.82	3026.6	66.3	3013.7	32.1	3005.2	30.3	1.01

PB
1397

186	1676	0.0295	60.8	0.0042	11.2	0.18	26.8	3.0	29.5	17.7	256.4	1508.1	0.10
256	316	0.0289	58.7	0.0043	8.2	0.14	27.4	2.2	28.9	16.8	161.9	1483.5	0.17
282	3201	0.0155	61.4	0.0043	5.1	0.08	27.4	1.4	15.6	9.5	NA	NA	#VALUE!
273	1999	0.0386	32.3	0.0043	5.3	0.16	27.9	1.5	38.4	12.2	757.0	688.4	0.04
333	4244	0.0324	16.5	0.0044	5.7	0.35	28.4	1.6	32.4	5.3	335.8	352.2	0.08
418	2495	0.0291	26.4	0.0047	4.6	0.17	29.9	1.4	29.1	7.6	-36.3	640.1	-0.82
262	3883	0.0284	30.5	0.0047	12.0	0.39	30.4	3.6	28.4	8.5	-136.1	704.6	-0.22
267	3285	0.0340	28.7	0.0048	6.4	0.22	30.8	2.0	33.9	9.6	260.8	654.2	0.12
586	4153	0.0378	42.0	0.0048	10.1	0.24	30.9	3.1	37.7	15.5	493.0	935.1	0.06
2312	11851	0.0328	3.8	0.0050	2.0	0.53	32.0	0.6	32.7	1.2	84.8	77.2	0.38
308	4704	0.0320	21.6	0.0051	5.7	0.26	32.5	1.8	32.0	6.8	-7.5	508.8	-4.34
506	5540	0.0314	26.1	0.0052	6.8	0.26	33.5	2.3	31.4	8.1	-127.4	631.5	-0.26
93	1941	-1.5898	4482.0	0.0054	14.9	0.00	34.5	5.1	#NUM!	#NUM!	NA	NA	#VALUE!
217	4204	0.0404	44.4	0.0054	9.4	0.21	34.9	3.3	40.2	17.5	369.5	1022.8	0.09
925	28558	0.0372	7.5	0.0055	2.1	0.28	35.4	0.7	37.1	2.7	143.9	169.9	0.25
322	5820	0.0400	26.9	0.0064	3.4	0.13	41.3	1.4	39.8	10.5	-47.8	659.0	-0.86
316	4849	0.0489	24.6	0.0074	2.6	0.10	47.8	1.2	48.5	11.6	83.6	587.4	0.57
288	7356	0.0543	15.6	0.0096	4.2	0.27	61.9	2.6	53.7	8.2	-297.9	386.1	-0.21
224	7057	0.0526	20.8	0.0102	2.5	0.12	65.6	1.7	52.1	10.6	-534.2	558.6	-0.12
70	2360	-3.2405	8807.7	0.0107	14.5	0.00	68.4	9.8	#NUM!	#NUM!	NA	NA	#VALUE!
430	25533	0.0720	12.9	0.0118	3.1	0.24	75.7	2.3	70.6	8.8	-99.8	309.5	-0.76
120	3274	0.0538	49.3	0.0118	7.3	0.15	75.8	5.5	53.3	25.6	-873.1	1478.7	-0.09
4556	99184	0.0780	2.2	0.0120	1.9	0.88	76.9	1.5	76.2	1.6	54.7	24.7	1.41
352	20491	0.0938	11.4	0.0144	3.1	0.27	92.2	2.8	91.0	9.9	61.2	261.3	1.51
298	8685	0.1014	11.3	0.0155	2.3	0.20	99.3	2.2	98.1	10.6	69.4	265.1	1.43
310	15145	0.1111	11.2	0.0174	1.6	0.14	111.0	1.7	107.0	11.3	18.8	266.2	5.89
271	21333	0.1774	11.5	0.0261	2.1	0.19	165.8	3.5	165.9	17.6	166.8	264.9	0.99
109	10600	0.1574	13.2	0.0261	5.8	0.44	165.9	9.5	148.4	18.2	-123.7	292.4	-1.34
272	40513	0.4143	2.1	0.0562	0.7	0.31	352.8	2.2	351.9	6.3	346.4	45.3	1.02
343	132950	0.4869	3.4	0.0639	2.4	0.70	399.4	9.2	402.8	11.2	422.7	53.2	0.94
297	77059	0.4923	4.0	0.0664	2.4	0.60	414.2	9.6	406.5	13.4	362.9	72.1	1.14

186	34048	0.6805	3.1	0.0842	1.6	0.51	521.1	7.8	527.1	12.7	553.3	58.0	0.94
126	83221	0.7564	5.0	0.0932	2.4	0.47	574.3	12.9	571.9	21.8	562.5	96.1	1.02
363	14170	0.8573	2.8	0.1011	2.5	0.89	620.7	14.9	628.7	13.2	657.3	27.0	0.94
87	24486	0.8786	4.5	0.1040	2.5	0.55	638.0	15.2	640.2	21.6	648.3	81.7	0.98
215	86142	1.6769	1.5	0.1672	0.9	0.60	996.9	8.0	999.8	9.2	1006.3	23.7	0.99
188	126559	1.9162	2.2	0.1842	1.9	0.85	1089.9	18.8	1086.8	14.7	1080.5	23.1	1.01
151	103925	2.0731	2.0	0.1950	1.5	0.74	1148.2	15.8	1139.9	14.0	1124.3	27.4	1.02
162	98843	2.1531	2.2	0.2012	2.1	0.93	1181.9	22.5	1166.1	15.5	1136.8	16.2	1.04
174	83047	2.1867	1.2	0.2027	0.9	0.77	1189.7	10.2	1176.8	8.5	1153.2	15.3	1.03
105	84270	2.1420	1.7	0.1977	1.3	0.75	1162.7	13.8	1162.5	11.9	1162.0	22.3	1.00
84	4517	2.1012	5.1	0.1917	3.6	0.72	1130.7	37.7	1149.2	34.9	1184.3	70.1	0.95
105	34821	2.2760	1.7	0.2058	1.2	0.72	1206.5	13.1	1204.9	11.7	1201.9	22.5	1.00
128	87424	2.2591	2.1	0.2037	1.7	0.79	1195.2	18.2	1199.6	14.8	1207.6	25.2	0.99
23	20314	2.1526	5.9	0.1932	1.9	0.32	1138.9	19.3	1165.9	40.6	1216.3	109.2	0.94
317	345296	2.4274	1.1	0.2136	1.0	0.92	1247.9	11.8	1250.7	8.1	1255.6	8.8	0.99
62	45733	2.5328	2.2	0.2192	1.3	0.59	1277.9	15.2	1281.5	16.3	1287.6	35.2	0.99
35	26013	2.6367	3.3	0.2257	1.7	0.52	1311.7	20.1	1310.9	24.1	1309.7	54.4	1.00
40	18810	2.8898	4.1	0.2401	2.3	0.57	1387.2	28.8	1379.3	30.7	1367.0	64.6	1.01
124	93725	2.9108	1.5	0.2407	1.4	0.96	1390.2	17.7	1384.7	11.2	1376.2	8.3	1.01
541	593312	2.9638	1.5	0.2425	1.4	0.96	1399.6	17.9	1398.4	11.3	1396.6	8.4	1.00
190	145465	2.9491	1.4	0.2408	1.3	0.96	1390.9	16.3	1394.6	10.3	1400.3	7.1	0.99
77	31643	3.0432	2.2	0.2478	1.3	0.61	1426.9	17.2	1418.5	16.8	1406.0	33.4	1.01
51	49070	3.0469	2.2	0.2459	1.1	0.50	1417.1	13.6	1419.5	16.5	1423.0	35.7	1.00
136	99403	3.1370	1.4	0.2530	1.1	0.79	1453.8	14.5	1441.8	10.8	1424.1	16.4	1.02
146	153103	3.0566	1.7	0.2449	1.6	0.96	1411.9	20.5	1421.9	13.0	1436.8	9.5	0.98
144	77844	3.0861	3.4	0.2472	3.1	0.93	1424.1	39.6	1429.2	25.7	1437.0	24.1	0.99
53	18759	3.1376	3.8	0.2510	1.3	0.34	1443.4	16.4	1442.0	29.1	1439.8	68.0	1.00
569	7485	2.8138	1.2	0.2250	1.2	0.97	1308.0	14.2	1359.2	9.3	1440.7	6.0	0.91
114	91100	3.1057	1.5	0.2483	1.3	0.88	1429.5	16.6	1434.1	11.4	1440.9	13.6	0.99
171	260776	3.1618	1.8	0.2527	1.7	0.93	1452.5	21.9	1447.9	13.9	1441.2	12.3	1.01
105	64322	3.2148	1.2	0.2569	0.7	0.62	1473.9	9.6	1460.7	9.0	1441.6	17.4	1.02
163	108271	3.1327	1.2	0.2502	0.9	0.70	1439.4	11.2	1440.8	9.5	1442.7	16.6	1.00
98	85963	3.2038	1.6	0.2559	1.2	0.74	1468.6	15.5	1458.1	12.4	1442.8	20.5	1.02

67	107702	3.1551	2.0	0.2516	0.7	0.37	1446.8	9.6	1446.3	15.2	1445.4	34.8	1.00
453	3580	2.2059	1.7	0.1752	1.6	0.94	1040.6	15.2	1182.9	11.7	1453.3	10.4	0.72
72	45299	3.1749	2.6	0.2503	2.5	0.94	1439.9	31.7	1451.1	20.3	1467.5	17.2	0.98
240	2946	2.9359	13.2	0.2313	12.6	0.96	1341.6	153.0	1391.2	100.4	1468.2	73.6	0.91
325	12652	3.3234	5.4	0.2559	3.5	0.65	1468.7	45.6	1486.6	41.9	1512.1	77.2	0.97
195	119411	3.5147	1.7	0.2660	1.7	0.97	1520.5	22.8	1530.5	13.7	1544.4	8.0	0.98
80	95749	4.2815	1.3	0.3016	1.0	0.73	1699.1	14.4	1689.8	10.9	1678.3	16.8	1.01
215	136431	4.3129	1.0	0.3029	1.0	0.95	1705.6	14.2	1695.8	8.3	1683.8	5.9	1.01
110	46717	4.2649	2.8	0.2993	2.7	0.97	1687.8	39.7	1686.6	22.6	1685.1	12.0	1.00
204	91786	4.3174	1.1	0.3025	0.9	0.79	1703.5	13.0	1696.7	9.1	1688.2	12.5	1.01
201	288659	4.5156	1.0	0.3154	1.0	0.96	1767.1	15.0	1733.8	8.4	1694.0	4.9	1.04
90	113495	4.1822	1.5	0.2915	1.1	0.76	1648.8	16.3	1670.5	12.1	1697.9	17.8	0.97
181	49270	4.3665	1.4	0.3026	1.1	0.83	1704.3	17.1	1706.0	11.3	1708.2	13.8	1.00
494	362267	4.2831	2.7	0.2961	2.6	0.99	1672.0	38.8	1690.1	21.8	1712.7	5.8	0.98
53	35592	4.4531	2.1	0.3078	1.5	0.73	1729.7	23.5	1722.3	17.7	1713.2	27.0	1.01
168	210161	4.4012	1.6	0.3033	1.5	0.96	1707.6	22.3	1712.6	12.9	1718.6	8.5	0.99
788	480218	4.3115	1.6	0.2970	1.6	1.00	1676.3	24.2	1695.6	13.6	1719.4	2.8	0.97
143	111465	4.7088	1.5	0.3162	1.5	0.96	1771.0	22.7	1768.8	12.8	1766.1	7.6	1.00
327	192018	4.8499	1.0	0.3235	1.0	0.96	1806.8	15.7	1793.6	8.7	1778.3	5.0	1.02
158	111730	4.7325	1.5	0.3156	1.4	0.93	1768.3	21.5	1773.0	12.5	1778.5	9.7	0.99
256	290573	4.8205	1.4	0.3204	1.3	0.96	1791.5	20.3	1788.5	11.4	1785.0	7.0	1.00
218	12701	4.8535	1.2	0.3216	0.9	0.79	1797.4	14.9	1794.2	10.1	1790.5	13.3	1.00
288	392803	4.8426	0.8	0.3206	0.7	0.97	1792.4	11.5	1792.3	6.4	1792.2	3.1	1.00
329	725788	6.1897	2.3	0.3737	2.2	0.97	2047.0	38.9	2003.0	20.1	1957.9	10.5	1.05
398	8681	12.2058	5.3	0.5064	5.3	1.00	2641.1	114.9	2620.4	49.9	2604.4	6.5	1.01
1027	75597	12.2590	0.9	0.5016	0.9	0.99	2620.5	19.8	2624.4	8.7	2627.5	2.6	1.00
299	8273	11.5403	6.3	0.4605	6.3	1.00	2441.8	128.0	2567.8	58.9	2668.9	3.2	0.91
156	202048	13.4269	5.1	0.5341	4.8	0.95	2758.5	108.6	2710.2	48.3	2674.3	26.9	1.03
191	177795	13.5286	3.0	0.5350	2.9	0.99	2762.5	66.0	2717.3	27.9	2683.8	5.2	1.03
92	127784	13.9778	1.5	0.5397	1.4	0.97	2782.4	32.3	2748.2	14.0	2723.2	5.8	1.02
1284	151953	15.3945	4.0	0.4638	3.8	0.96	2456.4	78.3	2840.0	38.0	3124.7	17.2	0.79

BP
110

146	1238	0.0190	88.8	0.0037	11.3	0.13	24.0	2.7	19.1	16.8	-551.4	3115.6	-0.04
142	2146	0.0223	76.7	0.0037	13.9	0.18	24.1	3.3	22.4	17.0	-156.1	2212.9	-0.15
507	7158	0.0201	27.2	0.0039	3.4	0.13	25.4	0.9	20.2	5.5	-557.1	739.0	-0.05
922	10331	0.0246	15.6	0.0040	3.3	0.21	25.8	0.9	24.7	3.8	-77.0	374.0	-0.33
768	11110	0.0222	25.1	0.0041	3.7	0.15	26.1	1.0	22.3	5.5	-368.6	650.9	-0.07
127	1744	0.0909	206.2	0.0041	14.2	0.07	26.2	3.7	88.4	176.2	2473.8	162.3	0.01
349	1976	0.0194	39.2	0.0041	9.2	0.23	26.3	2.4	19.5	7.6	-762.5	1104.7	-0.03
1087	15086	0.0291	14.5	0.0046	2.0	0.14	29.7	0.6	29.1	4.2	-19.7	349.2	-1.51
408	11200	0.0280	31.9	0.0046	3.6	0.11	29.8	1.1	28.1	8.8	-122.9	799.2	-0.24
346	7683	0.0308	57.0	0.0049	3.8	0.07	31.8	1.2	30.8	17.3	-49.7	1500.6	-0.64
94	1438	-1.1644	3886.6	0.0050	15.7	0.00	32.1	5.0	#NUM!	#NUM!	NA	NA	#VALUE!
114	1796	0.0301	73.9	0.0052	9.9	0.13	33.1	3.3	30.1	21.9	-203.4	2135.6	-0.16
272	4652	0.0195	57.7	0.0052	9.4	0.16	33.2	3.1	19.7	11.2	NA	NA	#VALUE!
257	6082	0.0298	46.5	0.0052	5.1	0.11	33.7	1.7	29.8	13.7	-269.3	1232.3	-0.13
114	2493	0.0878	209.6	0.0053	9.5	0.05	34.2	3.2	85.4	173.4	1948.9	220.7	0.02
723	8546	0.0339	18.9	0.0053	4.5	0.24	34.3	1.5	33.9	6.3	5.5	446.4	6.18
1035	15287	0.0357	12.6	0.0054	3.9	0.31	34.8	1.3	35.6	4.4	90.9	285.4	0.38
1149	16313	0.0354	8.3	0.0055	3.0	0.36	35.4	1.1	35.4	2.9	35.8	186.3	0.99
1013	14791	0.0374	8.3	0.0055	2.5	0.31	35.4	0.9	37.3	3.0	162.5	185.5	0.22
729	17529	0.0307	18.9	0.0055	2.1	0.11	35.4	0.7	30.7	5.7	-321.8	485.1	-0.11
292	3803	0.0433	24.0	0.0055	5.6	0.23	35.5	2.0	43.0	10.1	488.2	520.6	0.07
103	2072	0.0482	68.3	0.0055	17.5	0.26	35.5	6.2	47.8	31.9	718.0	1592.2	0.05
265	4348	0.0348	46.5	0.0056	8.9	0.19	36.1	3.2	34.7	15.9	-59.2	1168.3	-0.61
212	2837	0.0240	94.3	0.0056	11.3	0.12	36.2	4.1	24.1	22.5	-1063.3	2100.3	-0.03
101	1520	10.8173	######	0.0059	11.8	0.00	37.7	4.4	2507.6	#NUM!	NA	NA	#VALUE!
727	25974	0.0450	12.0	0.0066	2.0	0.17	42.7	0.8	44.6	5.2	152.3	278.1	0.28
175	4624	0.0370	53.9	0.0066	8.3	0.15	42.7	3.5	36.9	19.5	-325.2	1462.5	-0.13
291	6411	0.0387	57.8	0.0071	4.1	0.07	45.5	1.9	38.6	21.9	-373.6	1619.2	-0.12
127	4008	0.0347	80.7	0.0078	10.0	0.12	50.1	5.0	34.7	27.5	-939.7	2815.3	-0.05
1222	22197	0.0594	6.3	0.0089	1.5	0.23	57.1	0.8	58.6	3.6	122.4	143.3	0.47
959	27072	0.0586	5.1	0.0092	1.5	0.29	59.0	0.9	57.8	2.9	8.2	118.3	7.16
228	5262	0.0924	10.9	0.0118	4.1	0.38	75.6	3.1	89.7	9.4	483.9	223.3	0.16

816	27566	0.0978	6.3	0.0150	1.2	0.19	95.8	1.2	94.7	5.7	67.4	148.1	1.42
1428	75152	0.1033	3.6	0.0155	2.2	0.63	99.3	2.2	99.8	3.4	111.7	65.2	0.89
72	5113	0.1649	37.6	0.0228	9.5	0.25	145.5	13.7	155.0	54.0	303.5	853.8	0.48
157	11397	0.1518	14.3	0.0256	2.7	0.19	162.7	4.3	143.5	19.1	-163.3	350.8	-1.00
123	6842	0.1579	17.4	0.0259	3.1	0.18	164.8	5.1	148.9	24.1	-97.5	423.2	-1.69
429	47417	0.1742	6.3	0.0261	1.5	0.24	166.3	2.5	163.1	9.5	117.4	145.2	1.42
241	13753	0.1765	6.7	0.0262	1.9	0.28	166.6	3.1	165.0	10.2	141.6	150.5	1.18
210	12063	0.1814	9.5	0.0267	2.8	0.30	170.0	4.7	169.2	14.8	158.7	212.5	1.07
1845	146476	0.1969	1.0	0.0287	0.7	0.68	182.3	1.2	182.5	1.6	184.7	16.7	0.99
1350	203322	0.2487	1.8	0.0351	0.8	0.45	222.1	1.8	225.5	3.6	261.4	36.7	0.85
1381	89946	0.2560	2.3	0.0359	1.8	0.79	227.4	4.0	231.4	4.7	272.4	32.1	0.83
811	73913	0.2595	1.9	0.0367	1.1	0.58	232.1	2.6	234.2	4.1	255.3	36.6	0.91
138	45691	0.5099	5.5	0.0675	2.2	0.41	421.1	9.0	418.4	18.7	403.5	111.8	1.04
152	28116	0.4920	4.4	0.0675	1.1	0.25	421.1	4.5	406.3	14.9	322.9	97.8	1.30
204	27706	0.5542	2.8	0.0730	0.9	0.33	454.5	4.1	447.8	10.1	413.3	58.6	1.10
143	79374	1.7491	1.6	0.1723	1.0	0.66	1025.0	9.9	1026.8	10.2	1030.7	24.1	0.99
500	183078	1.8626	0.8	0.1812	0.6	0.76	1073.3	5.7	1067.9	5.0	1056.9	9.9	1.02
76	24308	1.8210	2.0	0.1764	0.9	0.47	1047.1	9.1	1053.1	13.2	1065.4	35.8	0.98
49	28194	1.9370	3.5	0.1876	1.4	0.40	1108.4	14.2	1094.0	23.6	1065.4	65.1	1.04
448	503136	1.8992	1.1	0.1836	0.9	0.82	1086.4	9.1	1080.8	7.4	1069.6	12.8	1.02
86	20099	1.8203	4.7	0.1749	1.5	0.31	1039.2	14.1	1052.8	31.0	1081.2	90.1	0.96
223	98534	1.9260	1.7	0.1848	1.4	0.78	1093.4	13.6	1090.2	11.6	1083.7	22.0	1.01
144	5649	1.5507	2.0	0.1476	1.3	0.67	887.8	11.0	950.8	12.3	1099.7	29.7	0.81
224	89774	1.9090	6.8	0.1813	6.8	0.99	1073.8	67.0	1084.2	45.5	1105.3	16.4	0.97
82	31712	2.1653	2.4	0.2005	1.6	0.66	1178.2	17.3	1170.0	16.8	1154.8	35.9	1.02
1002	215379	2.2258	0.9	0.2029	0.9	0.98	1190.8	9.9	1189.2	6.5	1186.3	3.5	1.00
246	42242	2.0616	4.2	0.1877	4.1	0.98	1108.7	41.6	1136.1	28.5	1188.9	16.0	0.93
189	237023	2.9096	1.4	0.2373	1.2	0.86	1372.4	14.4	1384.4	10.3	1402.9	13.4	0.98
103	75056	3.0636	1.4	0.2478	0.9	0.69	1427.4	12.1	1423.6	10.5	1418.1	19.0	1.01
342	253183	3.1651	1.0	0.2531	0.9	0.97	1454.5	12.3	1448.7	7.6	1440.2	4.9	1.01
90	64566	3.1938	2.3	0.2551	1.7	0.73	1464.8	21.9	1455.7	17.6	1442.3	29.6	1.02
118	41409	3.0594	9.9	0.2344	7.8	0.79	1357.4	95.4	1422.6	75.7	1521.6	114.6	0.89
358	7376	2.9391	5.4	0.2158	5.2	0.95	1259.7	59.4	1392.0	41.3	1601.0	30.5	0.79

94	119239	4.1582	2.2	0.2958	1.8	0.84	1670.2	27.1	1665.8	18.0	1660.2	22.2	1.01
163	115457	4.2415	1.6	0.2986	1.6	0.97	1684.1	23.3	1682.1	13.3	1679.5	7.6	1.00
1234	8251	3.9265	1.5	0.2763	1.5	0.99	1572.7	21.2	1619.2	12.4	1680.1	3.3	0.94
148	119680	4.4653	2.4	0.3135	2.3	0.95	1758.0	35.7	1724.5	20.2	1684.2	13.6	1.04
280	209734	4.2793	2.3	0.3003	2.3	0.99	1692.8	33.9	1689.4	19.0	1685.1	6.8	1.00
446	319804	4.3040	1.6	0.3013	1.5	0.96	1697.8	22.4	1694.1	12.8	1689.6	7.7	1.00
154	110426	4.3064	0.9	0.3010	0.8	0.81	1696.2	11.2	1694.6	7.6	1692.6	9.9	1.00
132	91887	4.4324	1.7	0.3066	1.4	0.80	1724.1	20.6	1718.4	14.1	1711.5	18.8	1.01
498	560558	4.4393	1.1	0.3068	1.1	0.99	1724.7	17.0	1719.7	9.4	1713.6	3.3	1.01
355	4369	3.4016	7.2	0.2344	7.0	0.97	1357.3	86.1	1504.8	56.8	1719.0	30.8	0.79
124	42671	4.4293	1.6	0.3044	0.9	0.58	1713.2	13.6	1717.8	12.9	1723.5	23.4	0.99
346	400180	4.5681	0.9	0.3118	0.8	0.93	1749.4	12.2	1743.5	7.2	1736.4	6.0	1.01
155	162640	4.4922	1.2	0.3051	1.1	0.89	1716.8	15.9	1729.5	9.8	1745.0	9.8	0.98
347	74792	4.4521	3.2	0.2983	3.1	0.97	1682.8	45.9	1722.1	26.6	1770.1	14.9	0.95
129	67851	4.5388	3.3	0.2945	3.3	0.99	1664.1	47.7	1738.1	27.4	1828.4	9.6	0.91
107	77012	5.2672	1.3	0.3378	1.2	0.92	1876.0	19.5	1863.6	11.1	1849.7	9.0	1.01
814	33570	5.2422	1.6	0.3295	1.5	0.95	1836.1	24.6	1859.5	13.8	1885.7	9.0	0.97
82	95295	5.7087	1.3	0.3517	0.8	0.57	1942.9	12.6	1932.7	11.4	1921.8	19.4	1.01
87	103367	10.5541	1.0	0.4713	0.7	0.74	2489.2	15.2	2484.7	9.2	2480.9	11.3	1.00
197	225564	10.5761	1.1	0.4713	1.1	0.99	2489.1	23.1	2486.6	10.5	2484.6	2.7	1.00
205	6062	7.8540	4.4	0.3325	4.0	0.92	1850.5	65.0	2214.4	39.4	2570.5	28.0	0.72
953	848121	11.2135	1.4	0.4606	1.4	1.00	2442.0	28.6	2541.0	13.2	2621.0	1.4	0.93
103	106535	12.4367	2.7	0.4951	2.6	0.99	2592.9	56.1	2638.0	25.1	2672.7	7.5	0.97
156	236117	12.9941	0.9	0.5115	0.8	0.97	2663.0	18.3	2679.2	8.2	2691.5	3.6	0.99
69	146559	13.5393	1.0	0.5202	0.9	0.93	2700.2	20.4	2718.0	9.4	2731.3	6.2	0.99

DB 37

781	11035	0.6072	12.0	0.0334	11.8	0.99	212.0	24.7	481.8	45.9	2121.0	31.0	0.10
625	489218	1.8324	2.0	0.1783	1.9	0.94	1057.9	18.5	1057.2	13.2	1055.7	13.5	1.00
647	3458	0.0221	38.6	0.0038	6.0	0.16	24.7	1.5	22.2	8.5	-235.3	992.3	-0.10
156	54448	2.0801	3.3	0.1923	2.5	0.76	1134.0	26.2	1142.3	22.7	1158.0	42.7	0.98
380	41917	0.4843	2.1	0.0640	1.1	0.56	399.7	4.4	401.0	6.8	408.4	38.4	0.98

557	762	0.0410	18.8	0.0051	9.7	0.51	33.0	3.2	40.8	7.5	522.2	356.6	0.06
930	27865	0.4119	2.9	0.0561	2.4	0.83	352.0	8.2	350.3	8.6	338.9	37.0	1.04
302	118669	4.0423	2.1	0.2891	2.1	0.98	1637.2	29.9	1642.8	17.2	1649.8	7.8	0.99
114	12803	0.3726	15.9	0.0539	2.2	0.13	338.7	7.1	321.6	44.0	199.3	369.0	1.70
1388	30184	0.0325	10.4	0.0050	1.8	0.17	32.4	0.6	32.5	3.3	36.0	246.9	0.90
386	6158	0.0368	23.4	0.0071	9.2	0.39	45.8	4.2	36.7	8.4	-529.6	582.5	-0.09
343	2889	0.0674	139.2	0.0040	9.4	0.07	25.6	2.4	66.3	89.6	2001.3	131.9	0.01
297	159	0.0715	44.6	0.0038	8.7	0.20	24.7	2.2	70.1	30.2	2168.5	806.2	0.01
645	8164	0.0325	25.1	0.0060	2.5	0.10	38.3	1.0	32.5	8.0	-377.3	655.9	-0.10
413	3342	0.0274	32.7	0.0046	8.0	0.25	29.6	2.4	27.4	8.9	-162.0	806.7	-0.18
137	153713	4.0598	1.8	0.2850	0.6	0.36	1616.4	9.3	1646.3	14.9	1684.6	31.5	0.96
149	40475	1.6862	3.6	0.1694	3.2	0.88	1009.0	29.9	1003.3	23.1	991.0	34.4	1.02
592	5763	0.0278	25.3	0.0044	5.1	0.20	28.5	1.5	27.8	6.9	-26.6	607.9	-1.07
449	7226	0.0265	43.1	0.0059	5.4	0.13	37.7	2.0	26.6	11.3	-890.5	1286.9	-0.04
609	8256	0.0269	24.9	0.0047	4.1	0.16	30.4	1.2	27.0	6.6	-268.6	632.6	-0.11
254	1751	0.0325	49.7	0.0041	11.8	0.24	26.4	3.1	32.5	15.9	512.2	1125.3	0.05
288	11933	2.2904	8.4	0.1864	8.3	1.00	1102.0	84.3	1209.3	59.1	1406.3	12.9	0.78
1935	175555	3.1082	1.6	0.2522	1.6	0.99	1449.6	20.5	1434.7	12.3	1412.7	4.5	1.03
112	45492	2.1282	3.0	0.1976	2.5	0.83	1162.2	26.4	1158.0	20.8	1150.1	33.7	1.01
391	120869	0.9453	2.3	0.1117	1.4	0.61	682.7	9.3	675.6	11.5	652.2	39.6	1.05
573	7509	0.0242	28.5	0.0042	5.1	0.18	27.3	1.4	24.3	6.8	-264.7	722.5	-0.10
177	1676	0.0480	128.8	0.0039	17.1	0.13	25.3	4.3	47.6	60.0	1396.0	210.8	0.02
683	17085	0.0399	19.4	0.0060	2.3	0.12	38.8	0.9	39.8	7.6	100.3	459.8	0.39
287	38435	4.5928	6.4	0.2986	5.6	0.88	1684.4	83.3	1748.0	53.1	1824.8	54.1	0.92
314	164809	12.3533	3.7	0.4992	3.7	1.00	2610.4	78.7	2631.6	34.6	2648.0	5.0	0.99
295	36541	0.2285	7.3	0.0339	2.1	0.29	215.0	4.5	208.9	13.7	140.6	163.5	1.53
177	356952	10.2131	1.1	0.4554	1.0	0.91	2419.1	19.8	2454.3	9.9	2483.5	7.4	0.97
227	104354	4.4852	2.6	0.3056	2.3	0.92	1718.9	35.4	1728.2	21.2	1739.5	18.8	0.99
259	192608	3.7305	5.9	0.2657	5.9	0.99	1518.9	79.2	1577.9	47.2	1657.8	12.9	0.92
680	99290	0.4186	2.5	0.0563	2.1	0.85	353.4	7.4	355.1	7.6	366.1	30.1	0.97
147	1222	-0.9924	3820.0	0.0038	14.0	0.00	24.2	3.4	-4959.4	#NUM!	0.0	132.5	#DIV/0!
199	75578	2.2569	3.0	0.2056	2.8	0.92	1205.5	30.7	1198.9	21.3	1187.2	23.4	1.02
122	179142	5.4376	1.6	0.3389	1.3	0.77	1881.3	20.4	1890.8	14.0	1901.2	18.8	0.99

261	350527	13.0270	1.5	0.5237	1.4	0.97	2715.1	32.0	2681.6	14.1	2656.5	6.1	1.02
171	52855	10.0325	7.8	0.4033	7.8	1.00	2184.0	145.1	2437.8	72.5	2656.9	6.7	0.82
30	17278	2.3734	8.4	0.2029	1.7	0.21	1190.7	18.9	1234.6	59.9	1312.1	159.2	0.91
92	105531	12.7856	4.5	0.5059	4.4	0.99	2639.0	95.8	2664.0	42.1	2683.0	10.4	0.98
3689	57183	0.0307	3.2	0.0047	1.6	0.50	30.0	0.5	30.7	1.0	82.5	64.8	0.36
859	7320	0.0346	16.1	0.0056	4.3	0.27	36.1	1.6	34.5	5.5	-75.7	381.3	-0.48
112	99869	4.1188	2.1	0.2958	1.4	0.64	1670.5	20.0	1658.0	17.4	1642.3	30.3	1.02
332	39195	4.2392	1.7	0.2964	1.5	0.92	1673.5	22.6	1681.7	13.7	1691.8	12.1	0.99
495	16986	11.8766	4.8	0.4882	4.8	1.00	2562.9	100.6	2594.7	44.6	2619.6	3.4	0.98
170	109744	6.9528	4.4	0.3829	4.3	1.00	2089.9	77.6	2105.4	38.8	2120.7	7.4	0.99
128	52902	1.7249	3.1	0.1683	1.7	0.54	1002.6	15.9	1017.8	20.2	1050.7	53.2	0.95
209	1695	0.0154	77.9	0.0046	19.1	0.25	29.8	5.7	15.5	12.0	-1886.0	797.7	-0.02
80	24394	1.8351	3.7	0.1787	2.4	0.66	1059.8	23.7	1058.1	24.2	1054.6	55.9	1.00
106	25497	2.1542	4.1	0.1972	3.3	0.81	1160.4	35.3	1166.4	28.6	1177.6	48.4	0.99
1225	12071	0.0277	9.7	0.0048	4.1	0.42	30.6	1.3	27.8	2.7	-210.6	220.7	-0.15
125	95166	4.8295	1.5	0.3183	1.0	0.71	1781.6	16.2	1790.1	12.3	1799.9	18.7	0.99
321	2575	-0.1707	1138.6	0.0041	9.5	0.01	26.7	2.5	-190.0	#NUM!	0.0	646.6	#DIV/0!
373	5399	0.0321	31.7	0.0052	15.8	0.50	33.6	5.3	32.1	10.0	-80.3	682.2	-0.42
2560	2009	0.0329	6.7	0.0047	3.7	0.55	30.5	1.1	32.9	2.2	211.8	129.4	0.14
111	100774	4.2140	1.6	0.2999	1.3	0.79	1690.8	19.3	1676.7	13.5	1659.2	18.9	1.02
103	190942	4.6717	1.5	0.3221	1.0	0.67	1799.8	16.1	1762.2	12.7	1717.9	20.7	1.05
187	975	0.0200	90.4	0.0042	15.3	0.17	26.7	4.1	20.1	18.0	-710.5	3285.0	-0.04
499	820	0.0303	28.6	0.0039	15.8	0.55	25.2	4.0	30.3	8.5	458.0	534.6	0.06
118	47554	3.1213	2.9	0.2531	1.4	0.50	1454.3	18.7	1438.0	22.0	1413.8	47.4	1.03
573	5832	0.0230	24.4	0.0040	5.8	0.24	25.8	1.5	23.1	5.6	-250.3	606.8	-0.10
1088	102035	4.6962	4.9	0.3232	4.9	1.00	1805.3	77.0	1766.6	41.2	1721.0	8.7	1.05
205	1431	0.0306	86.4	0.0040	13.9	0.16	25.5	3.5	30.6	26.1	452.4	2486.2	0.06
272	4368	0.0218	97.9	0.0054	7.9	0.08	34.4	2.7	21.9	21.3	-1200.2	0.0	-0.03
1148	10731	0.0271	19.3	0.0042	4.5	0.23	27.1	1.2	27.1	5.2	31.6	453.8	0.86
385	4412	0.0262	52.6	0.0042	11.0	0.21	27.0	3.0	26.2	13.6	-38.9	1332.3	-0.69
1953	33293	0.0351	6.8	0.0055	1.8	0.27	35.5	0.6	35.0	2.3	6.9	158.2	5.14
1175	8502	0.0272	10.1	0.0043	3.2	0.31	27.7	0.9	27.3	2.7	-10.8	233.3	-2.58
67	29853	4.0023	3.0	0.2874	2.4	0.81	1628.6	34.8	1634.7	24.3	1642.4	32.6	0.99

151	107341	4.9540	2.9	0.3258	2.8	0.96	1818.2	43.8	1811.5	24.3	1803.8	14.5	1.01
423	2476	0.0251	47.0	0.0044	12.4	0.26	28.4	3.5	25.1	11.7	-277.4	1208.6	-0.10
203	1242	0.0512	121.3	0.0042	17.7	0.15	27.3	4.8	50.7	60.1	1373.5	181.7	0.02
1814	1747	0.0402	29.0	0.0047	2.1	0.07	30.1	0.6	40.0	11.4	683.0	629.6	0.04
360	4540	0.0472	112.7	0.0051	8.0	0.07	33.1	2.6	46.8	51.6	823.4	514.1	0.04
95	26864	1.8302	3.7	0.1751	2.3	0.63	1040.2	22.6	1056.3	24.4	1089.8	57.7	0.95
284	2239	0.0556	263.1	0.0041	12.8	0.05	26.3	3.4	55.0	141.6	1598.7	735.7	0.02
1195	7875	0.0304	13.8	0.0042	2.9	0.21	27.2	0.8	30.4	4.1	294.4	310.2	0.09
1157	7155	0.0264	15.6	0.0042	3.3	0.21	27.1	0.9	26.5	4.1	-32.5	372.6	-0.83
176	99295	3.2569	2.1	0.2536	1.5	0.73	1457.1	20.2	1470.8	16.4	1490.6	27.3	0.98
300	4195	0.0306	46.0	0.0054	8.0	0.17	34.9	2.8	30.6	13.9	-294.8	1210.8	-0.12
718	96941	1.7593	1.6	0.1725	1.1	0.70	1025.6	10.7	1030.6	10.5	1041.1	23.5	0.99
62	36297	13.6121	2.4	0.5229	2.2	0.92	2711.3	49.0	2723.1	22.7	2731.8	15.2	0.99
250	1295	0.0217	80.3	0.0039	16.8	0.21	25.3	4.3	21.8	17.3	-348.4	2435.6	-0.07
141	105929	4.1189	2.3	0.2946	2.1	0.92	1664.3	31.2	1658.1	18.9	1650.2	16.9	1.01
982	294	0.0312	45.6	0.0044	6.8	0.15	28.5	1.9	31.2	14.0	246.8	1091.2	0.12
325	9813	0.1733	16.3	0.0271	2.2	0.13	172.5	3.7	162.3	24.5	16.0	390.4	10.81

SP 15

405	100360	3.1654	1.8	0.2523	1.7	0.94	1450.2	22.4	1448.8	14.1	1446.6	11.4	1.00
758	35777	0.1776	4.2	0.0261	2.9	0.68	165.8	4.7	166.0	6.5	169.2	71.8	0.98
144	41551	4.0638	2.1	0.2876	1.8	0.85	1629.3	25.4	1647.1	16.8	1669.8	19.9	0.98
384	11230	0.2545	8.4	0.0340	2.0	0.24	215.5	4.3	230.3	17.3	384.2	183.8	0.56
284	41678	0.8657	3.2	0.1037	1.8	0.55	636.0	10.7	633.3	15.1	623.3	57.7	1.02
304	568362	14.0745	3.8	0.5202	3.8	1.00	2700.0	84.3	2754.7	36.3	2795.1	4.1	0.97
83	62608	4.3171	1.8	0.2963	1.1	0.61	1673.0	16.6	1696.6	15.2	1725.9	26.7	0.97
760	8299	0.0235	27.1	0.0040	11.1	0.41	25.4	2.8	23.6	6.3	-164.2	622.1	-0.15
359	3663	0.0395	30.6	0.0068	6.4	0.21	43.9	2.8	39.3	11.8	-231.3	768.3	-0.19
128	54790	2.1963	1.8	0.2025	1.1	0.62	1188.8	12.2	1179.9	12.7	1163.4	28.3	1.02
603	209962	1.9489	2.9	0.1866	2.8	0.97	1103.0	28.2	1098.1	19.2	1088.4	13.0	1.01
553	7731	0.0366	23.4	0.0056	3.4	0.15	36.2	1.2	36.5	8.4	52.6	557.8	0.69
162	1846	-0.2257	852.2	0.0045	19.2	0.02	29.0	5.6	-259.7	#NUM!	0.0	56.0	#DIV/0!

911	69565	0.2445	3.0	0.0350	1.8	0.61	221.8	4.0	222.1	6.1	225.0	55.9	0.99
450	23612	0.1766	7.3	0.0257	3.1	0.43	163.8	5.1	165.1	11.1	184.1	153.6	0.89
166	2759	0.0646	66.5	0.0109	15.5	0.23	69.7	10.7	63.6	41.0	-161.5	1791.8	-0.43
331	156	0.0416	28.0	0.0054	13.8	0.49	34.5	4.7	41.3	11.3	459.8	547.0	0.08
643	4788	0.0263	27.8	0.0041	8.7	0.32	26.3	2.3	26.3	7.2	26.2	641.3	1.00
589	44691	4.2085	2.3	0.2952	2.3	0.99	1667.5	33.9	1675.7	19.1	1685.9	6.7	0.99
191	126037	4.3587	0.8	0.2973	0.8	0.91	1678.0	11.3	1704.5	7.0	1737.3	6.5	0.97
425	3881	0.0306	27.1	0.0057	13.9	0.51	36.6	5.1	30.6	8.2	-423.5	615.6	-0.09
209	1845	0.0397	41.6	0.0040	9.4	0.23	26.0	2.4	39.5	16.1	968.2	861.6	0.03
520	7214	0.0368	33.7	0.0056	5.0	0.15	35.7	1.8	36.7	12.2	106.1	807.9	0.34
497	322482	4.2079	1.7	0.2941	1.7	0.99	1661.9	25.3	1675.6	14.4	1692.7	5.5	0.98
669	37112	0.1817	5.2	0.0271	2.9	0.56	172.2	4.9	169.6	8.1	133.2	101.3	1.29
280	23524	0.4541	5.3	0.0605	1.3	0.25	378.5	4.9	380.2	16.8	390.4	115.1	0.97
360	277460	9.7855	3.5	0.4459	3.5	1.00	2376.8	69.5	2414.8	32.3	2447.0	3.2	0.97
255	3402	0.0311	42.6	0.0041	11.5	0.27	26.6	3.0	31.1	13.1	400.1	957.1	0.07
95	50756	3.1554	3.6	0.2517	2.6	0.72	1447.0	34.0	1446.3	28.0	1445.3	47.7	1.00
208	89169	1.8870	4.1	0.1817	3.7	0.91	1076.5	36.5	1076.5	27.0	1076.6	34.6	1.00
360	331178	13.4932	1.9	0.5146	1.9	0.99	2676.2	41.8	2714.8	18.3	2743.6	5.3	0.98
59	8638	0.1145	70.4	0.0260	9.6	0.14	165.4	15.6	110.0	73.5	-970.1	2316.7	-0.17
401	274134	3.2184	2.1	0.2498	2.1	0.97	1437.2	26.7	1461.6	16.5	1497.2	9.3	0.96
180	138797	5.1353	1.3	0.3250	1.2	0.87	1814.3	18.3	1842.0	11.4	1873.3	12.0	0.97
157	18822	1.8126	3.3	0.1656	2.8	0.85	987.6	25.6	1050.0	21.6	1182.2	34.3	0.84
448	219905	4.8050	1.7	0.3272	1.7	0.99	1825.0	26.3	1785.8	14.0	1740.3	3.8	1.05
497	146724	1.5655	1.6	0.1607	1.3	0.81	960.4	11.9	956.7	10.2	948.0	19.5	1.01
269	138999	4.9353	2.2	0.3234	2.2	0.98	1806.2	34.7	1808.3	19.0	1810.8	8.0	1.00
163	64032	2.6377	2.2	0.2231	1.6	0.71	1298.3	18.7	1311.2	16.5	1332.4	30.5	0.97
214	158212	4.5786	1.2	0.3070	1.0	0.88	1725.9	15.9	1745.4	9.9	1768.8	10.2	0.98
58	13311	1.9398	4.8	0.1808	2.5	0.53	1071.5	25.0	1094.9	32.2	1141.9	81.1	0.94
226	147394	2.8597	1.8	0.2335	1.5	0.83	1353.1	18.1	1371.4	13.4	1400.0	18.8	0.97
361	16326	3.3713	1.9	0.2660	1.1	0.59	1520.3	15.4	1497.7	15.1	1465.9	29.6	1.04
202	122502	4.4706	3.4	0.3033	3.3	0.96	1707.6	48.9	1725.5	28.1	1747.3	16.5	0.98
292	4357	0.0358	66.1	0.0056	14.9	0.23	36.0	5.4	35.7	23.2	17.9	1724.7	2.01
112	40378	1.9051	4.4	0.1818	3.1	0.72	1077.0	31.2	1082.9	29.1	1094.8	60.8	0.98

386	2709	0.4182	12.8	0.0550	5.3	0.41	345.1	17.8	354.7	38.3	418.5	260.5	0.82
194	77785	1.5513	3.3	0.1561	2.8	0.86	935.2	24.5	951.0	20.2	987.9	34.0	0.95
336	163074	2.1281	2.5	0.1960	2.2	0.91	1153.7	23.7	1158.0	17.0	1165.9	20.2	0.99
1527	930747	3.7487	2.1	0.2329	2.0	0.97	1349.5	24.5	1581.8	16.7	1907.1	9.8	0.71
38	23978	1.7820	8.2	0.1666	5.0	0.61	993.4	46.0	1038.9	53.7	1136.1	130.7	0.87
462	340112	4.5759	1.5	0.3096	1.5	0.98	1738.8	22.6	1744.9	12.6	1752.2	5.3	0.99
174	17686	0.4710	10.5	0.0658	3.3	0.32	410.8	13.3	391.8	34.1	281.7	228.0	1.46
87	38616	2.2224	5.9	0.2007	5.3	0.90	1178.9	57.5	1188.1	41.3	1204.8	49.5	0.98
548	13526	2.5674	4.6	0.2244	4.4	0.96	1305.1	51.8	1291.4	33.3	1268.8	24.2	1.03
170	60678	4.2677	1.2	0.3004	1.0	0.83	1693.2	14.8	1687.2	9.9	1679.7	12.5	1.01
57	20140	2.9931	3.9	0.2425	2.0	0.52	1399.5	25.1	1405.9	29.3	1415.5	63.1	0.99
201	9288	0.2143	14.5	0.0328	4.0	0.27	208.2	8.1	197.1	26.0	65.9	333.1	3.16
491	5807	0.0390	16.1	0.0051	7.8	0.49	32.5	2.5	38.9	6.2	454.7	314.2	0.07
315	12254	0.0826	29.3	0.0141	13.6	0.46	90.3	12.2	80.6	22.7	-199.6	660.0	-0.45
351	301130	3.5350	3.3	0.2648	3.1	0.96	1514.2	42.4	1535.1	25.9	1564.0	17.2	0.97
124	56862	4.2252	1.7	0.2921	1.4	0.86	1652.2	21.1	1678.9	13.8	1712.5	15.5	0.96
457	3573	0.0283	22.0	0.0035	8.2	0.37	22.8	1.9	28.4	6.1	528.9	450.7	0.04
94	39984	2.1757	3.3	0.2006	1.9	0.56	1178.5	20.1	1173.3	23.2	1163.8	54.7	1.01
267	221532	4.3672	1.3	0.3018	1.1	0.85	1700.2	16.2	1706.2	10.5	1713.4	12.2	0.99
152	2587	0.0383	116.4	0.0050	19.0	0.16	32.3	6.1	38.2	43.6	425.9	827.2	0.08
565	991	0.0339	18.6	0.0047	4.3	0.23	30.0	1.3	33.8	6.2	314.3	415.3	0.10
233	2126	0.0328	48.4	0.0052	18.4	0.38	33.5	6.1	32.8	15.6	-19.6	1133.9	-1.71
285	4621	0.0270	83.4	0.0042	13.0	0.16	26.9	3.5	27.1	22.3	45.7	2470.7	0.59
323	11973	2.3916	10.9	0.1950	10.8	0.99	1148.1	113.6	1240.1	78.2	1403.6	29.8	0.82
502	4330	0.0202	53.2	0.0054	5.0	0.09	34.4	1.7	20.3	10.7	-1448.0	1844.7	-0.02
150	14833	0.2533	12.9	0.0354	4.3	0.33	224.4	9.4	229.3	26.5	279.6	279.2	0.80
362	7388	0.0481	26.1	0.0092	11.1	0.42	59.2	6.5	47.7	12.2	-495.4	636.9	-0.12
254	21895	0.1904	9.2	0.0261	3.8	0.42	166.2	6.3	176.9	14.9	322.9	190.2	0.51
398	5305	0.0344	163.9	0.0035	17.2	0.10	22.8	3.9	34.3	55.4	942.2	760.2	0.02
53	32229	3.9623	3.0	0.2865	1.8	0.59	1623.9	25.3	1626.5	24.3	1629.9	45.1	1.00
320	129587	1.6384	2.0	0.1651	1.9	0.94	985.0	17.1	985.1	12.6	985.4	14.3	1.00
507	347242	3.9471	5.5	0.2643	5.4	0.97	1511.7	72.4	1623.4	44.8	1771.4	23.5	0.85
591	51046	0.2451	4.7	0.0354	1.7	0.35	224.2	3.7	222.6	9.4	206.2	102.2	1.09

1164	7633	0.0325	18.0	0.0052	2.7	0.15	33.3	0.9	32.5	5.8	-31.3	434.7	-1.07
408	1274	0.0208	93.8	0.0037	6.5	0.07	23.8	1.5	20.9	19.5	-293.7	1201.0	-0.08
148	90996	5.0224	1.0	0.3251	0.6	0.63	1814.7	9.5	1823.1	8.0	1832.7	13.4	0.99
1765	76505	0.0474	5.5	0.0074	1.3	0.24	47.4	0.6	47.1	2.5	32.4	128.1	1.46
696	85600	0.4634	3.2	0.0624	2.3	0.73	390.2	8.9	386.6	10.3	365.0	49.8	1.07
1154	8610	0.0173	15.4	0.0029	3.9	0.26	19.0	0.7	17.4	2.7	-196.1	375.0	-0.10
618	122119	1.8649	1.4	0.1799	1.2	0.86	1066.4	11.7	1068.7	9.1	1073.4	13.9	0.99
459	306	0.0370	27.3	0.0061	9.1	0.33	39.1	3.6	36.9	9.9	-106.0	642.6	-0.37
370	3456	0.0292	83.1	0.0027	16.5	0.20	17.3	2.9	29.2	23.9	1164.4	2069.0	0.01
76	882	0.3783	649.8	0.0058	13.6	0.02	37.5	5.1	325.8	#NUM!	4151.3	350.1	0.01
312	50291	0.4384	4.0	0.0588	1.8	0.44	368.5	6.3	369.1	12.4	372.7	81.0	0.99
257	3786	0.4526	6.8	0.0594	2.6	0.39	371.8	9.5	379.1	21.4	424.1	139.3	0.88
733	3053	0.4770	8.0	0.0478	7.3	0.91	301.0	21.4	396.0	26.1	996.4	65.5	0.30
227	179399	4.1394	2.4	0.2926	2.4	0.97	1654.3	34.4	1662.1	19.9	1672.0	11.1	0.99
621	8894	0.0405	28.0	0.0072	4.0	0.14	46.5	1.9	40.3	11.1	-317.7	722.8	-0.15
114	55494	3.2504	3.4	0.2612	3.0	0.86	1495.8	39.7	1469.3	26.7	1431.1	33.0	1.05

CB 26

783	8229	0.0466	12.6	0.0066	2.4	0.19	42.6	1.0	46.3	5.7	239.2	287.0	0.18
389	21619	0.1264	6.0	0.0181	4.2	0.70	115.7	4.9	120.8	6.9	222.6	99.7	0.52
384	4020	0.0285	42.8	0.0039	5.7	0.13	25.3	1.4	28.5	12.0	308.9	1007.1	0.08
356	2811	0.0200	34.3	0.0045	8.0	0.23	29.0	2.3	20.1	6.8	-948.0	998.9	-0.03
253	5621	0.0364	50.0	0.0071	8.8	0.18	45.6	4.0	36.3	17.8	-538.7	1392.4	-0.08
115	44562	2.9386	2.0	0.2397	1.6	0.79	1385.0	19.9	1391.9	15.2	1402.6	23.4	0.99
429	104761	1.8147	2.2	0.1752	2.0	0.91	1040.7	19.1	1050.8	14.2	1071.7	17.9	0.97
247	17240	0.1651	8.1	0.0264	3.1	0.39	168.0	5.2	155.1	11.6	-37.5	181.0	-4.48
222	355	0.1195	29.2	0.0131	8.3	0.28	84.0	6.9	114.6	31.6	808.0	595.8	0.10
66	17525	0.7528	9.2	0.0890	4.2	0.46	549.7	22.1	569.8	40.0	650.8	175.3	0.84
400	18449	0.0501	15.9	0.0074	4.0	0.25	47.5	1.9	49.6	7.7	152.6	362.0	0.31
239	2113	0.5969	3345.3	0.0045	13.9	0.00	29.0	4.0	475.3	#NUM!	0.0	693.1	#DIV/0!
623	5325	0.0247	26.2	0.0048	3.9	0.15	30.7	1.2	24.8	6.4	-515.4	702.7	-0.06
326	16732	0.1732	8.5	0.0249	5.7	0.67	158.6	8.9	162.2	12.8	214.4	147.4	0.74

199	11266	0.1693	14.3	0.0228	3.7	0.26	145.2	5.3	158.8	21.0	367.5	311.8	0.40
121	6769	0.1294	27.9	0.0225	6.4	0.23	143.6	9.1	123.6	32.5	-247.6	697.0	-0.58
393	7249	0.0298	30.7	0.0043	9.4	0.31	27.5	2.6	29.8	9.0	217.8	689.3	0.13
137	8186	0.1590	29.1	0.0266	6.2	0.21	169.3	10.4	149.8	40.5	-148.4	716.2	-1.14
227	140738	1.8996	2.7	0.1826	1.8	0.65	1081.3	17.8	1080.9	18.2	1080.2	41.8	1.00
22	26947	6.1295	5.4	0.3650	4.4	0.82	2005.8	75.9	1994.5	47.0	1982.7	55.2	1.01
46	22897	2.6187	4.3	0.2215	3.0	0.71	1290.0	35.2	1305.9	31.3	1332.1	58.3	0.97
103	99534	3.3711	7.8	0.2665	7.7	0.99	1523.0	103.8	1497.7	60.8	1462.0	23.5	1.04
129	2898	0.0445	44.4	0.0087	14.1	0.32	55.9	7.9	44.2	19.2	-556.9	1178.8	-0.10
96	71280	4.3126	2.7	0.3021	2.3	0.87	1701.5	35.1	1695.8	22.3	1688.7	24.9	1.01
135	50449	1.7494	3.1	0.1715	1.7	0.56	1020.4	16.3	1027.0	19.8	1041.0	51.1	0.98
261	32752	5.8958	1.4	0.3508	1.3	0.95	1938.4	21.9	1960.6	12.0	1984.1	7.7	0.98
143	1080	0.0632	316.2	0.0042	13.8	0.04	27.1	3.7	62.2	193.0	1780.8	799.3	0.02
264	42013	0.4907	5.1	0.0662	3.3	0.64	413.2	13.1	405.4	17.2	361.4	89.7	1.14
423	2656	0.0220	38.7	0.0045	8.5	0.22	28.7	2.4	22.1	8.4	-655.3	1069.7	-0.04
197	196857	16.0012	2.1	0.5646	2.1	0.98	2885.4	48.4	2876.9	20.2	2870.9	6.1	1.01
84	62399	4.2860	2.2	0.2963	1.9	0.87	1672.8	28.6	1690.7	18.5	1713.0	20.7	0.98
87	24788	0.6896	7.9	0.0865	2.9	0.36	534.8	14.7	532.6	32.9	522.9	162.8	1.02
301	18762	0.5087	3.6	0.0655	2.8	0.76	409.1	11.0	417.6	12.5	464.7	52.6	0.88
383	3157	0.0225	42.8	0.0045	10.7	0.25	28.7	3.1	22.6	9.6	-592.0	1167.1	-0.05
245	3423	0.0439	119.0	0.0044	19.8	0.17	28.4	5.6	43.6	50.9	987.0	431.2	0.03
72	27683	2.3234	3.8	0.2087	2.6	0.67	1221.9	28.5	1219.5	27.1	1215.1	55.8	1.01
242	3592	0.0456	41.2	0.0053	9.7	0.24	34.2	3.3	45.3	18.2	680.8	888.7	0.05
218	126642	1.7486	2.1	0.1655	1.8	0.84	987.5	16.4	1026.6	13.8	1110.9	22.9	0.89
50	20202	2.9514	2.6	0.2448	1.5	0.56	1411.4	18.7	1395.2	20.1	1370.5	42.3	1.03
288	4015	0.0393	40.8	0.0060	5.7	0.14	38.8	2.2	39.2	15.7	59.5	999.9	0.65
504	5263	0.0275	25.7	0.0050	7.9	0.31	32.4	2.5	27.5	7.0	-375.5	643.1	-0.09
114	66305	3.0378	3.2	0.2472	1.9	0.60	1424.0	24.5	1417.2	24.6	1406.9	49.4	1.01
328	19452	0.1759	10.9	0.0250	3.0	0.27	158.9	4.7	164.5	16.6	245.9	242.8	0.65
192	4739	0.0815	30.5	0.0115	6.6	0.22	74.0	4.9	79.6	23.4	249.5	700.1	0.30
1584	17939	2.4260	1.7	0.1936	1.5	0.91	1140.9	16.0	1250.3	12.1	1444.1	13.3	0.79
289	10437	0.0655	35.6	0.0117	8.2	0.23	75.0	6.1	64.5	22.3	-312.7	911.8	-0.24
849	40837	0.0348	12.9	0.0057	4.0	0.31	36.7	1.5	34.8	4.4	-97.1	302.1	-0.38

379	129317	1.9206	3.4	0.1738	3.3	0.97	1033.0	31.7	1088.3	22.8	1200.7	15.7	0.86
218	192277	4.5369	2.1	0.3077	1.9	0.94	1729.4	29.4	1737.8	17.2	1747.8	13.1	0.99
629	2503	0.0291	16.2	0.0042	7.0	0.43	27.0	1.9	29.2	4.6	210.5	339.5	0.13
568	6666	0.0365	18.2	0.0050	3.8	0.21	32.4	1.2	36.4	6.5	309.3	408.8	0.10
187	84302	2.6865	2.8	0.2254	2.5	0.89	1310.5	29.9	1324.8	21.1	1347.9	25.4	0.97
436	118968	0.4903	3.4	0.0650	1.8	0.54	406.1	7.2	405.1	11.3	399.3	64.0	1.02
542	14602	0.0216	39.6	0.0043	8.5	0.22	27.8	2.4	21.7	8.5	-615.8	1089.2	-0.05
381	11017	0.0558	26.0	0.0088	5.7	0.22	56.2	3.2	55.1	14.0	7.3	620.2	7.67
111	503	0.1775	20.5	0.0238	5.2	0.25	151.5	7.7	165.9	31.5	376.9	451.2	0.40
147	27549	1.7651	2.8	0.1749	1.9	0.67	1039.2	17.9	1032.7	18.1	1018.9	42.2	1.02
680	15324	0.0631	14.8	0.0091	6.0	0.40	58.5	3.5	62.1	8.9	201.8	316.4	0.29
247	49628	2.9790	1.5	0.2435	1.0	0.63	1404.8	12.2	1402.3	11.6	1398.5	22.8	1.00
60	99712	1.6654	5.1	0.1665	3.2	0.62	993.0	29.1	995.5	32.1	1000.9	80.4	0.99
382	3146	0.0391	57.5	0.0038	16.8	0.29	24.4	4.1	39.0	22.0	1059.4	1203.0	0.02
161	74398	3.3821	2.5	0.2585	2.4	0.96	1482.3	32.4	1500.3	20.0	1525.7	13.5	0.97
253	4293	0.0360	55.5	0.0079	3.4	0.06	50.4	1.7	35.9	19.6	-851.0	1702.2	-0.06
60	45391	4.3823	3.8	0.3037	3.5	0.91	1709.5	52.7	1709.0	31.8	1708.4	29.1	1.00
269	2808	0.0262	36.6	0.0057	9.1	0.25	36.7	3.3	26.3	9.5	-851.6	1044.6	-0.04
119	120072	3.1484	2.5	0.2515	2.0	0.80	1446.3	25.7	1444.6	19.1	1442.2	28.3	1.00
38	46327	3.0782	4.9	0.2422	2.1	0.42	1398.0	26.0	1427.3	37.4	1471.2	83.9	0.95
47	29529	2.8425	3.9	0.2375	2.2	0.57	1373.9	27.6	1366.8	29.4	1355.7	62.0	1.01
82	57857	4.1602	2.3	0.2967	1.7	0.73	1675.2	25.3	1666.2	19.2	1655.0	29.5	1.01
265	2107	0.0215	49.1	0.0044	9.8	0.20	28.1	2.7	21.6	10.5	-647.8	1389.4	-0.04
520	3690	0.0202	46.9	0.0047	3.9	0.08	30.1	1.2	20.3	9.4	-1037.3	1462.1	-0.03
598	2569	0.0430	21.8	0.0057	5.2	0.24	36.6	1.9	42.8	9.1	403.0	478.7	0.09
392	178349	4.3455	1.0	0.3014	1.0	0.94	1698.2	14.2	1702.0	8.4	1706.7	6.6	1.00
638	15530	0.0330	13.7	0.0052	6.6	0.48	33.7	2.2	33.0	4.5	-19.1	291.9	-1.76
288	143176	2.6841	4.1	0.2277	3.9	0.96	1322.7	46.9	1324.1	30.1	1326.3	21.1	1.00
1590	10789	0.0298	10.4	0.0043	3.9	0.38	27.4	1.1	29.9	3.1	232.1	222.7	0.12
80	38515	2.7244	3.2	0.2284	2.2	0.69	1326.3	26.7	1335.1	23.9	1349.2	44.9	0.98
123	19204	0.4987	8.0	0.0691	2.9	0.36	431.0	12.0	410.8	27.0	298.9	170.4	1.44
216	3428	3.6716	3.6	0.2624	3.1	0.85	1502.1	40.9	1565.2	28.5	1651.3	34.4	0.91
773	254477	4.6896	2.5	0.3133	2.5	0.99	1756.7	38.1	1765.4	20.9	1775.7	5.8	0.99

332	179137	2.1067	3.4	0.1925	2.9	0.87	1135.1	30.5	1151.0	23.2	1181.0	32.7	0.96
188	101662	2.2276	3.2	0.2044	2.9	0.91	1198.7	31.7	1189.8	22.4	1173.5	27.0	1.02
246	13627	0.1789	17.5	0.0276	4.5	0.26	175.7	7.8	167.2	27.0	48.0	407.3	3.66
332	105367	4.5478	7.7	0.3092	7.7	1.00	1736.6	117.6	1739.8	64.5	1743.6	8.8	1.00
562	31297	0.2797	3.4	0.0391	2.6	0.78	247.4	6.4	250.4	7.5	278.4	48.7	0.89

References

Aleinikoff, J.N., Muhs, D.R., Bettis, E.A., III, Johnson, W.C., Fanning, C.M., and Benton, R., 2008, Isotopic evidence for the diversity of late Quaternary loess in Nebraska: Glaciogenic and nonglaciogenic sources: Geological Society of America Bulletin, v. 120, no. 11/12, p. 1362-1377.

Amato, J.M., Boullion, A.O., Serna, A.M., Sanders, A.E., Farmer, G.L., Gehrels, G.E., and Wooden, J.L., 2008, Evolution of the Mazatzal province and the timing of the Mazatzal orogeny: Insights from U-Pb geochronology and geochemistry of igneous and metasedimentary rocks in southern New Mexico: Geological Society of America Bulletin, v. 120, no. 3-4, p. 328-346.

An, Z., Liu, T., Lu, Y., Porter, S.C., Kukla,G., Wu., X., and Huan, Y., 1990, The long-term paleomonsoon variation recorded by the loess-paleosol sequence in central China: Quaternary International, v. 7-8, p. 91-95, doi: 10.1016/1040-6182(90)90042-3.

Anders, M.H., Saltzman, J., and Hemming, S.R., 2009, Neogene tephra correlations in eastern Idaho and Wyoming: Implications for Yellowstone hotspot-related volcanism and tectonic activity: Geological Society of America Bulletin, v. 121, no. 5-6, p. 837-856.

Anderson, J.L., 1983, Proterozoic anorogenic granite plutonism of North America, *in* Medaris, L.G., Byers, C.W., Mickelson, D.M., and Shank, W.C., eds., Proterozoic Geology: Selected Papers from an International Proterozoic Symposium: Geological Society of America Memoir 161, p. 133-154.

Anderson, T.H., and Silver, L.T., 1981, An overview of Precambrian rocks in Sonora: Universidad Autónoma de México Instituto de Geología Revista, v. 5, p. 131-139.

Armstrong, R.L., and Ward, P.L., 1993, Late Triassic to earliest Eocene magmatism in the North American Cordillera: Implications for the Western Interior Basin, *in* Caldwell, W.G.E., and Kauffman, E.G., eds., Evolution of the Western Interior Basin: Geological Association of Canada Special Paper 39, p. 49-72.

Barth, A.P., and Wooden, J.L., 2006, Timing of magmatism following initial convergence at a passive margin, southwestern U.S. Cordillera, and ages of lower crustal magma sources: The Journal of Geology, v. 114, p. 231-245, doi:10.1086/499573.

Barth, A.P., Wooden, J.L., Coleman, D.S., and Vogel, M.B., 2009, Assembling and disassembling California: A zircon and monazite geochronologic framework for Proterozoic crustal evolution in southern California: The Journal of Geology, v. 117, p. 221-239, doi:10.1086/597515.

Best, M.G., and Christiansen, E.H., 1991, Limited extension during peak Tertiary volcanism, Great Basin of Nevada and Utah: Journal of Geophysical Research, v. 96, p. 13,509-13,528.

Best, M.G., Christiansen, E.H., and Gromme, S., 2013, The 36–18 Ma southern Great Basin, USA, ignimbrite province and flareup: Swarms of subduction-related supervolcanoes: Geosphere, v. 9, p. 260-274, doi:10.1130/GES00870.1.

Bickford, M.E., Van Schmus, W.R., and Zietz, I., 1986, Proterozoic history of the midcontinent region of North America: Geology, v. 14, p. 492-496, doi:10.1130 /0091-7613(1986)14<492:PHOTMR>2.0.CO;2.

Bryson, R.A., and Hare, F.K., 1974, The climates of North America, *in* Bryson, R.A., and Hare, F.K., eds., Climates of North America (world survey of climatology, volume 11), New York, Elsevier, p.1-47.

Buffler, R.T., 2003, The Browns Park Formation in the Elkhead region, northwestern Colorado–south central Wyoming: Implications for Late Cenozoic sedimentation, *in* Raynolds, R.G., and Flores, R.M., eds., Cenozoic systems of the Rocky Mountain region: Cenozoic Systems of the Rocky Mountain Region: Denver, Colorado, Rocky Mountain SEPM, p. 183-212.

Cassiliano, M., 2008, A new genus and species of Stenomylinae (Camelidae, Artiodactyla) from the Moonstone Formation (late Barstovian-early Hemphillian) of central Wyoming: Rocky Mountain Geology, v. 43, no. 1, p. 41-110.

Cather, S.M., Connell, S.D., Chamberlin, R.M., McIntosh, W.C., Jones, G.E., Potochnik, A.R., Lucas, S.G., and Johnson, P.S., 2008, The Chuska erg: Paleogeomorphic and paleoclimatic implications of an Oligocene sand sea on the Colorado Plateau: Geological Society of America Bulletin, v. 120, p. 13-33.

Cather, S.M., Chapin, C.E., and Kelley, S.A., 2012, Diachronous episodes of Cenozoic erosion in southwestern North America and their relationship to surface uplift, paleoclimate, paleodrainage and paleoaltimetry: Geosphere, v. 8, no. 6, p. 1177-1206.

Chamberlain, K.R., Frost, C.D., and Frost, B.R., 2003, Early Archean to Mesoproterozoic evolution of the Wyoming Province: Archean origins to modern lithospheric architecture: Canadian Journal of Earth Sciences, v. 40, p. 1357-1374, doi:10.1139/e03-054.

Chapin, C.E., Wilks, M., and McIntosh, W.C., 2004a, Space-time patterns of Late Cretaceous to present magmatism in New Mexico—comparison with Andean volcanism and potential for future volcanism: New Mexico Bureau of Geology & Mineral Resources, Bulletin 160, p. 13-40.

Chapin, C.E., McIntosh, W.C., and Chamberlin, R.M., 2004b, The late Eocene-Oligocene peak of Cenozoic volcanism in southwestern New Mexico, *in* Mack, G.H., and Giles, K.A., eds., The geology of New Mexico: A geologic history: New Mexico Geologic Society Special Publication 11, p. 271-293.

Chen, J.H., and Moore, J.G., 1982, Uranium-lead isotopic ages from the Sierra Nevada Batholith, California: Journal of Geophysical Research, v. 87, p. 4761-4784.

Childs, O.E., Steele, G., Salvador, A., and Lindberg, F.A., 1988, Correlation of stratigraphic units in North America (COSUNA) Project: AAPG, Tulsa, Oklahoma, 20 map sheets.

Condie, K.C., 1982, Plate-tectonics model for Proterozoic continental accretion in the southwestern United States: Geology, v. 10, p. 37-42, doi:10.1130 /00917613(1982)10<37:PMFPCA>2.0.CO;2.

Cunningham, C.G., Rowley, P.D., Steven, T.A., and Rye, R.O., 2007, Geologic evolution and mineral resources of the Marysvale volcanic field, west-central Utah, *in* Willis, G.C.,

Hylland, M.D., Clark, D.L., and Chidsey, T.C., Jr., eds., Central Utah: Diverse Geology of a Dynamic Landscape: Utah Geological Association Publication 36, p. 143-161.

Damon, P.E., 1970, Correlation and chronology of ore deposits and volcanic rocks: Tucson, University of Arizona, U.S. Atomic Energy Commission Contract AT (11-1)-689, Annual Progress Report COO-689-130, 77 p.

Daniel, C.G., Pfeifer, L.S., Jones, J.V., III, and McFarlane, C.M., 2013, Detrital zircon evidence for non-Laurentian provenance, Mesoproterozoic (ca. 1490–1450 Ma) deposition and orogenesis in a reconstructed orogenic belt, northern New Mexico, USA: Defining the Picuris orogeny: Geological Society of America Bulletin, v. 125, no. 9-10, p. 1423-1441, doi:10.1130/B30804.1.

DeCelles, P.G., 2004, Late Jurassic to Eocene evolution of the Cordilleran thrust belt and foreland basin system, western U.S.A.: American Journal of Science, v. 304, p. 105-168.

Denson, N.M., 1965, Miocene and Pliocene rocks of central Wyoming, *in* Cohee, G.V., and West, W.S., Changes in stratigraphic nomenclature by the U.S. Geological Survey: U.S. Geological Survey Bulletin, v. 1224—A, p. A70-A77, figs. 1-14, 1 table.

Dickinson, W.R., 1985, Interpreting provenance relations from detrital modes of sandstones, *in* Zuffa, G.C., ed., Provenance of Arenites: Hingham, Massachusetts, D. Reidel Publishing Company, p. 333-361.

Dickinson, W.R., 2004, Evolution of the North American Cordillera: Annual Review of Earth and Planetary Sciences, v. 32, p. 13-45.

Dickinson, W.R., 2008, Impact of differential zircon fertility of granitoid basement rocks in North America on age populations of detrital zircons and implications for granite petrogenesis: Earth and Planetary Science Letters, v. 275, p. 80–92, doi:10.1016/j.epsl.2008.08.003.

Dickinson, W.R., and Gehrels, G.E., 2003, U-Pb ages of detrital zircons from Permian and Jurassic eolian sandstones of the Colorado Plateau, USA: Paleogeographic implications: Sedimentary Geology, v. 163, p. 29-66, doi: 10.1016/S0037-0738(03)00158-1.

Dickinson, W.R., and Gehrels, G.E., 2008, Sediment delivery to the Cordilleran foreland basin: Insights from U-Pb ages of detrital zircons in Upper Jurassic and Cretaceous strata of the Colorado Plateau: American Journal of Science, v. 308, p. 1041-1082.

Dickinson, W.R., and Gehrels, G.E., 2009, U-Pb ages of detrital zircons in Jurassic eolian and associated sandstones of the Colorado Plateau: Evidence for transcontinental dispersal and intraregional recycling of sediment: Geological Society of America Bulletin, v. 121, p. 408-433.

Dickinson, W.R., and Snyder, W.S., 1978, Plate tectonics of the Laramide orogeny, *in* Matthews, V., ed., Laramide folding associated with basement block faulting in the western United States: Geological Society of America Memoir 151, p. 355-366.

Dickinson, W.R., and Suczek, C., 1979, Plate tectonics and sandstone compositions: The American Association of Petroleum Geologists Bulletin, v. 63, p. 2164-2182.

Dickinson, W.R., Beard, L.S., Brakenridge, G.R., Erjavec, J.L., Ferguson, R. C., Inman, K.F., Knepp, R.A., Lindberg, F.A., and Ryberg, P.T., 1983, Provenance of North American Phanerozoic sandstones in relation to tectonic setting: Geological Society of America Bulletin, v. 94, p. 222-235.

Dickinson, W.R., Klute, M.A., Hayes, M.J., Janecke, S.U., Lundin, E.R., McKittrick, M.A., and Olivares , M.D., 1988, Paleogeographic and paleotectonic setting of Laramide sedimentary basins in the central Rocky Mountain region: Geological Society of America Bulletin, v. 100, p. 1023-1039, doi:10.1130/00167606(1988)100<1023:PAPSOL>2.3.CO;2.

Dickinson, W.R., Lawton, T.F., and Gehrels, G.E., 2009, Recycling detrital zircons: A case study from the Cretaceous Bisbee Group of southern Arizona: Geology, v. 37, p. 503-506, doi:10.1130/G25646A.1.

Duller, R.A., Whittaker, A.C., Swinehart, J.B., Armitage, J.J., Sinclair, H.D., Bair, A., and Allen, P.A., 2012, Abrupt landscape change post-6 Ma on the central Great Plains, USA: Geology, v. 40, p. 871-874.

Eaton, G.P., 1982, The Basin and Range province: origin and tectonic significance: Annual Reviews of Earth and Planetary Science, v. 10, p. 409-440.

Emry, R. J., 1973, Stratigraphy and preliminary biostratigraphy of the Flagstaff Rim Area, Natrona County, Wyoming: Smithsonian contributions to paleobiology, v. 18, p. 1-43.

Emry, R. J., 1975, Revised Tertiary stratigraphy and paleontology of the Western Beaver Divide, Fremont County, Wyoming: Smithsonian contributions to paleobiology, v. 25, p. 1-20.

Emry, R. J., Russell, L.S., and Bjork, P.R., 1987, Chadronian, Orellan, and Whitneyan North American land mammal ages, *in* Woodburne, M.O., ed., Cenozoic mammals of North America, Geochronology and biostratigraphy: Berkeley, University of California Press, p. 118-152.

Eriksson, K.A., Campbell, I.H., Palin, J.M., and Allen, C.M., 2003, Predominance of Grenvillian magmatism recorded in detrital zircons from modern Appalachian rivers: The Journal of Geology, v. 111, p. 707-717, doi:10.1086/378338.

Evanoff, E., 1990a, Late Eocene and early Oligocene paleoclimates as indicated by the sedimentology and nonmarine gastropods of the White River Formation near Douglas, Wyoming: (Order No. 9117043, University of Colorado at Boulder), 493 p.

Evanoff, E., 1990b, Early Oligocene paleovalleys in southern and central Wyoming: Evidence of high local relief on the late Eocene unconformity: Geology, v. 18, p. 443-446.

Evanoff, E., and Chapin, C.E., 1994, Composite nature of the “late Eocene surface” of the Front Range and adjacent regions, Colorado and Wyoming: Geological Society of America Abstracts with Programs, v. 26, no. 6, p. 12.

Evanoff, E., Prothero, D.R., and Lander, R.H., 1992, Eocene-Oligocene change in North America: the White River Formation near Douglas, east-central Wyoming, *in* Prothero, D.R. and Berggren, W.A., eds., Eocene-Oligocene climatic and biotic evolution: Princeton, Princeton University Press, p. 116-130.

Evernden, J. F., Savage, D. E., Curtis, G. H., and James, C.T., 1964, Potassium Argon dates and the Cenozoic mammalian Chronology of North America: American Journal of Science, v. 262, no. 2, p. 145-208.

Ewing, T.E., 1979, Geology of the Kamloops Group (921/9, 10, 15, 16), *in* Geological Fieldwork 1978: British Columbia Ministry of Energy, Mines and Petroleum Research Paper 1979-1, p. 119-123.

Fan, M., and Dettman, D.L., 2009, Late Paleocene high Laramide ranges in northeast Wyoming: Oxygen isotope study of ancient river water: Earth and Planetary Science Letters, v. 286, p. 110-121, doi: 10.1016/ j.epsl.2009.06.024.

Fan, M., DeCelles, P.G., Gehrels, G. E., Dettman, D.L., and Peyton, S. L., 2011, Sedimentology, detrital zircon geochronology, and stable isotope geochemistry of the lower Eocene strata in the Wind River Basin, central Wyoming: GSA Bulletin, v. 123, no. 5/6, p. 979-996.

Ferrari, L., Valencia-Moreno, M., and Bryan, S., 2007, Magmatism and tectonics of the Sierra Madre Occidental and its relation with the evolution of the western margin of North America, *in* Alaniz-Álvarez, S.A., and Nieto-Samaniego, Á.F., eds., Geology of México: Celebrating the Centenary of the Geological Society of México: Geological Society of America Special Paper 422, p. 1-39.

Flanagan, K.M., 1990, Late Cenozoic geology of the Pathfinder region, central Wyoming, with tectonic implications for adjacent areas [Ph.D. dissert.]: Laramie, Wyoming, University of Wyoming, 185 p.

Flanagan, K.M., and Montagne, J., 1993, Neogene stratigraphy and tectonics of Wyoming, *in* Snoke, A.W., Steidtmann, J.R., and Roberts, S.M., eds., Geology of Wyoming: Laramie, Geological Survey of Wyoming Memoir No. 5, p. 572-607.

Folk, R.L., 1974, Petrology of sedimentary rocks: Austin, Texas, Hemphill Publishing Co., second edition, 182 p.

Folk, R.L., 1980, Petrology of Sedimentary Rocks: Austin, Texas, Hemphill Publishing Company, 184 p.

Galloway, W.E., Whiteaker, T.L., and Ganey-Curry, P., 2011, History of Cenozoic North American drainage basin evolution, sediment yield, and accumulation in the Gulf of Mexico Basin: Geosphere, v. 7, p. 938-973.

Gehrels, G.E., and Dickinson, W.R., 1995, Detrital zircon provenance of Cambrian to Triassic miogeoclinal and eugeoclinal strata in Nevada: American Journal of Science, v. 295, p. 18-48, doi:10.2475/ajs,295.1.18.

Gehrels, G.E., and Stewart, J.H., 1998, Detrital zircon U-Pb geochronology of Cambrian to Triassic miogeoclinal and eugeoclinal strata of Sonora, Mexico: Journal of Geophysical Research, v. 103, p. 2471-2487, doi:10.1029/97JB03251.

Gehrels, G.E., Dickinson, W.R., Ross, G.M., Stewart, J.H., and Howell, D.G., 1995, Detrital zircon reference for Cambrian to Triassic miogeoclinal strata of western North America: Geology, v. 23, p. 831-834, doi:10.1130/0091-7613(1995)023<0831:DZRFCT>2.3. CO;2.

Gehrels, G.E., Valencia, V., and Pullen, A., 2006, Detrital zircon geochronology by laser-ablation multicollector ICPMS at the Arizona Laserchron Center, *in* Olszewski, T., and Huff, W., eds., Geochronology: Emerging opportunities: Philadelphia, Paleontological Society Short Course, Oct. 21, 2006, p. 1-10.

Gehrels, G.E., Valencia, V., and Ruiz, J., 2008, Enhanced precision, accuracy, efficiency, and spatial resolution of U-Pb ages by laser ablation–multicollector–inductively coupled plasma–mass spectrometry: Geochemistry Geophysics Geosystems, v. 9, p. Q03017, doi: 10.1029/2007GC001805.

Gehrels, G.E., Blakey, R., Karlstrom, K.E., Timmons, J.M., Dickinson, B., and Pecha, M., 2011, Detrital zircon U-Pb geochronology of Paleozoic strata in the Grand Canyon, Arizona: Lithosphere, v. 3, p. 183-200, doi:10.1130/L121.1.

Gleason, J.D., Gehrels, G.E., Dickinson, W.R., Patchett, P.J., and Kring, D.A., 2007, Laurentian sources for detrital zircon grains in turbidite and deltaic sandstones of the Pennsylvanian Haymond Formation, Marathon assemblage, west Texas, USA: Journal of Sedimentary Research, v. 77, p. 888-900, doi:10.2110/jsr.2007.084.

Gong, D., Wang, S., and Zhu, J., 2001, East Asian winter monsoon and Arctic Oscillation: Geophysical Research Letters, v. 28, no. 10, p. 2073-2076.

Grambling, J.A., Williams, M.L., and Mawer, C.K., 1988, Proterozoic tectonic assembly of New Mexico: Geology, v. 16, p. 724-727, doi:10.1130/0091-7613(1988)016<0724:PTAONM>2.3.CO;2.

Hayes, F. G., 2005, Paleomagnetics and biostratigraphy of the Pine Ridge Arikaree Group (late Oligocene--early Miocene), Nebraska: (Order No. 3151434, The University of Nebraska - Lincoln), ProQuest Dissertations and Theses, 221 p.

Heller, P.L., Dueker, K., and McMillan, M.E., 2003, Post-Paleozoic alluvial gravel transport as evidence of continental tilting in the U.S. Cordillera: Geological Society of America Bulletin, v. 115, p. 1122-1132.

Hoffman, P.F., 1988, United plates of America, the birth of a craton: Early Proterozoic assembly and growth of Laurentia: Annual Review of Earth and Planetary Sciences, v. 16, p. 543-603, doi:10.1146/annurev.ea .16.050188.002551.

Hoffman, P.F., 1989, Speculations on Laurentia's first gigayear (2.0 to 1.0 Ga): Geology, v. 17, p. 135-138, doi:10.1130 /0091-7613(1989)017<0135:SOLSFG>2.3.CO;2.

Hoganson, J.W., Murphy, E.C., and Forsman, N.F., 1998, Lithostratigraphy, paleontology, and biochronology of the Chadron, Brule, and Arikaree Formations in North Dakota, *in* Terry, D.O., Jr., LaGarry, H.E., and Hung, R.M., Jr., eds., Depositional Environments, Lithostratigraphy, and Biostratigraphy of the White River and Arikaree Groups (Late Eocene to Early Miocene, North America): Boulder, Colorado, Geological Society of America Special Paper 325, p. 185-196.

Honey, J.G., and Izett, G.A., 1988, Paleontology, taphonomy, and stratigraphy of the Browns Park Formation (Oligocene and Miocene) near Maybell, Moffat County, Colorado: U.S. Geological Survey Professional Paper 1358, 52 p.

Ingersoll, R.V., Bullard, T.F., Ford, R.L., Grimm, J.P., Pickle, J.D., and Sares, S.W., 1984, The effect of grain size on detrital modes: A test of the Gazzi-Dickinson point-counting method: Journal of Sedimentary Petrology, v. 54, p. 103-116.

Ingersoll, R.V., Cavazza, W., and Graham, S.A., 1987, Provenance of impure calclithites in the Laramide foreland of southwestern Montana: Journal of Sedimentary Petrology, v. 57, no. 6, p. 995-1003.

Izett, G.A., 1975, Late Cenozoic sedimentation and deformation in northern Colorado and adjoining areas, *in* Curtis, B.F., ed., Cenozoic history of the Southern Rocky Mountains: Geological Society of America Memoir 144, p. 179-209.

Izett, G.A., and Obradovich, J.D., 2001, 40Ar/39Ar ages of Miocene tuffs in basin-fill deposits (Santa Fe Group, New Mexico, and Troublesome Formation, Colorado) of the Rio Grande rift system: The Mountain Geologist, v. 38, p. 77-86.

Jacobson, C.E., Grove, M., Pedrick, J.N., Barth, A.P., Marsaglia, K.M., Gehrels, G.E., and Nourse, J.A., 2011, Late Cretaceous-early Cenozoic tectonic evolution of the southern California margin inferred from provenance of trench and forearc sediments: Geological Society of America Bulletin, v. 123, p. 485-506, doi:10.1130/B30238.1.

Jones, J.V., III., and Thrane, K., 2012, Correlating Proterozoic synorogenic metasedimentary successions in southwestern Laurentia: New insights from detrital zircon U-Pb geochronology of Paleoproterozoic quartzite and metaconglomerate in central and northern Colorado, U.S.A.: Rocky Mountain Geology, v. 47, p. 1-35.

Jones, J.V., III, Shaw, C.A., Allen, J.L., and Housh, T., 2013, U-Pb zircon age constraints on two episodes of Paleoproterozoic magmatism and development of the Grizzly Creek shear zone, White River Uplift, western Colorado, U.S.A.: Rocky Mountain Geology, v. 48, no. 1, p. 15-39.

Kapp, P., Pelletier, J.D., Rohrmann, A., Heermance, R., Russell, J., and Ding, L., 2011, Wind erosion in the Qaidam basin, central Asia: implications for tectonics, paleoclimate, and the source of the Loess Plateau: Geological Society of America Bulletin v. 21, p. 4-10.

Karlstrom, K.E., Dallmeyer, R.D., and Grambling, J.A., 1997, 40Ar/39Ar evidence for 1.4 Ga regional metamorphism in New Mexico: Implications for thermal evolution of lithosphere in the southwestern USA: The Journal of Geology, v. 105, p. 205-224, doi:10.1086 /515912.

Karlstrom, K.E., Amato, J.M., Williams, M.L., Heizler, M.T., Shaw, C.A., Read, A.S., and Bauer, P., 2004, Proterozoic tectonic evolution of the New Mexico region: A synthesis, *in* Mack, G.H., and Giles, K.A., eds., The Geology of New Mexico; A Geologic History: New Mexico Geological Society Special Publication 11, p. 1-34.

Kauffman, E.G., 1985, Cretaceous evolution of the Western Interior Basin of the Unites States, *in* Pratt, L.M., Kauffman, E.G., and Zelt, F.B., eds., Fine-grained deposits and biofacies of the Cretaceous Western Interior Seaway: Evidence of cyclic sedimentary processes: Society of Economic Paleontologists and Mineralogists, 1985 Midyear Meeting, Golden, Colorado, Field Trip Guidebook No. 4, p. iv-xiii.

LaGarry, H.E., 1998, Lithostratigraphic revision and redescription of the Brule Formation (White River Group) of northwestern Nebraska, *in* Terry, D.O., Jr., LaGarry, H.E., and Hunt, R.M., Jr., eds., Depositional Environments, Lithostratigraphy, and Biostratigraphy of the White River and Arikaree Groups (Late Eocene to Early Miocene, North America): Boulder, Colorado, Geological Society of America Special Paper 325, p. 63-92.

LaGarry, H.E., and LaGarry, L.A., 1997, Geology of the Montrose, Orella, Wolf Butte, Roundtop, and Horn 7.5' Quadrangles, Sioux and Dawes Counties, Nebraska: University of Nebraska—Lincoln Conservation and Survey Division Open-File Report 48, 159 p.

Larson, E.E., and Evanoff, E., 1998, Tephrostratigraphy and source of the tuffs of the White River sequences, *in* Terry, D.O., LaGarry, H.E., and Hunt, R.M., Jr., eds., Depositional environments, lithostratigraphy, and biostratigraphy of the White River and Arikaree Groups (late Eocene to Early Miocene, North America): Geological Society of America Special Paper 325, p. 1-14.

Lillegraven, J.A., 1993, Correlation of Paleogene strata across Wyoming—a users' guide, *in* Snoke, A.W., Steidtmann, J.R., and Roberts, S.M., eds., Geology of Wyoming: Geological Survey of Wyoming Memoir No. 5, p. 417-477.

Lipman, P.W., 2007, Incremental assembly and prolonged consolidatioin of Cordilleran magma chambers: Evidence from the Southern Rocky Mountain volcanic field: Geosphere, v. 3, no. 1, p. 42-70.

Liter, M.R., Prothero, D.R., and Hopkins, S.B., 2008, Magnetic stratigraphy of the late Hemingfordian-?Barstovian (lower to middle Miocene) Split Rock Formation, Central Wyoming: New Mexico Museum of Natural History and Science Bulletin, v. 44, p. 25-30.

Liu, L., and Gurnis, M., 2010, Dynamic subsidence and uplift of the Colorado Plateau: Geology, v. 38, p. 663-666, doi:10.1130/G30624.1.

Liu, L., Eronen, J. R., and Fortelius, M., 2009, Significant mid-latitude aridity in the middle Miocene of East Asia: Paleogeography, Paleoclimatology, Paleoecology, v. 279, p. 201-206.

Liu, M., 1996, Dynamic interactions between crustal shortening, extension, and magmatism in the North American Cordillera: Pure and Applied Geophysics, v. 146, no 3-4, p. 447-467.

Liu, T., 1988, Loess in China (2nd edition), Beijing: China Ocean Press, Berlin: Springer-Verlag, 224 p.

Love, J. D., 1961, Split Rock Formation (Miocene) and Moonstone Formation (Pliocene) in central Wyoming: U.S. Geological Survey Bulletin 1121-I, 39 p.

Love, J.D., 1970, Cenozoic geology of the Granite Mountains area, central Wyoming: U.S. Geological Survey Professional Paper 495-C, 154 p.

Love, J.D., and Christiansen, A.C., 1985, Geologic Map of Wyoming: U.S. Geological Survey, scale 1:500,000.

Ludwig, K. L., 2008, Isoplot 3.70. A geochronological toolkit for Microsoft Excel: Berkeley Geochronology Center Special Publication 4, p. 1-77.

MacFadden, B.J., and Hunt, R.M., Jr., 1998, Magnetic polarity stratigraphy and correlation of the Arikaree Group, Arikarean (late Oligocene–early Miocene) of northwestern Nebraska, *in* Terry, D.O., LaGarry, H.E., and Hunt, R.M., Jr., eds., Depositional Environments, Lithostratigraphy, and Biostratigraphy of the White River and Arikaree Groups: Geological Society of America Special Paper 325, p. 143-165.

Mackey, G.N., Horton, B.K., and Milliken, K.L., 2012, Provenance of the Paleocene-Eocene Wilcox Group, western Gulf of Mexico basin: Evidence for integrated drainage of the southern Laramide Rocky Mountains and Cordilleran arc: Geological Society of America Bulletin, v. 124, no. 5/6, p. 1007-1024.

May, J.S., and Russell, L.R., 1994, Thickness of the syn-rift Santa Fe Group in the Albuquerque Basin and its relation to structural style: Geological Society of America Special Paper 291, p. 113-123.

McIntosh, W.C., and Cather, S.M., 1994, 40Ar/39Ar geochronology of basaltic rocks and constraints on Late Cenozoic stratigraphy and landscape development in the Red Hill-Quemado area, New Mexico: New Mexico Geological Society, Guidebook 45, p. 209-215.

McIntosh, W.C., and Chamberlin, R.M., 1994, 40Ar/39Ar geochronology of middle to late Cenozoic ignimbrites, mafic lavas, and volcaniclastic rocks in the Quemado region, New Mexico: New Mexico Geological Society, Guidebook 45, p. 165-185.

McIntosh, W.C., Chapin, C.E., Ratte, J.C., and Sutter, J.F., 1992, Time-stratigraphic framework for the Eocene-Oligocene Mongollon-Datil volcanic field, southwest New Mexico: Geological Society of America Bulletin, v. 104, p. 851-871.

McKenna, M.C. and Love, J.D., 1972, High-level strata containing early Miocene mammals on the Bighorn Mountains, Wyoming: American Museum Novitiates, no. 2490, 31 p.

McMillan, M.E., Heller, P.L., and Wing, S.L., 2006, History and causes of post-Laramide relief in the Rocky Mountain orogenic plateau: Geological Society of America Bulletin, v. 118, p. 393-405.

Miller, D.M., Nilsen, T.H., and Bilodeau, W.L., 1992, Late Cretaceous to early Eocene geological evolution of the U.S. Cordillera, *in* Burchfiel, B.C., Lipman, P.W., and Zoback, M.L., eds., The Cordilleran Orogen: Conterminous U.S.: Boulder, Colorado, Geological Society of America, The Geology of North America, v. G-3, p. 205-260.

Mix, H.T., Mulch, A., Kent-Corson, M.L., and Chamberlain, C.P., 2011, Cenozoic migration of topography in the North American Cordillera: Geology, v. 39, p. 87-90.

Moecher, D.P., and Samson, S.D., 2006, Differential zircon fertility of source terranes and natural bias in the detrital zircon record: implications for sedimentary provenance analysis: Earth and Planetary Science Letters, v. 247, p. 252-266.

Moucha, R., Forte, A.M., Rowley, D.B., Mitrovica, J.X., Simmons, N.A., and Grand, S.P., 2008, Mantle convection and the recent evolution of the Colorado Plateau and the Rio Grande Rift valley: Geology, v. 36, p. 439-442.

Moye, F.J., Hackett, W.R., Blakley, J.D., and Snider, L.G., 1988, Regional geologic setting and volcanic stratigraphy of the Challis volcanic field, central Idaho, *in* Link, P.K., and Hackett, W.R., eds., Guidebook to the Geology of Central and Southern Idaho: Idaho Geological Survey Bulletin 27, p. 87-97.

Muhs, D.R., and Bettis, E.A., III, 2003, Quaternary loess-paleosol sequences as examples of climate-driven sedimentary extremes, *in* Chan, M.A., and Archer, A.W., eds., Extreme depositional environments: Mega end members in geologic time: Boulder, Colorado, Geological Society of America Special Paper 370, p. 53-74.

Muhs, D.R., Aleinikoff, J.N., Stafford, T.W., Jr., Kihl, R., Been, J., Mahan, S., and Cowherd, S.D., 1999a, Late Quaternary loess in northeastern Colorado, I: Age and paleoclimatic significance: Geological Society of America Bulletin, v. 111, p. 1861-1875, doi: 10.1130/0016-7606(1999)111<1861:LQLINC>2.3.CO;2.

Muhs, D.R., Swinehart, J.B., Loope, D.B., Aleinikoff, J.N., and Been, J., 1999b, 200,000 years of climate change recorded in eolian sediments of the High Plains of eastern Colorado and western Nebraska, *in* Lageson, D.R., Lester, A.P., and Trudgill, B.D., eds., Colorado and

adjacent areas: Boulder, Colorado, Geological Society of America Field Guide 1, p. 71-91.

Muhs, D.R., Reynolds, R.L., Been, J., and Skipp, G., 2003, Eolian sand transport pathways in the southwestern United States: importance of the Colorado River and local sources: Quaternary International, v. 104, p. 3-18.

Muhs, D.R., Bettis, E. A., III, Aleinikoff, J., McGeehin, J. P., Beann, J., Skipp, G., Marshall, B. D., Roberts, H. M., Johnson, W. C., and Benton, R., 2008, Origin and paleoclimatic significance of late Quaternary loess in Nebraska: Evidence from stratigraphy, chronology, sedimentology, and geochemistry: Geological Society of America Bulletin, v. 120, p.1378-1407, doi: 10.1130/B26221.1.

Naeser, C.W., Izett, G.A., and Obradovich, J.D., 1980, Fission-track and K-Ar ages of natural glasses: U.S. Geological Survey Bulletin, v. 1489, 31 p.

Nourse, J.A., Premo, W.R., Iriondo, A., and Stahl, E.R., 2005, Contrasting Proterozoic basement complexes near the truncated margin of Laurentia, northwestern Sonora–Arizona international border region, *in* Anderson, T.H., Nourse, J.A., McKee, J.W., and Steiner, M.B., eds., The Mojave-Sonora Megashear Hypothesis: Development, Assessment, and Alternatives: Geological Society of America Special Paper 393, p. 123-182.

Pedrick, J.N., Karlstrom, K.E., and Bowring, S.A., 1998, Reconciliation of conflicting tectonic models for Proterozoic rocks of northern New Mexico: Journal of Metamorphic Geology, v. 16, p. 687-707, doi:10.1111 /j.1525-1314.1998.00165.x.

Pelletier, J.D., 2009, The impact of snowmelt on the late Cenozoic landscape of the southern Rocky Mountains, USA: GSA Today, v. 19, p. 4-10, doi: 10.1130/ GSATG44A.1.

Prothero, D.R., 1995, Geochronology and magnetostratigraphy of Paleogene North American Land Mammal Mammal “Ages”: an update *in* Berggren, W.A., Kent, D.V., Aubry, M.P., and Hardenbol, J., eds., Geochronology, time scales, and global stratigraphic correlations: Unified temporal framework for a historical geology: Tulsa, Oklahoma, Society for Sedimentary Geology, SEPM Special Publication 54, p. 305-316.

Prothero, D.R., and Sanchez, F., 2004, Magnetic stratigraphy of the middle to upper Eocene section at Beaver Divide, Fremont County, Wyoming. New Mexico Museum of Natural History and Science Bulletin, v. 26, p. 149-152.

Pye, K., and Tsoar, H., 1990, Aeolian sand and sand dunes, Springer, London, 396 p.

Retallack, G.J., 2007, Cenozoic paleoclimate on land in North America: The Journal of Geology, v. 115, p. 271-294.

Roberts, H.M., Muhs, D.R., Wintle, A.G., Duller, G.A.T., and Bettis, E.A., III, 2003, Unprecedented last-glacial mass accumulation rates determined by luminescence dating of loess from western Nebraska: Quaternary Research, v. 59, p. 411-419, doi: 10.1016S0033-5894(03)00040-1.

Roberts, G.G., White, N.J., Martin-Brandis, G.L., and Crosby, A.G., 2012, An uplift history of the Colorado Plateau and its surroundings from inverse modeling of longitudinal river profiles: Tectonics, v. 31, p. 1-25.

Robinson, P.L., 1973, A problematic reptile from the British Upper Triassic: Journal of the Geological Society, v. 129, p. 457-479.

Scott, J.W., 2002, the upper Miocene Moonstone Formation of central Wyoming: Linking vertebrate biostratigraphy and uranium-lead geochronology with post-Laramide tectonism, Masters Thesis, University of Wyoming, 236 p.

Scott, J., and Bowring, S.A., 2000, High precision U/Pb geochronology of Oligocene tuffs from the White River Formation, Douglas, Wyoming: Society of Vertebrate Paleontology, v. 20, no. 3, p. 69A.

Sheldon, N.D., 2009, Non-marine records of climatic change across the Eocene-Oligocene transition, *in* The late Eocene Earth-Hothouse, Icehouse, and Impacts: Geological Society of America Special Paper 452, p. 241-248.

Sheldon, N. D., and Retallack, G. J., 2004, Regional paleoprecipitation records from the late Eocene and Oligocene of North America: Journal of Geology, v. 112, no. 4, p. 487-494.

Snoke, A.W., 1993, Geologic history of Wyoming within the tectonic framework of the North American Cordillera, *in* Snoke, A.W., Steidtmann, J.R., and Roberts, S.M., eds., Geology of Wyoming: Geological Survey of Wyoming Memoir No. 5, p. 2-56.

Steidtmann, J.R., and Middleton, L.T., 1991, Fault chronology and uplift history of the southern Wind River Range, Wyoming: Implicaitons for Laramide and post-Laramide deformation in the Rocky Mountain foreland: Geological Society of America Bulletin, v. 103, p. 472-485.

Steidtmann, J.R., Middleton, L.T., and Schuster, M.W., 1989, Post-Laramide (Oligocene) uplift in the Wind River Range, Wyoming: Geology, v. 17, p. 38-41, doi:10.1130/00917613(1989)017<0038:PLOUIT >2.3.CO;2.

Stewart, J.H., Gehrels, G.E., Barth, A.P., Link, P.K., Christie-Blick, N., and Wrucke, C.T., 2001, Detrital zircon provenance of Mesoproterozoic to Cambrian arenites in the western United States and northwestern Mexico: Geological Society of America Bulletin, v. 113, p. 1343-1356, doi:10.1130/0016-7606(2001)113<1343:DZPOMT >2.0.CO;2.

Strömberg, C.A.E., 2004, Using phytolith assemblages to reconstruct the origin and spread of grass-dominated habitats in the Great Plains of North America during the late Eocene to early Miocene: Palaeogeography, Palaeoclimatology, Palaeoecology, v. 207 no. 3-4, p. 239-275.

Sun, J., Ye, J., Wu, W., Ni, X., Bi, S., Zhang, Z., Liu, W., and Meng, J., 2010, Late Oligocene–Miocene mid-latitude aridification and wind patterns in the Asian interior: Geology, v. 38, p. 515-518.

Swinehart, J. B., and Diffendal, R. F, Jr., 1987, Duer Ranch, Morrill County, Nebraska: Contrast between Cenozoic fluvial and eolian deposition: Geological Society of America Centennial Field Guide-North-Central Section, p. 23-28.

Swinehart, J.B., Souders, V.L., DeGraw, H.M., and Diffendal, R.F., Jr., 1985, Cenozoic paleogeography of western Nebraska, *in* Flores, R.M., and Kaplan, S.S., eds., Cenozoic paleogeography of west-central United States: Rocky Mountain Paleogeography

Symposium 3, Rocky Mountain Section: Tulsa, Society of Economic Paleontologists and Mineralogists, p. 209-229.

Swisher, C.C., III, and Prothero, D.R., 1990, Single crystal 40Ar/39Ar dating of the Eocene-Oligocene transition in North America: Science, v. 249, p. 760-762.

Tedford, R.H., and Barghoorn, S., 1999, Santa Fe Group (Neogene) Ceja del Rio Puerco, northwestern Albuquerque Basin, Sandoval County, New Mexico: New Mexico Geological Society, Guidebook 50, p. 327-335.

Terry, D.O. Jr., 1998, Lithostratigraphic revision and correlation of the lower part of the White River Group: South Dakota to Nebraska, *in* Terry, D.O., LaGarry, H.E., and Hunt, R.M., Jr., eds., Depositional Environments, Lithostratigraphy, and Biostratigraphy of the White River and Arikaree Groups: Geological Society of America Special Paper 325, p. 15-38.

Tolan, T.L., Reidel, S.P., Beeson, M.H., Anderson, J.L., Fecht, K.R., and Swanson, D.A., 1989, Revisions to the estimates of the areal extent and volume of the Columbia River Basalt Group *in* Reidel, S.P., and Hooper, P.R., eds., Volcanism and tectonism in the Columbia River flood-basalt province: Geological Society of America Special Paper 239, p. 1-20.

Torres, R., Ruiz, J., Patchett, P.J., and Grajales, J.M., 1999, Permo-Triassic continental arc in eastern Mexico: Tectonic implicaitons for reconstructions of southern North America, *in* Bartolini, C., Wilson, J.L., and Lawton, T.F., eds., Mesozoic Sedimentary and Tectonic History of North-Central Mexico: Geological Society of America Special Paper 340, p. 191-196.

Tsoar, H., and Pye, K., 1987, Dust transport and the question of desert loess formation: Sedimentology, v. 34, p. 139-153.

Van Houten, F.B., 1964, Tertiary geology of the Beaver Rim area, Fremont and Natrona Counties, Wyoming: U.S. Geological Survey Bulletin, v. 1164, 99 p.

Vermeesch, P., 2004, How many grains are needed for a provenance study?: Earth and Planetary Science Letters, v. 224, n. 3-4, p. 441-451.

Whitmeyer, S. J., and Karlstrom, K. E., 2007, Tectonic model for the Proterozoic growth of North America: Geosphere, v. 3, no. 4, p. 220-259.

Woodburne, M.O., and Swisher, C.C., III, 1995, Land mammal high-resolution geochronology, intercontinental overland dispersals, sea level, climate and vicariance, *in* Berggren, W.A., Kent, D.V., Aubry, M.P., and Hardenbol, J., eds., Geochronology, time scales, and global stratigraphic correlations: Unified temporal framework for a historical geology: Tulsa, Oklahoma, Society for Sedimentary Geology, SEPM Special Publication 54, p. 337-364.

Wu, B., and Wang, J., 2002, Winter Arctic oscillation, Siberian High and East Asian winter monsoon: Geophysical Research Letters, v. 29, no. 19, p. 3-1-3-4.

Zachos, J.C., Shackleton, N.J., Revenaugh, J.S., Palike, H., and Flower, B.P., 2001a, Climate response to orbital forcing across the Oligocene-Miocene boundary: Science, v. 292, p. 274-278.

Zachos, J.C., Pagani, M., Sloan, L., Thomas, E., and Billups, K., 2001b, Trends, rhythms, and aberrations in global climate 65 Ma to present: Science, v. 292, p. 686-693.

Zhisheng, A., Kutzbach, J.E., Prell, W.L., and Porter, S.C., 2001, Evolution of Asian monsoons and phased uplift of the Himalaya-Tibetan plateau since Late Miocene times: Nature, v. 411, p. 62-66.

Biographical Information

Jillian Rowley is a native Texan. She was born in Lake Jackson and raised in Liverpool. She attended Alvin High School and graduated in May 2006. Upon graduation, she attended Kilgore College and belonged to the world famous Kilgore College Rangerettes where she served as Right Lieutenant. At Kilgore College, Jillian discovered her love of geology in Dr. Paul Buchanan's Physical Geology class. She applied to the University of Texas at Austin and graduated from the Jackson School of Geosciences in August 2008. Following graduation, she began an internship with XTO Energy and attended the University of Texas at Arlington to pursue a master's degree in Geology. Upon completion of her degree, she will begin a career as a petroleum geologist with the Exploration Company at ExxonMobil Corporation.